POWER QUALITY IMPROVEMENT OF DISTRIBUTION SYSTEM BY OPTIMAL ALLOCATION OF DISTRIBUTED ENERGY RESOURCES USING META HEURISTIC TECHNIQUES

Thesis Submitted for the Award of the Degree of

DOCTOR OF PHILOSOPHY

in

Electrical Engineering

By

Shaik Aarif

Registration Number: 41800011

Supervised By

Dr. Suresh Kumar Sudabattula (21628)

Power System (Associate Professor) Lovely Professional University, Punjab

Co-Supervised by

Dr. Sachin Mishra (20444)

Power System (Professor) Lovely Professional University, Punjab

LOVELY PROFESSIONAL UNIVERSITY, PUNJAB

2025

DECLARATION

I, hereby declared that the presented work in the thesis entitled "Power Quality Improvement of Distribution System by Optimal Allocation of Distributed Energy Resources using Metaheuristic Techniques" in fulfilment of degree of **Doctor of Philosophy (Ph.D.)** is outcome of research work carried out by me under the supervision of **Dr. Suresh Kumar Sudabattula**, working as Associate Professor, in the School of Electronics and Electrical Engineering of Lovely Professional University, Punjab, India and under the Co-supervision of **Dr. Sachin Mishra** , working Professor, in the School of Electronics and Electrical Engineering of Lovely Professional University, Punjab India. In keeping with general practice of reporting scientific observations, due acknowledgements have been made whenever work described here has been based on findings of other investigator. This work has not been submitted in part or full to any other University or Institute for the award of any degree.

(Signature of Scholar)

Name of the scholar: Shaik.Aarif

Registration No.: 41800011

Department/school: Department of Electrical Engineering

Lovely Professional University,

Punjab, India

CERTIFICATE

This is to certify that the work reported in the Ph.D. thesis entitled "**Power Quality Improvement of Distribution System by Optimal Allocation of Distributed Energy Resources using Metaheuristic Techniques**" submitted in fulfilment of the requirement for the reward of degree of **Doctor of Philosophy (Ph.D.)** in the Department of Electrical Engineering, is a research work carried out by Shaik. Aarif 41800011, is bonafide record of his original work carried out under my supervision and that no part of thesis has been submitted for any other degree, diploma or equivalent course.

(Signature of Supervisor)

Name of supervisor: Dr. Suresh Kumar Sudabattula

Designation: Associate Professor

Department/school: School of Electronics and Electrical Engineering

University: Lovely Professional University.

(Signature of Co-Supervisor)

Name of Co-Supervisor: Dr. Sachin Mishra

Designation: Professor

Department School of Electronics and Electrical Engineering

University: Lovely Professional University.

ABSTRACT

Due to the increasing importance of renewable energy sources, such as solar and wind power, scientists have intensified efforts to reduce environmental pollution caused by burning fossil fuels. This shift toward renewables has been accompanied by a growing advocacy for a sustainable energy supply. However, despite increasing support for renewable energy, the transition has been too slow to meet global energy demands. In 2022, the number of people lacking access to energy services grew significantly, underscoring the vulnerability of the global energy system. While progress has been made in using renewables like wind and solar power, other critical sources, such as biomass and geothermal energy, remain underutilized.

In 2022, energy markets were highly volatile and unpredictable. The rapid recovery from the COVID-19 pandemic and the Russian Federation's invasion of Ukraine drove up energy prices. This rise in gas and oil prices caused higher costs for energy, food, and basic necessities. Governments responded with various policies, such as the European Union’s initiatives and the US Inflation Reduction Act, to mitigate the impact of rising costs. However, climate change-related natural disasters worsened the situation. Ironically, many nations increased subsidies for fossil fuels, boosting global coal and fossil fuel usage. Rising costs also delayed advancements in technologies aimed at providing universal energy access.

Global primary energy demand grew by only 1.1% in 2022, compared to 5.5% in 2021. Although solar and wind energy expanded, fossil fuels still dominated, contributing over 80% of global energy supply. Fossil fuel price volatility and supply disruptions prompted more consumers to consider sustainable energy sources. Between 2011 and 2021, global energy consumption increased by 16%. The share of renewables in the Total Final Energy Consumption (TFEC) grew from 30 EJ to 50 EJ in six years, while fossil fuels’ share decreased marginally from 81.2% to 78.9%. However, fossil fuel consumption still increased by 35 EJ during this period.

In 2020, Iceland led the TFEC with 83% of its energy sourced from renewables, followed by Norway (74%) and Paraguay (73%). Between 2010 and 2020, renewable energy shares in the Lao People's Democratic Republic increased by 20%, with Denmark, Sweden, and Norway also showing significant growth.

Heat energy accounted for nearly half of the global energy supply in 2022, 4% higher than in 2010. Transport fuel and electricity made up 28.6% and 22.7% of the global supply, respectively. Renewable heat contributed only 11.5% of the total heat demand, excluding

biomass. Renewable electricity and heat were expected to account for over 29.9% of global electricity production in 2022. Modern bioenergy sources, such as solar thermal, geothermal heat, and biomass, were expected to supply most of the renewable heat. Meanwhile, biofuels were projected to contribute just 0.4% to the transport sector's fuel supply.

Despite these advancements, solar and wind energy face inherent challenges due to the variability of solar radiation and wind speeds. These limitations must be considered when designing distribution systems. To address this, a Particle Swarm Optimization with Differential Velocities (PSODV) algorithm is proposed. This algorithm was implemented on an Indian 28-bus and IEEE 85-bus system, considering solar DG, wind DG, hybrid solar-wind DG, and residential, commercial, and industrial loads under various scenarios.

The optimal bus locations and DG sizes were calculated, and performance metrics, such as power loss (P_loss in kW), minimum voltage (V_min in p.u.), Voltage Stability Index (VSI_min in p.u.), and percentage reduction in power loss, were evaluated across all cases. The effectiveness of the proposed PSODV algorithm was benchmarked against the Firefly (FF) algorithm and Gorilla Troops Optimizer (GTO) algorithm. In all scenarios, the PSODV algorithm exhibited superior performance, demonstrating its potential for optimizing distributed power networks.

.

TABLE OF CONTENTS

LIST OF FIGURES

LIST OF TABLES

LIST OF ABBREVIATIONS & SYMBOLS

1. **DG** - Distributed Generation
2. **RDS** - Radial Distribution System
3. **PV** - Photovoltaic
4. **EV** - Electric Vehicle
5. **THD** - Total Harmonic Distortion
6. **PSODV** - Particle Swarm Optimization with Differential Velocities
7. **FF** - Firefly Algorithm
8. **GTO** - Gorilla Troops Optimizer
9. **TFEC** - Total Final Energy Consumption
10. **EJ** - Exajoule
11. **VSI** - Voltage Stability Index
12. **EU** - European Union
13. **P_loss** - Power loss (kW)
14. **V_min** - Minimum voltage (p.u.)
15. **VSI_min** - Minimum Voltage Stability Index (p.u.)
16. **% Reduction P_loss** - Percentage reduction in power loss

CHAPTER 1

INTRODUCTION

1.1 Preamble

Over the years, grid power systems has constructed with large power plants that amplify the input voltage of the electric power. These are designed to provide high-voltage power to the transmission networks of interconnected electric power plants. Then step down the voltage of electric power from high to medium voltage systems and then to low voltage systems. Finally, the power is then supplied to the loads through the distribution systems.

The utilization small power plant generation units at distribution level is termed as "Distributed Generation" (DG). The term Distributed Generation is used to describe small-scale electric power generation. It can be defined in different ways in different countries. IEA defines it as the generation of electricity at the customer's side or supporting the distribution system with voltage levels. According to the CIGRE, distribution generation includes the following characteristics[1]–[4].

- DG is smaller than 50000 kW to 100000 kW
- DG is not centrally dispatched or planned
- DG is connected directly to the distribution system

According to the Electric Power Research Institute, a distribution generation system is composed of units that are less than 50 kW. Many US states define it as embedded generation, while others refer to it as distributed generation. Europe, India, and other Asian nations refer to it as decentralized generation. The advantages of DG, such as it allows the market to operate more freely, it lowers the electric utility's reliance on fossil fuels, and it offers an alternative to building new transmission lines. It can be generated through various technological methods or through the utilization of more conventional sources. A distributed generation power plant is a type of energy source that uses various technologies such as solar photovoltaics, biomass, microturbines, and fuel cells.[5]–[8].

The large generating stations with interconnected systems along withdistributed generation are presented in Fig. 1.1. Local generation has the potential to impact decentralised energy networks. The DG makes it possible to consider the distribution grid with a steady, unidirectional power flow. Nevertheless, distributed generation impacts distribution system performance[9]–[15].The level of losses at distribution system is higher than that of a transmission system due to the presence of load tapping. Hence, it is essential to anticipate the losses at distribution system. The voltage profile of the system is uncertain, leading to higher losses. Uncertain voltage profiles can lead to variations in the current, causing higher power loss and cost along the distribution system. Hence its performance needs to be assessed and optimal planning is required[16]–[20].

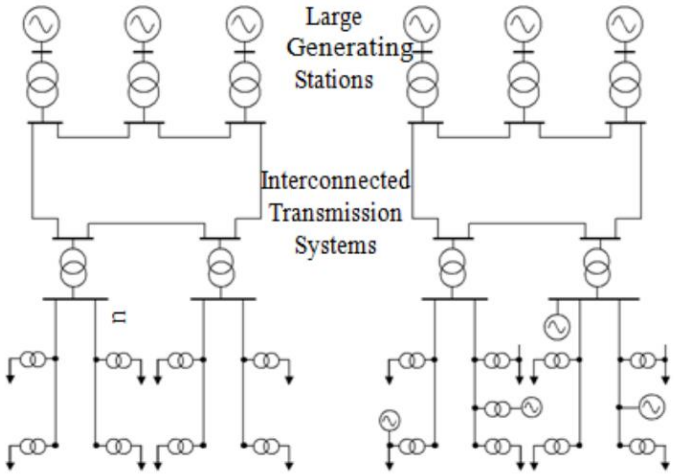

Fig. 1.1 Generating Stations

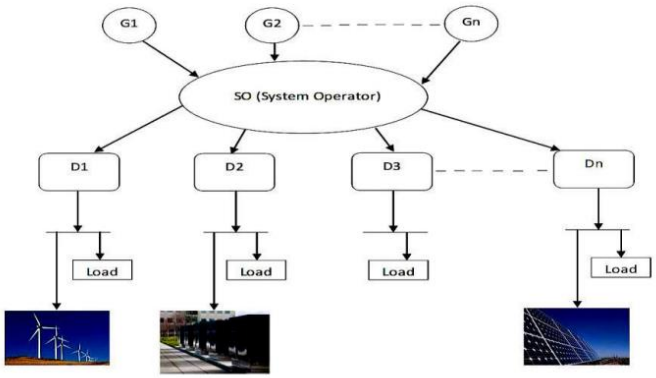

Fig. 1.2 DG Units

1.2 Distributed Generators

In the power industry, decentralized or distributed generation is a concept that's been around for a long time. In 1882, Thomas Edison established the Pearl Street electric plant in New York City. It provided 110 V DC power to 59 homes and businesses in lower Manhattan. By 1887, over a hundred Edison plants were supplying DC power to over a thousand businesses and homes in the US. Early generators usually rely on water or coal to power their operation. Through the use of alternating current electricity, these generators can carry electricity across long distances at a low cost.[21]–[26].

The concept of distributed generation, which involves the use of multiple sources of power, has gained widespread attention. It can be supported by various technologies, such as wind turbines, fuel cells, geothermal systems, and photovoltaic installations. The growth of distributed power generation is attributed to various factors such as the establishment of electric utility companies, technological advancements, and the environmental concerns surrounding the use of fossil fuels. The increasing number of distributed generation systems being implemented shows the growing importance of such technologies in the utility and smart grid sectors.[27]–[30].

With distributed generation, the electricity distribution system can be transformed from a passive to active, thereby increasing efficiency, enhancing load management, and decreasing the frequency of outages. Because of the complex behaviour of distribution system, designing, operating, and administering the power grid is challenging. To meet these challenges optimal planning is required.The schematic diagram of the distribution system is presented in Fig. 1.3

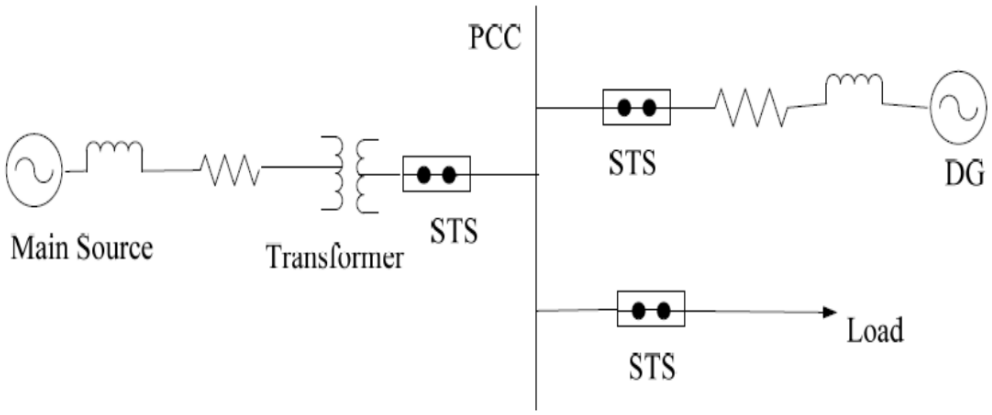

Fig. 1.3 Simple distributed system

During the early days of electrical power distribution, there were various feeders located radially from the substation. These were connected to the primary transformer. One of the major disadvantages of radial electric power distribution system is that it can't provide the associated consumers with power in case of a failure. This is because there's no alternative path to the transformer. If a transformer fails, the power supply to the consumer in the region would be interrupted. This means that the consumer would experience darkness until the transformer or feeder is fixed[31]–[34]. The advantages of Distribution system are presented in Fig. 1.4.

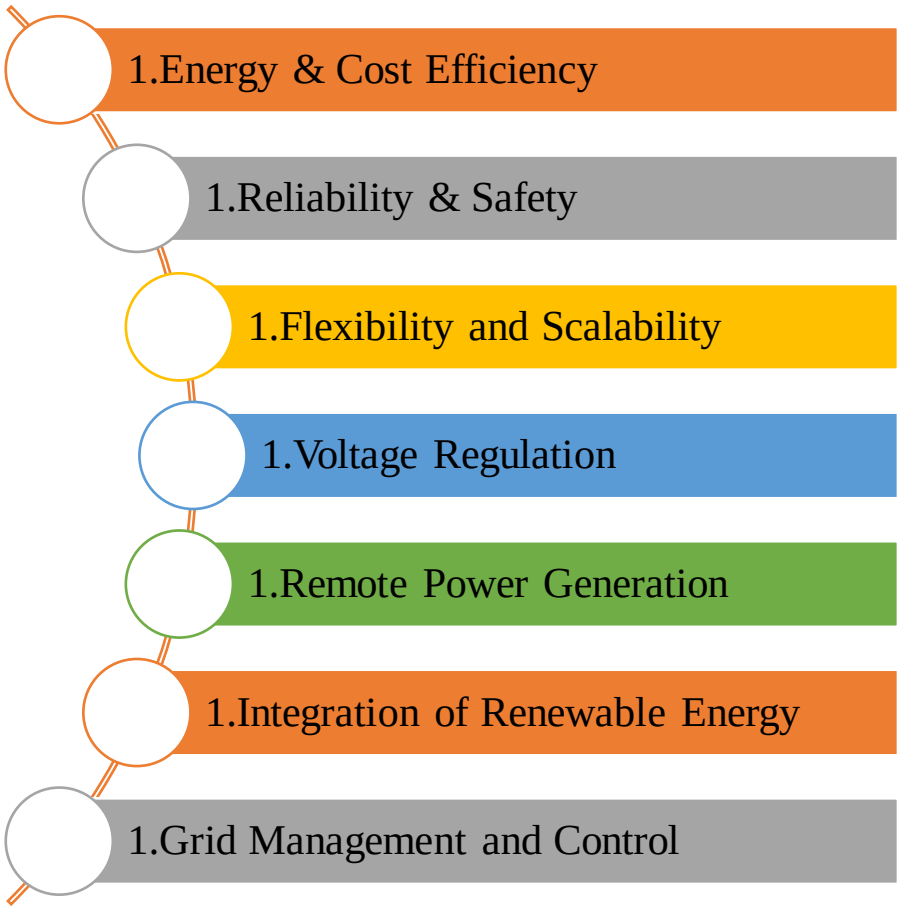

Fig. 1.4 Advantages of Distribution System

1.3 Significance of Distribution System

An electrical distribution system is the backbone of modern society, powering everything from homes to businesses. These intricate devices and components are designed to distribute electrical energy efficiently from the generation point to the end-users. The reliability of these systems is of utmost importance to ensure that the electricity supply is stable and reliable in the face of a constantly changing world. The

distribution of electricity is a vital part of modern society, as it allows us to seamlessly transmit power from our power plants to remote regions. This process helps us tap into various resources such as wind, water, and fossil fuels.

This infrastructure is essential for the advancement of society, as it enables industries, communities, and essential services to thrive. The importance of maintaining a reliable power supply is also a major factor that affects the operations of various businesses and organizations. A disruption in the electricity supply can have a significant impact on the quality of life and economic activities of the people. In order to guarantee a dependable supply of electricity, the design, construction, and maintenance of distribution systems are crucial. The design and construction of distribution systems are also important in order to promote sustainability and energy efficiency. As the world moves toward a more sustainable energy system, it is important that the distribution systems are equipped with the necessary equipment and technology to accommodate the growing number of renewable power sources. Modern smart grid technologies can help improve the efficiency and balance of the electricity supply by allowing real-time monitoring of the distribution system.

Besides power delivery, the design and construction of distribution systems also play a vital role in enhancing the energy quality of electricity. These components are equipped with various devices, such as voltage regulators and transformers, to ensure that the voltage levels are consistent. Power factor correction techniques can also be utilized in distribution systems to enhance the transmission of electricity. This technology helps minimize environmental impact and energy losses. The modernization of cities is a major issue that involves the distribution of electricity. Urbanization has increased the demand for electricity, which is mainly driven by the increasing number of smart buildings and transportation projects.

Distribution systems must be able to accommodate the needs of the future by adapting to the latest technologies and being able to integrate them seamlessly. Smart grids can help manage the energy resources of cities and improve their resilience. The rise of IoT and digitalization has created a new era for the electrical distribution industry. Various devices, such as smart meters, are being integrated into networks to provide real-time data regarding the performance of the equipment and the consumption of electricity. Through the use of data-driven strategies, utilities can make better

decisions and improve the efficiency of their distribution systems. This approach not only helps them maintain a reliable supply of electricity but also reduces their costs. The significance of the electrical distribution system cannot be overstated. These components play a vital role in powering the 21st century and are responsible for ensuring a secure and reliable supply of energy to promote sustainability and efficiency. As we transition to more sustainable energy sources and embrace new technologies, the evolution of these systems will play a crucial role in shaping the future energy consumption and distribution. The continuous optimization and advancement of distribution systems are needed to meet society's increasing demands and provide a resilient and sustainable energy infrastructure.

1.4 Renewable Energy Sources in Distribution System

Renewable energy sources are becoming increasingly important components of the electrical distribution system, which signifies a significant shift in how we generate, consume, and distribute power. The integration of such energy sources into the electrical grid is a crucial step towards a more resilient and sustainable future. When utilized as distributed generators, such as wind, solar, geothermal, and hydropower, these energy sources offer numerous advantages. One of these is their ability to capture and use resources that are both renewable and inexhaustible. This eliminates the risk of depleting the world's resources and contributes to the preservation of the environment. These sources are being utilized to support the global efforts toward a greener energy future. They help mitigate the effects of climate change and decrease reliance on non-renewable energy. The concept of distributed generation refers to the method of powering a home or business through the use of renewable energy. Unlike traditional power plants, which are usually situated far from the end-users, these generators are closer to the consumption area. This eliminates the need for large power plants and provides various benefits. When a disruption in the electrical system occurs, distributed generators can provide power to a nearby location. This eliminates the risk of power outages and enhances the system's overall reliability. One of the most common renewable energy sources that is being utilized for distributed generation is solar. This technology converts sunlight into electricity. It can be installed on various rooftops and in residential areas.

Not only does distributed solar energy contribute to the generation of clean energy, but it can also help alleviate the strain on the electrical grid during times of peak demand. As the cost of solar PV technology continues to decrease, it is expected that more people will start adopting this type of energy source. Another type of renewable energy source that is rapidly gaining popularity is wind power. These turbines are capable of capturing the wind's kinetic energy and converting it into electrical energy. These distributed wind projects are usually small and can be placed in different regions to maximize their efficiency. Integrating wind power into the electrical system can provide communities with a consistent and balanced source of renewable energy. One of the oldest forms of renewable energy is hydropower. This technology can be utilized to generate electricity at the local level through small-scale systems that are placed in streams and rivers. These generators can provide a steady supply of energy to regions with a plentiful water supply.

Hydropower technology's scalability enables it to be utilized in diverse settings, such as rural settlements and urban areas. It also contributes to a resilient electrical grid. The heat from the Earth's internal regions can be used to generate geothermal energy, which has the potential to be distributed. These power plants can be placed in regions with a plentiful water supply and are able to provide a constant supply of electricity. This type of energy source complements other renewable energy sources such as wind and solar. Advancements in energy storage have led to the integration of various renewable energy sources into distributed generators. These technologies allow for the capture of energy that has been produced during times of high renewable output. These energy storage systems can then be utilized to release this unused energy at times of peak demand. Through energy storage, distributed generators can improve the reliability of their operations by managing the fluctuations in their supply and ensuring a consistent supply of electricity to end-users.

The increasing popularity of distributed generators aligns with the concept of energy democracy, which allows people and communities to have a greater say in their energy consumption patterns and sources. Localized projects that are made up of renewable energy contribute to the development of an energy ecosystem that is more resilient. As distributed generators continue to expand their operations, they align with the notion of smart grids, which are composed of control and communication technologies that aim

to enhance the electrical system's efficiency and reliability. Integrating renewable resources into smart grids can provide various benefits, such as monitoring and data analytics. Predictive maintenance can be performed on distributed generators to enhance their performance and prevent failures. The installation of distributed generators has highlighted the importance of renewable energy in the electrical system. It contributes to the development of an energy ecosystem that is more resilient and sustainable. The adoption of these technologies has numerous advantages, such as energy independence, grid resilience, and environmental sustainability. Integrating renewable power sources into electrical grids is crucial as the world works toward tackling climate change and establishing a more sustainable future. The optimization, deployment, and growth of distributed power generation will have a significant impact on the future of distribution and generation

1.5 Distribution System Losses

The power generated from a plant is transported through various networks, such as overhead lines, power transformers, and underground cables. It reaches the end users through the distribution system. The term transmission system losses refer to the various incidents in the transmission system, while the latter is associated with the distribution system. The distribution system's losses are higher than those in the transmission system due to load tapping. It is important to anticipate the losses that the distribution system might experience due to the uncertainty regarding its voltage profile. This issue can lead to higher costs and power loss[35]–[38]. The distribution system losses are categorised in to the following

- Technical Losses
- Non-Technical Losses

1.5.1 Technical Losses

Unpredictable load changes can lead to technical losses in the distribution system. This is why the system should be planned correctly to prevent these losses. Technical losses can occur due to the power being dissipated by the loss of electrons at the conductor of the transmission line or electrical equipment. The reasons for the technical losses are presented in Fig. 1.5

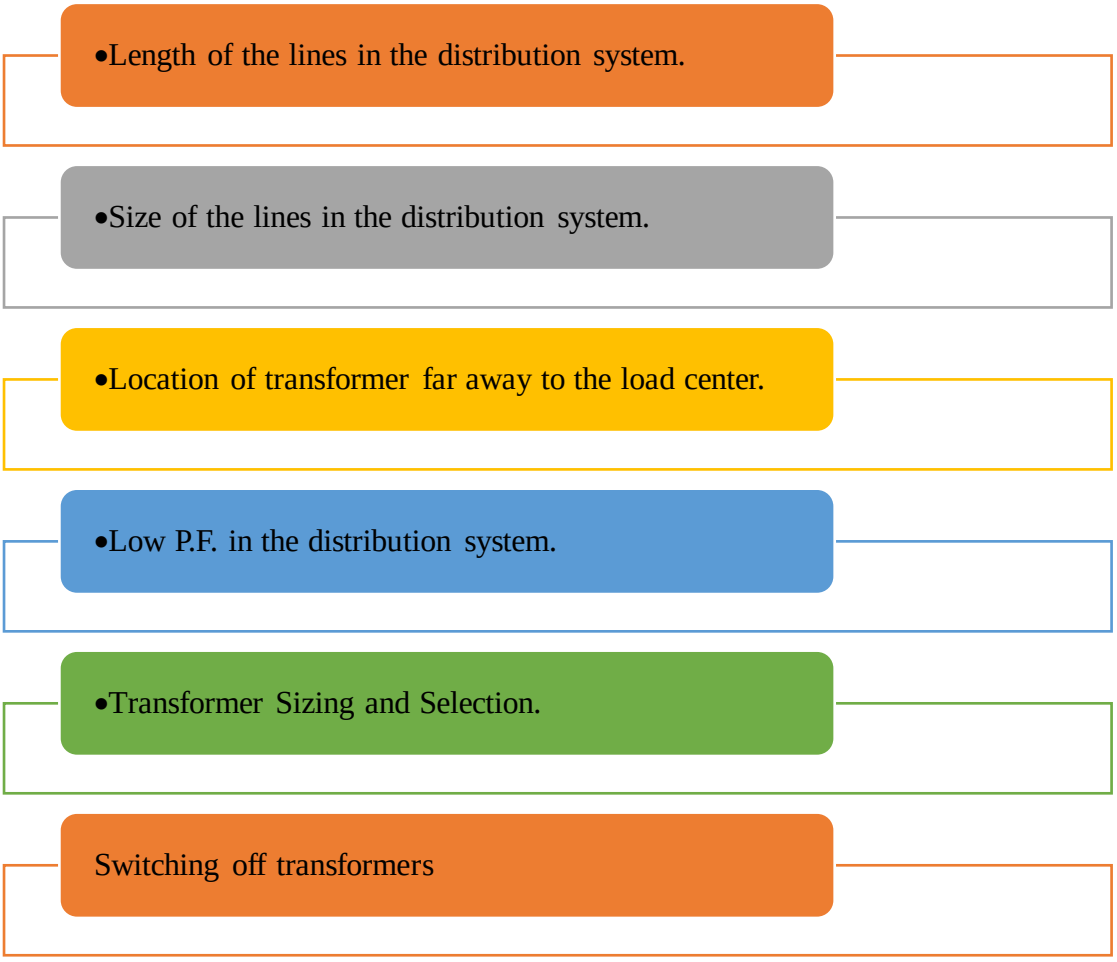

Fig. 1.5 Reasons for Technical Losses

1.5.2 Non-Technical Losses

A non-technical loss is referred to as commercial losses. It can be caused by various factors such as the theft of energy, the incorrect reading of meters, and defective meters.

1.6Distribution System Performance Improvement Methods

The performance index of the distribution system needs to be improved to maintain a healthy state. The system delivers power to different types of industrial, commercial, and domestic loads, which are often unpredictable[39]–[41]. To improve its performance, various methods are shown in Fig. 1.6.

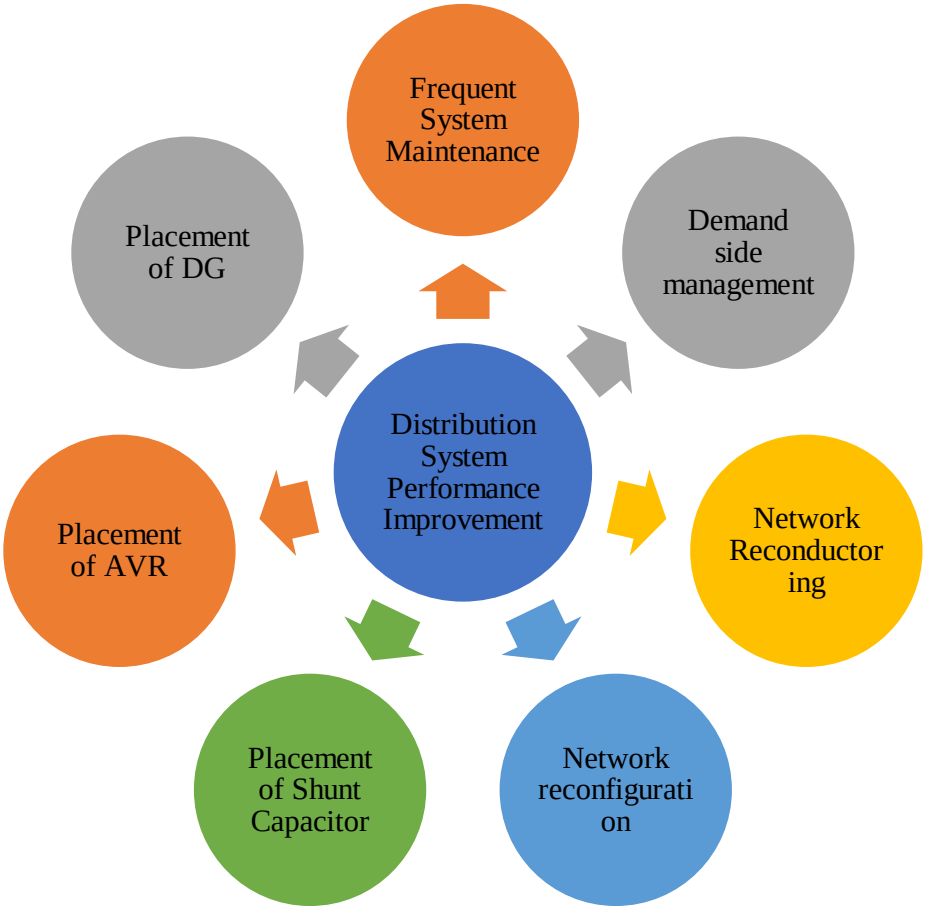

Fig. 1.6 Distribution System Performance Improvement

1.6.1 Frequent System Maintenance

The frequent maintenance of the distribution system helps improve its performance and prevents failures. It also ensures that the system is safe and efficient.

1.6.2 Demand Side Management

One of the most effective ways to improve the efficiency of the distribution system is DSM. This program aims to encourage the end users to reduce their energy consumption during the peak hours.

1.6.3 Network Reconductoring

A network reconductoring process involves replacing an existing conductor with a new one that has the ideal dimensions and size. This method is usually performed when the old conductor is not ideal in terms of its size and dimension. In addition to being able to provide a better conductor, the size of the conductor also determines the current and resistance of the network. This technique is being used in various emerging countries such as India. During the process, the old conductor is replaced with a new one that has a greater cross-sectional area. This means that the new conductor's resistance will decrease as the cross-sectional area gets bigger. This method can enhance the transmission capabilities of the network, as well as reduce the losses.

1.6.4 Network Reconfiguration

A network reconfiguration is a process that involves changing the distribution system's configuration to reduce the losses. It involves switching the load among the different feeders. The distribution system has a complex design and is designed to protect against overcurrent. The process of network reconfiguration is considered as a non-discriminatory optimization technique that can be utilized to improve the efficiency of the distribution network. It involves the reconfiguration of the distribution network in the most optimal way.

1.6.5 Placement of Shunt Capacitor

The optimal location and size of capacitors are some of the factors that are considered when it comes to optimizing the distribution system. Almost 80% of the energy that is generated is used to drive the rotating loads, such as induction motors. However, during the start-up phase, the motor consumes a huge amount of reactive power, which is required to magnetize its core. This is why it is important that the capacitor is placed in the right position and type. The advantages of optimal placement of shunt capacitors are presented in Fig. 1.7.

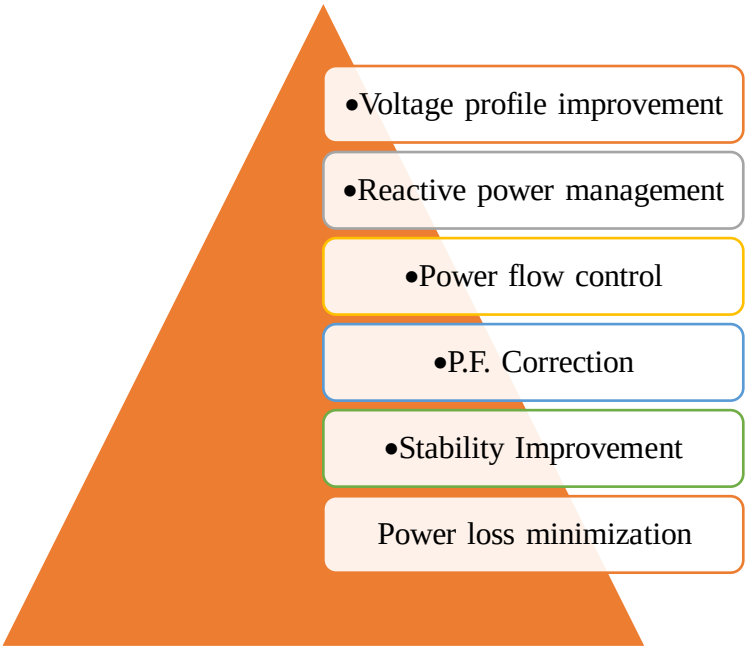

Fig. 1.7 Advantage of Optimal Placement of Shunt Capacitance

1.6.6 Placement of AVR

Researchers are still focused on finding the best possible solution to the issue of automatic voltage regulators. This topic is not a recent one, as it has been around for a long time. For instance, in order to maintain a voltage profile that's within the normal limits, power companies should use control units that are equipped with automatic voltage switches. When the duration of the feeding lines is long and the loads are high, the need for a suitable voltage control will be more critical. This is done through the use of automatic voltage regulators. Before they are used, several factors should be considered to ensure that they are optimal.

1.6.7 Placement of DG

In order to improve the performance of the distribution system, distributed generation is commonly used. This type of energy is generated using various non-conventional sources. Distributed generation units range from 1 kW to 1 MW. Distributed generation consists of various types of generators, such as wind, solar, tidal, biomass, diesel, and geo-thermal etc. Researchers classified the DG as shown in Fig. 1.8

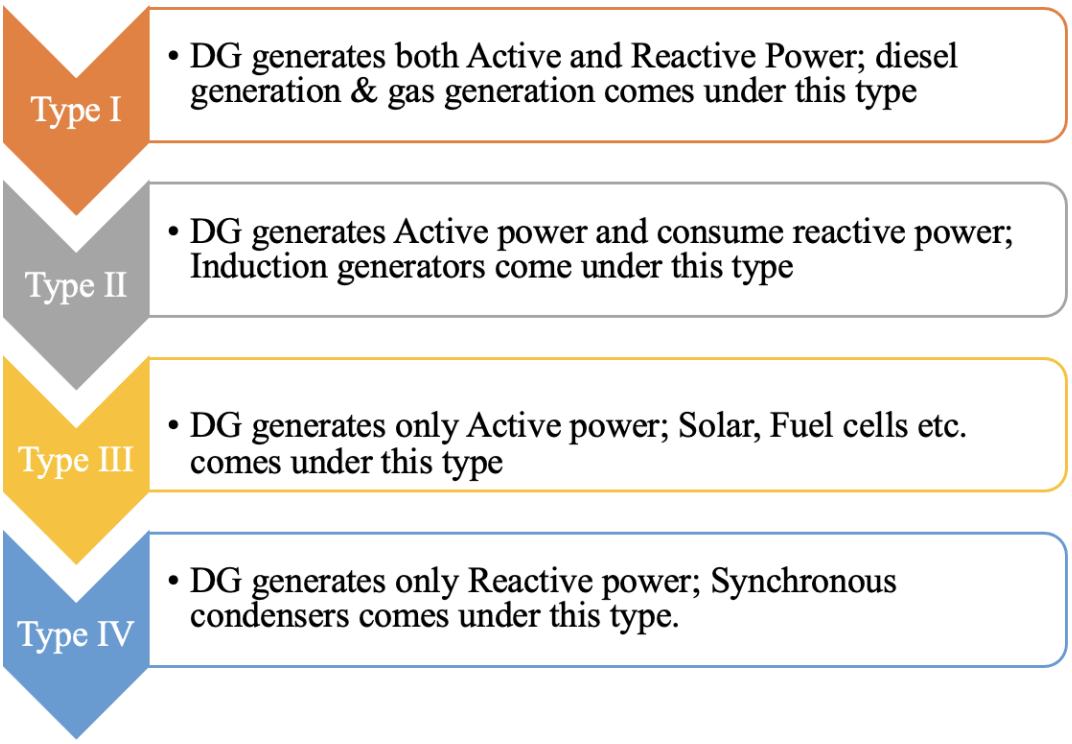

Fig. 1.8 Classification of DG

The advantages of DG Placements are presented in Fig. 1.9

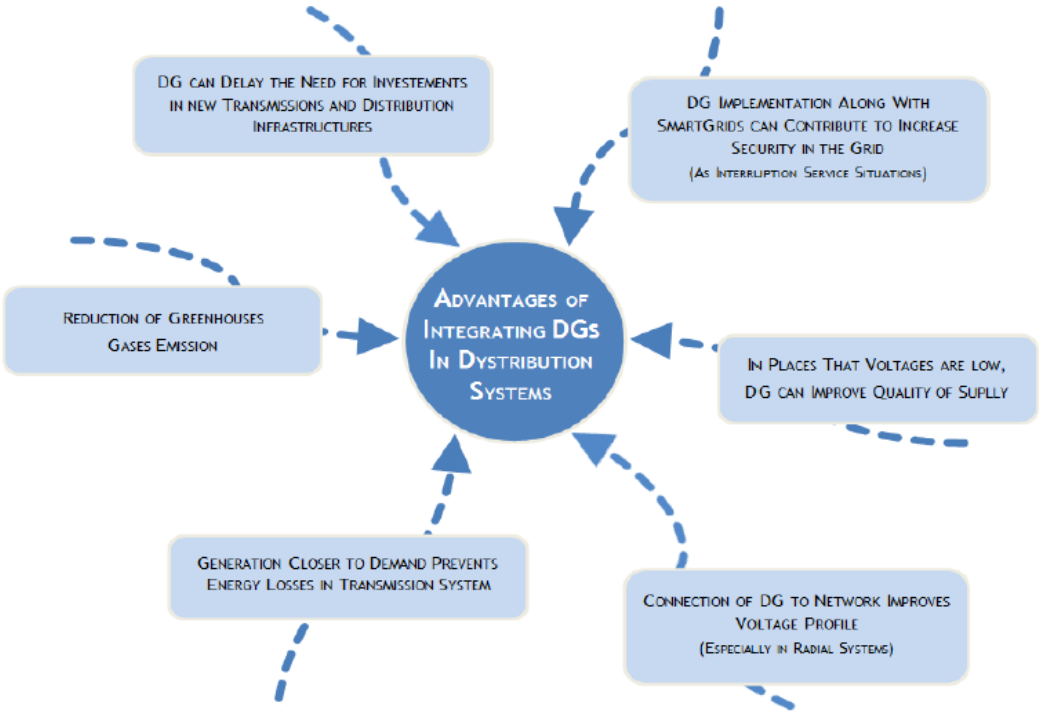

Fig. 1.9 Advantages of DG Placement

The optimal location of distributed generators is a complex optimization issue that involves considering various technical and environmental constraints. This can be done through the development of a strategy that takes into account the various factors that affect the system's performance. One of the most important factors that can be considered when it comes to the optimization of distributed generation is the size and location of the generators. The optimal performance index of DG depends on its location, size, and penetration level. Since this problem is non-convex and nonlinear, it cannot be solved using standard mathematical techniques.

1.7 Motivation

The rapid growth of the global economy and the increasing energy demands of the population have resulted in a significant increase in the energy consumption. This is met through the use of various conventional energy sources such as gas, coal, and oil. However, burning fossil fuels has a negative environmental impact. It is widely expected that the use of fossil fuels for power production will lead to depletion quickly. To address this issue, the international community has started focusing on renewable energy sources such as hydro, wind, solar, biomass, and geothermal. These sources have increased their application in DG systems and are expected to continue contributing to the development of the energy industry. Among the most popular renewable energy sources (RES) is solar photovoltaic (PV). This technology is easy to install and has various advantages, such as its eco-friendliness and accessibility. In 2020, over 760 gigawatts (GWP) of PV systems have been installed, and by 2050, it is estimated that the global PV capacity will provide 11% of the world's energy generation. The rapid emergence and evolution of the photovoltaic (PV) generation industry has been attributed to the increasing number of technological advancements and the lower cost of PV panels. The system is also becoming more integrated into the electricity distribution system. There is a rising number of PV producing stations in developing and industrial countries. In response to the increasing energy consumption, India's government has announced that it will install 100 gigawatts of solar photovoltaic power generation capacity by 2022.

The increasing gap between the demand and supply of electricity has an impact on the distribution network's performance. This issue can be solved by incorporating renewable DG technologies and sources. Besides reducing fossil fuel consumption, the

network can also benefit from other factors such as insulation and life deterioration. Harmonic distortion is a common issue that affects the stability of electrical systems. It is therefore important that the integrated DG is properly maintained. However, if it is not integrated properly it could cause problems such as overheating.

A simple PV array and the utility grid are shown in Figure 1.6 as components of a PV system. The array's performance is affected by environmental factors such as air temperature and sun radiation. The electronic converters that are used to connect the array to the grid are also shown in Fig. 1.6. The integration of a PV system with the electric grid is one of the most challenging factors that can affect the performance of this type of system. This is why it is important that the control schemes of electronic converters are designed to address these issues.

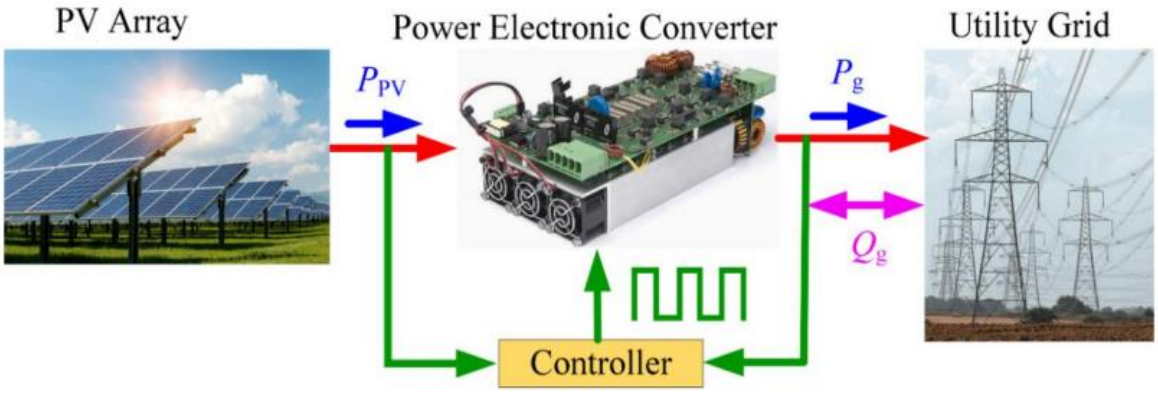

Fig. 1.10PV System with Grid Connected Mode

Overview PV systems are presented in Fig. 1.11. The photovoltaic systems have two power components: a DC-DC converter and an inverter. Because of its built-in DC-DC converter, PV panels are capable of maximum power point tracking (MPPT). The DC-AC inverter serves a dual purpose, adjusting the voltage of the intermediate DC bus and injecting alternating current (AC) into the power grid. However, the additional DC-DC stage in double-stage grid-connected PV systems results in lower efficiency, greater size, and higher cost. A single-stage grid-tied PV system has a more complex control architecture because a single controller must perform all controls, such as MPPT control, DC voltage regulation, and grid current regulation. High efficiency, economy,

and minimum cooling demands are some of the advantages of single-stage grid-connected PV systems.

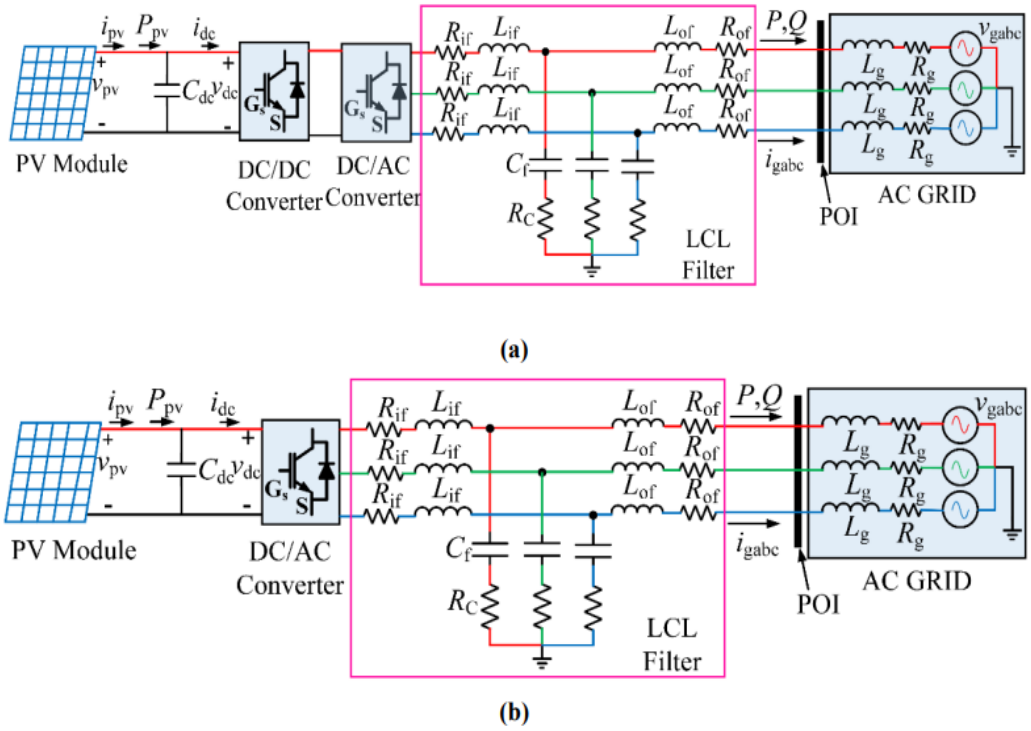

Fig. 1.11(a) A two-stage grid-connected PV system, and (b) a single-stage grid-connected PV system.

As the amount of PV yield increases, the control scheme for this sector will face various challenges. These include maintaining the power quality of the system, ensuring that the grid is stable, and preventing voltage fluctuations caused by unintentional islanding. The efficiency of a PV system is very important when it comes to providing electricity to the grid. There are various problems that can affect the quality of power that a PV system provides. Some of these include the frequency fluctuations and harmonics in the currents. The power quality of a PV system can affect its efficiency and production. In addition to higher line losses, it can also lead to various other issues such as reduced product quality and shorter lifespans of equipment. To avoid these issues, it is important that the system is regularly monitored and maintained according to international standards.

Increased utilization of nonlinear loads in the distribution grid, the issue of harmonic distortion has become a major concern for PV systems. One way to improve

the power quality is by minimizing the distortion caused by this equipment. The switching behavior of power electronic converters can affect the current being generated by a PV system. This issue can cause the harmonics in the current to increase. This can cause power fluctuations and grid overloading. The harmonics can interrupt the protection circuit of a PV system, which could lead to an unintentional disconnection from the grid. This issue can affect the stability and energy losses of large-scale PV systems. Another issue that can cause the failure of a grid-tied device is the broad range of impedance. It becomes harder to limit the amount of harmonics in the current injected by a PV system. To meet the latest standards for harmonics, a robust mechanism for regulating the current is required.

The quality of power supplied to PV systems is one of the most critical issues that utilities face when it comes to regulating the electricity supply to their customers. Most of the time, voltage spikes and dips are caused by the large capacitor switching that occurs in the system. Due to the importance of these systems to the grid, they have developed new grid codes. Previously, it was common for PV arrays to disconnect from the grid and reconnect once the issue was resolved. Unfortunately, this method would lead to higher power loss due to the increased power penetration of PV. To avoid this issue, systems should maintain a connection to a grid-tied inverter. They should also have LVRT capability to operate under grid faults. The control system of a PV system should be able to keep the power quality constant while maintaining the LVRT requirements in the grid fault mode. This is done through the use of MPPT and reactive electricity.

Many international organizations develop grid codes to help utilities manage their interactions with the electric power system. These codes are used to monitor various aspects of the electric power system, such as fault ride-through and islanding detection. A grid-connected photovoltaic system should be able to provide adequate power to the grid while also meeting the needs of its users. This can be done through the use of system rating specifications that limit the available reactive and active power. Having a method to calculate these limits can help with regulation schemes.

1.8 Overview of DG technologies

1.8.1. DG technology

Distributed-generation (DG) systems can connect to the grid using induction or synchronous generators. These are commonly used for various types of power equipment, such as gas turbines, internal combustion engines, and solar thermal and biomass generators. In micro and wind power plants, induction generators are commonly used with DG. These are also utilized in fuel cells and solar photovoltaic systems[42]–[45].

1.8.2 Internal Combustion Engines

Internal combustion engine (ICEs) are devices that convert the heat from a burning fuel into rotary motion. They then drive generators.

One of the most common types of generators used for DG is an ICE. They are generally cheaper than other technologies, and they can be used in various applications such as emergency power supplies and standby generators. In addition to their low capital cost, they also provide good operating reliability and are capable of starting up quickly in case of a power outage.

ICE usage is hindered mainly by high fuel and maintenance costs, as well as their higher NOX emissions than other DG technologies.

1.8.3 Gas Turbines

A gas turbine is a type of power-generating unit that uses the rotational energy of a gas to produce electric power. It comprises a combustor, a turbine-generator, and a compressor.

A gas turbine can be used in various applications, such as power generation and combined heat and power. The small industrial gas turbines are commonly used in applications that require high temperature steam. Compared to reciprocating engines, gas turbines are relatively less costly to maintain. They also emit lower NOX emissions than their combustion counterparts.

1.8.4 CCGTP Plant

It uses a combination of gas turbine and water boiler to produce steam. The water then flows into the boiler and the exhaust gas, which then exchanges energy with the water. The steam then expands and produces shaft work, which is used to generate additional electric energy.

This process is commonly referred to as a combined cycle power plant. The efficiency of this type of power plant is very high, but it is not commonly used in installations with a capacity of less than 10 MW.

1.8.5 Solar Photovoltaic

It converts solar light to electricity using the semiconductor devices. These eco-friendly systems are easy to use and can be powered by either solar light or a battery. They are also very low in emissions and require no additional fuel. However, they require a lot of space and the initial cost is high. The Schematic Diagram of PV system is presented in Fig. 1.12

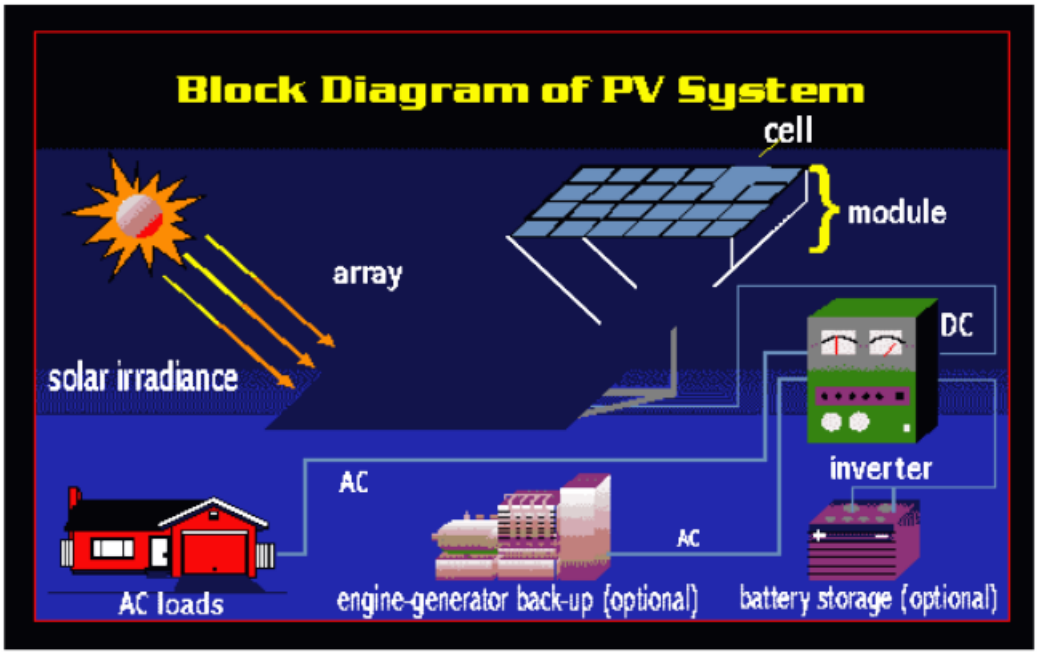

Fig. 1.12Photovoltaic system Schematic diagram

1.9Challenges in Distribution Grid Operation

The efficient and reliable distribution of electricity is a major challenge in the distribution grid operation the major challenges are presented in Fig. 1.13.

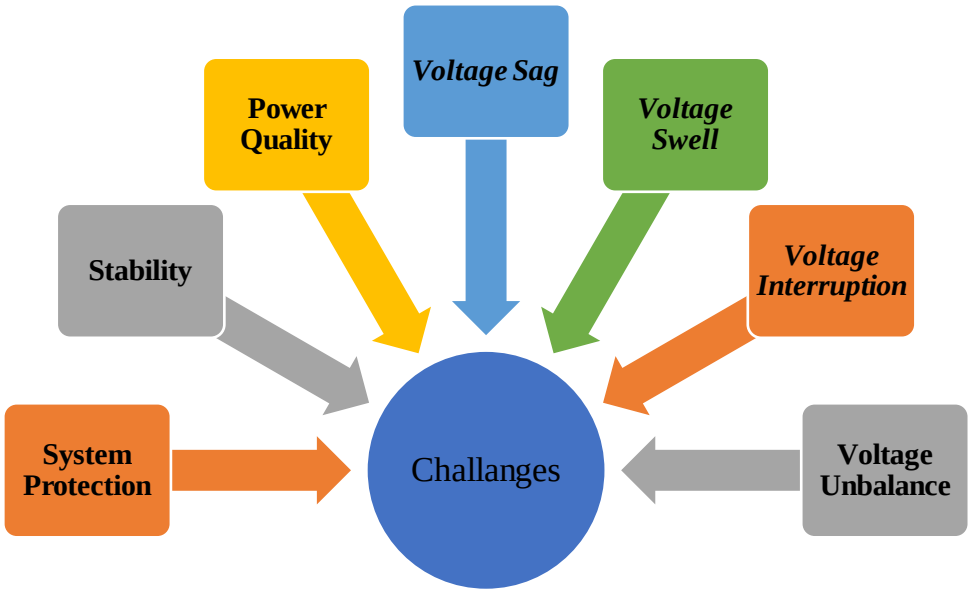

Fig. 1.13 Challenges in Distribution Grid Operation

The flow diagram for the power quality problems are presented in Fig. 1.14.

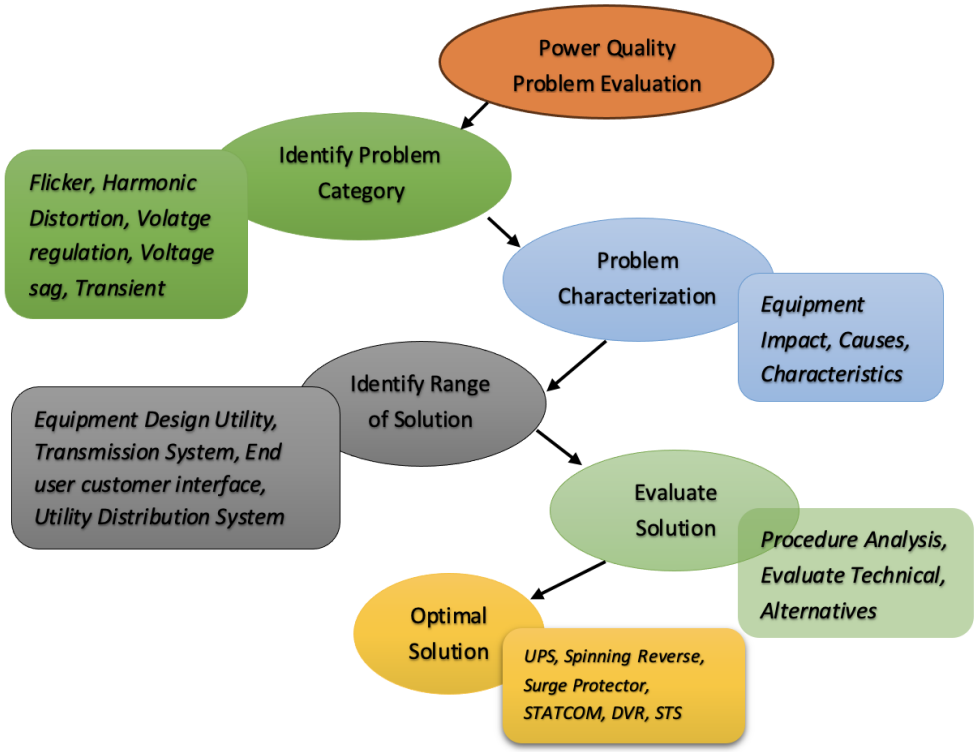

Fig 1.14. Flow diagram for the evaluation of power quality problems

The sources of power quality issues are presented in Fig. 1.15.

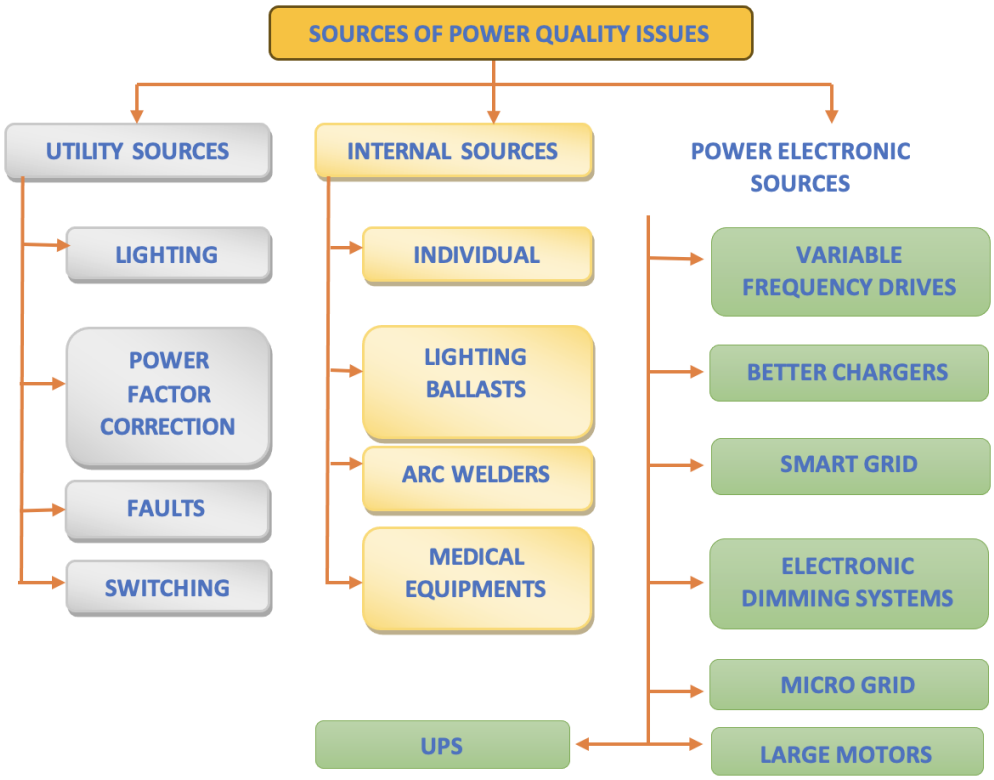

Fig. 1.15 Sources of power quality problems

The power quality monitoring techniques are presented in Fig. 1.6.

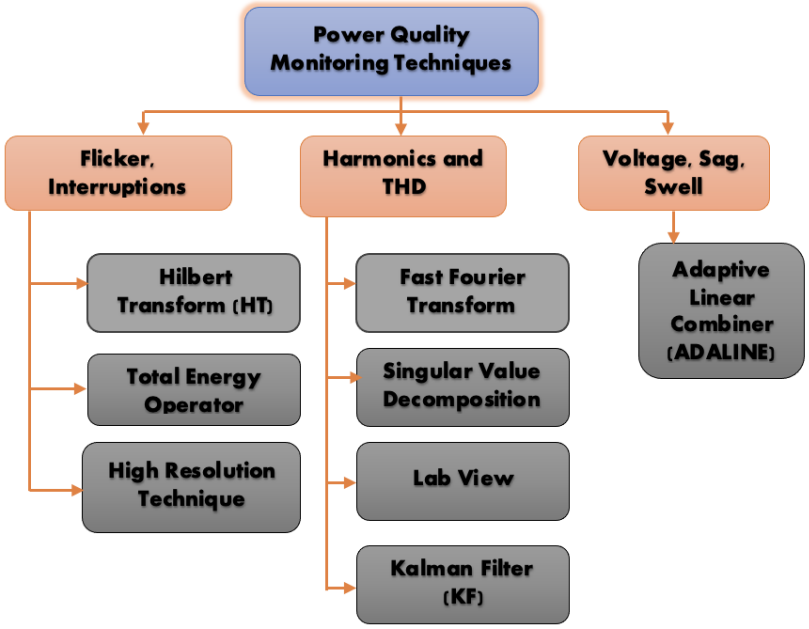

Fig. 1.16 Power Quality Monitoring Techniques

Problems of power quality disturbances are presented in Fig. 1.17

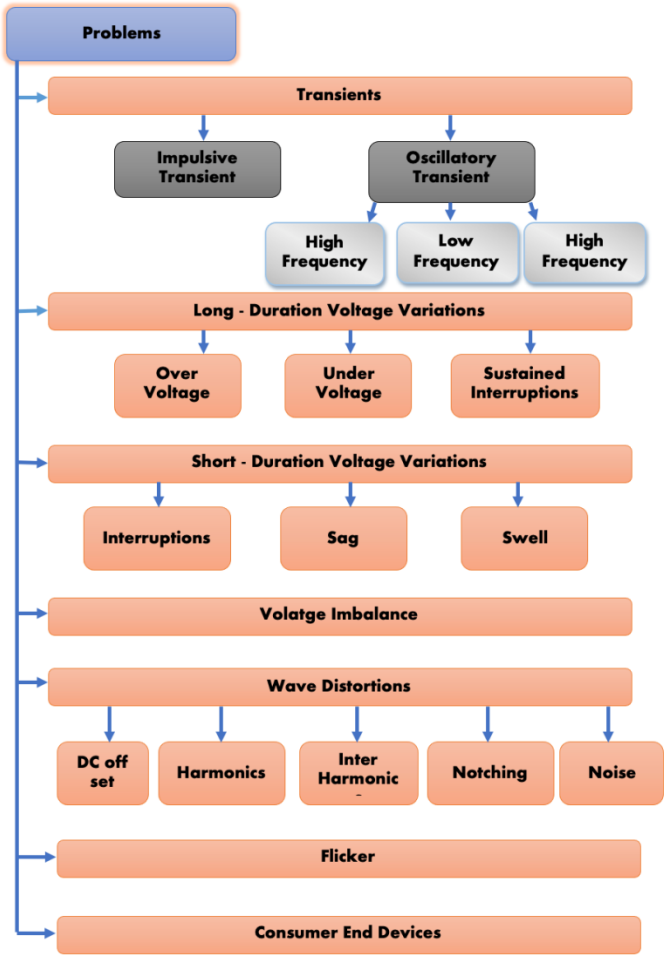

Fig. 1.17 Problems of power quality disturbances

1.10Global PV Potential

In 2022, the global PV market continued to grow, reaching a total capacity of 1 185 gigawatts (Gw). Despite the various factors that affected the industry, such as the post-covid price hike and the political conflicts in Europe, the PV sector is still expected to continue contributing to the reduction of greenhouse gas emissions and electricity costs. The Chinese market continued to grow at a robust rate, adding over 106 gigawatts of new capacity, more than twice as much as that of Europe. This impressive growth follows the previous years' achievements, when the country's PV market grew by over 54 gigawatts in 2021 and 48 gigawatts in 2020.The Indian market continued to grow at a fast pace, with a total capacity of 18,1 gigawatts, which is mainly concentrated in centralised systems. Other regional markets such as Australia and Korea also contributed to the industry's growth.

The Japanese market continued to grow, with a total capacity of 6,5 gigawatts, unchanged from the previous year. The European PV market continued to grow at a strong pace, with a total capacity that reached 39 gigawatts. Some of the major countries that contributed to this region's growth were Germany, Spain, Poland, and the Netherlands. Due to the high electricity prices, several countries have enacted policies to accelerate the PV industry.

The US market contracted during the year, as various factors such as grid connection backlogs and trade issues affected the industry. On the other hand, Brazil's PV market experienced a robust growth rate, adding 9,9 gigawatts during the year.Several countries, including Spain, Greece, and Chile, have over 10% penetration rates. Despite the challenges that grid congestion has presented, various technological solutions and policies have been implemented to address this issue.

Although individual markets are sensitive to policy support, it is shifting toward indirect measures to address issues such as grid congestion or accelerating permitting. China's increasing concerns about the upstream supply chain have prompted several initiatives to support local manufacturing. In 2022, two-thirds of the new renewable energy capacity added in the electricity sector was powered by PV, which helped reduce the annual CO2 emissions by over 50%. This is an important contribution to the reduction of greenhouse gas emissions, as it accounts for around 10% of the total heat and electricity sector emissions. As the industry continues to develop, it is positioned as one of the leading solutions to address climate change.

1.11Global Wind Potential

The year 2022 was the third-best year for new capacity additions, with 78 gigawatts being added globally. The global installed capacity reached 906 gigawatts during the year. This represents an annual growth rate of 9%. It is expected that the world will add over a hundred gigawatts of new capacity in 2023, which would be a record for any year. According to the GWEC Market Intelligence, the year-on-year growth rate is expected to be 15%. The GWEC Market Intelligence projects that the global installed capacity will reach over 680 gigawatts by 2027.The firm's outlook for the next decade is positive, with an additional 143 gigawatts expected to be added by

2030. It previously estimated that the world would build over 1078 gigawatts from 2022 to 2030. This estimate has been increased to 1221 gigawatts by 2030.

The rapid emergence and evolution of the wind industry will be a crucial factor that will determine the global energy supply and climate change. This year, wind energy is expected to reach the milestone of 1 trillion installed capacity. Despite the challenges that it has faced, the next generation of wind energy will be able to meet the needs of the world's largest economies. The policies that are being pursued by the major economies in both the West and the Global South are expected to support the development of new renewable energy sources. The goal of these policies is to bring about 2 TW of new wind energy capacity to be installed by 2030. They are driven by various factors, such as the increasing urgency to address climate change, the high prices of fossil fuels, and the success of the wind industry in scaling up.

Despite the industry's rapid emergence and evolution, the last few years have been very challenging for the wind industry. Due to the policies introduced by the government, many of the manufacturers have experienced financial losses. These include the implementation of race to the bottom pricing policies, as well as the high logistics and inflation costs. The various projects that have been launched in the past few years have been delayed or stopped due to the lack of proper licensing and permitting rules. This has created a bizarre paradox regarding the energy markets' rewarding of fossil fuel companies with huge profits while renewable energy firms have struggled to breakeven. The report indicates that despite the various factors that have affected the wind industry, the market has continued to stall. In 2022, the industry only recorded a total of 77.6 gigawatts of new wind energy capacity.

Despite the significant progress that has been made in addressing the climate and energy crises, the world's policymakers still have a long way to go to meet their goals for wind energy. In 2023, the start of a new era will see a significant increase in the number of wind turbines installed. The US enacted the Inflation Reduction Act, which significantly changed the rules for both offshore and onshore wind. In the EU, policymakers are working on introducing new regulations to support the rapid deployment of renewable energy. In China, the country's rapid economic growth is expected to continue as COVID-19 restrictions are lifted. Despite the significant progress that has been made in addressing the climate and energy crises, the world's

policymakers still have a long way to go to meet their goals for wind energy. In 2023, the start of a new era will see a significant increase in the number of wind turbines installed. The US enacted the Inflation Reduction Act, which significantly changed the rules for both offshore and onshore wind. In the EU, policymakers are working on introducing new regulations to support the rapid deployment of renewable energy. In China, the country's rapid economic growth is expected to continue as COVID-19 restrictions are lifted.

Several economies, such as the Philippines and Vietnam, are expected to increase their wind energy production. India is also expected to gain momentum as it continues to develop its wind energy industry. The Global Wind Energy Council (GWEC) is forecasting that by 2024, the world will have installed over a hundred gigawatts of onshore wind turbines. On the other hand, it is expected that the number of offshore wind turbines will reach 25 gigawatts in 2025.The global wind energy market is expected to change due to the competition and the need for more robust supply chains. This will require the establishment of the next generation of Wind Energy Supply Chains. According to Ben Backwell, the most important factors that will determine the success of the industry are the availability of capital and the efficiency of regulators. The global power equipment market is expected to change due to the lack of supply chain capacity. This will affect the demand for various equipment, such as wind turbines and power transmission equipment.

Wind energy is expected to meet the needs of society and policymakers at large, and it is crucial that the industry begins investing in new plants and training programs now. Failure to do so could threaten the industry's ability to deliver on its promises and lead to policymakers resorting to other less efficient alternatives. Despite the current economic conditions, the wind energy industry is still expected to grow. Despite the obstacles that it has faced, the leaders of the industry are still optimistic about the future. They have already started investing in new facilities. Wind energy needs new partnerships with other organizations such as governments, investors, and customers to drive its next generation of growth. In order to secure the necessary policies, the wind industry and its partners need to work together. Together, we can create a framework that will allow the industry to attract trillions in investments and create millions of jobs. The Wind Energy Industry has to adopt a new mindset in order to keep up with the

changes brought about by the energy transition. It is no longer the hobby industry it was 40 years ago, and its technology is now mature and resilient. To ensure that the industry can deliver on its promises, it needs to have a strong and confident confidence in its ability to move forward.

1.12 Chapter Summar

In this chapter, introduction to distribution system is presented, background is presented. Types of DGs are presented. A Para-diagram of distribution system is discussed. Distribution system losses are discussed. Distribution system performance improvement methods are presented. Distribution system advantages are discussed. Finally, motivation for research and DG technology is presented.

CHAPTER 2

LITERATURE REVIEW, RESEARCH OBJECTIVE AND METHODOLOGY

2.1 Literature Review

A distribution system is a network of interconnected equipment that connects the transmission and generation systems. It is designed to provide efficient and effective control of the various functions of the system. The configuration of this system is usually done radially. The optimal distribution system design requires the use of suitable methods. In order to operate continuously, the system's efficiency should be improved and its operating costs minimized.

To minimize the losses, voltage index should be improved, the line loading should be reduced, and the power losses should be minimized. Various factors such as the reconfiguration of the feeder system, the placement of Capacitors, and the use of DGs are also required to achieve this. The objectives can be presented as single or multi-objective problems. The field of optimal distribution has been continuously studied and updated in recent years. The goal of this research is to improve the efficiency of the system and reduce the power loss. The objective of optimizing the distribution system is to find the optimal topology that is appropriate for its various determinative factors. These include power shortages, operating efficiency, and energy demand.

2.1.1 Optimal Placement of DG in the Distribution System

Distributed generation (DGs) are the energy sources that are utilized at the distribution level. The increasing power demands caused by the growing population and the development of new facilities are forcing the need for more power generation. Installing DGs is the ideal solution to meet these demands. Installing DGs in the distribution system can improve the technical performance of the system by reducing the power loss and improving the voltage profile. However, this process can be very complex and time-consuming. To effectively integrate these into the system, the optimal allocation of resources is required.

In [46] proposed IEO (Improved Equilibrium Optimization) method for determining the allocation of DGUs in a distribution system. This will reduces the total power loss and enhance the system's efficiency. In [47] presented a classification method that can be used to determine the optimal placement and size of DSTATCOMs, EVCSs, and DGUs in 69-bus radial distribution networks. In [48] proposed the use of the classification method for placement of DGUs in a radial distribution network. It takes into account the design and construction of these generators that are powered by wind and PV cells. The study of wind and PV generation is carried out in this system according to the wind velocity and radiation data.

In [49] presented an optimized offshore wind farm placement and sizing on IEEE33 model bus. The multi-objective approach developed for this study includes the size constraints and location of the farms. In [50] a study was carried out to find out how distributed generation could be used to improve the quality of power in Onitsha's distribution line network. The recent studies on optimal placement of distributed generation is presented in Table 2.1

Table 2.1 Recent studies on optimal placement of distributed generation

Reference	**Objective/Method**	**Test System**	**Year**
[51]	Graph Based Approach	--	2024
[52]	Multi Objective Optimization	--	2024
[53]	The work proposes two strategies, one is bi-directional change in the current, the second is active power sensitivity analysis.	--	2021
[54]	Active distribution network & several soft open points	IEEE 33 Bus system	2021
[55]	Artificial gorilla troops optimizer (GTO	IEEE 69 & Egyptian	2022

		distribution grid of 30 bus system	
[56]	Mixed-integer linear programming	IEEE 33 Bus system	2022
[57]	Spider monkey optimization	IEEE 33 Bus system	2022
[58]	Harris Hawk Optimization Algorithm	--	2022
[59]	Artificial ecosystem optimizer	59-bus Cairo distribution system	2022
[60]	Pareto dominance-based hybrid methodology	118 radial bus system	2022
[61]	Gorilla troop's optimizer	94 bus system	2022
[62]	Genetic Algorithm & Fuzzy inference system	6 bus radial system	2021
[63]	Honey Badger Algorithm	IEEE 69 Bus system	2022
[64]	Barnacles Mating Optimization	--	2022
[65]	n-1 criterion	IEEE – 33 & 69 Bus system	2021
[66]	Dandelion Optimization Algorithm	IEEE – 33 Bus system	2022
[67]	Hybrid Fuzzy-Metaheuristic Strategy	IEEE – 33 & 69 Bus system	2022
[68]	Data-driven multi-objective optimization	33 Radial Bus System	2022
[69]	NSGA-III algorithm	--	2022
[70]	Modified Flower Pollination Algorithm	IEEE – 33 & 69 Bus system	2022
[71]	Coyote algorithm	69& 119node systems	2021

[72]	Metaphor-less based AI technique	IEEE – 33 Bus system	2021

2.1.2 Optimal Placement of Solar PV in the Distribution System

The optimal placement of photovoltaic installations is a complex process that involves taking into account various factors. In [73] presented a novel Bi-level MO approach for planning the placement of solar photovoltaic-battery storage systems in the Smart Grid distribution system. In [74]explores the various effects of solar radiation on the load conditions of the electricity distribution system. It also covers the changes in load conditions caused by the PV placement and size. In [75] proposed a method that aims to reduce the losses and improve the bus voltages in the electricity distribution system by implementing a distributed generation system (DG). This method involves the use of small renewable energy sources such as solar PV and wind. The recent studies on optimal placement of Solar PV in the distribution system is presented in Table 2.2

Table 2.2 Recent Studies on Optimal Placement of Solar PV in the Distribution System

Reference	Objective/Method	Test System	Year
[76]	Local search optimization	IEEE 9 bus system	2022
[77]	Modified analytical approach	IEEE 33 bus system	2021
[78]	Genetic Algorithm	IEEE – 33 & 69 Bus system	2023
[79]	Genetic Algorithm	IEEE – 33 & 14 Bus system	2021
[80]	GA & GIS	IEEE 33 bus system	2020
[81]	Communal spider optimization algorithm	69 & 15 Bus system	2022
[82]	Multi objective grey wolf optimization	IEEE 123 bus system	2022

[83]	GIS & Optimization, Integration	--	2014
[84]	Genetic algorithm With Newton-Raphson approach	162 bus system	2018
[85]	Genetic Algorithm	--	2018
[86]	Stochastic planning	IEEE 34 node feeder	2019
[87]	Operational planning model	IEEE 15 & 33 bus system	2023
[88]	COVID-19 herd immunity algorithm	IEEE – 33 & 69 Bus system	2023
[89]	FPA Pareto optimal algorithm	51 & 85 bus systems	2022

2.1.3 Optimal Placement of Wind in the Distribution System

Optimal placement of Wind generator in the distribution system improves the performance. In [90] proposed an optimization method that can be used to determine the optimal location and sizing of SMESs and WTGs in a distribution system. It utilizes an efficient algorithm known as EO along with a loss sensitivity factor. In [91] proposed a method that combines the data clustering and optimization techniques to determine the optimal location and sizing of wind farms in a radial distribution system. In [92] presented a framework for optimizing wind turbine installations, taking into account their reactive power capacities, wind speeds, and their demand curves. The recent studies on optimal placement of Wind in the distribution system is presented in Table 2.3

Table 2.3 Recent Studies on Optimal Placement of Solar PV in the Distribution System

Reference	**Objective/Method**	**Test System**	**Year**
[93]	Linear Optimization and Wind speed modelling	--	2017

[94]	Self-sorting analytical approach	IEEE 14 bus system	2022
[95]	Flower pollination algorithm	--	2021
[96]	Genetic Algorithm	IEEE – 33 & 69 Bus system	2015
[97]	Active and Reactive power dynamic modeling of wind generator	33 bus system	2018
[98]	Grey Wolf Optimization	IEEE 30 bus system	2023
[99]	Wind plant wake analysis	IEEE – 28 & 69 Bus system	2020
[100]	Particle Swarm Optimization	IEEE – 16 & 30 Bus system	2017
[101]	Clayton-Copula method	IEEE 57 bus system	2017

2.1.4 Optimal Placement of Solar PV and Wind in the Distribution System

Combined Optimal placement of Solar PV & Wind generator in the distribution system improves the performance. The recent studies on optimal placement of Wind in the distribution system is presented in Table 2.4

Table 2.4 Recent Studies on Optimal Placement of Solar PV and Wind in the Distribution System

Reference	**Objective/Method**	**Test System**	**Year**
[102]	Matrix mothflame algorithm	IEEE 33 bus system	2020
[103]	Quantum particle swarm algorithm	IEEE 33 bus system	2017
[104]	Particle swarm algorithm	IEEE – 15, 33 & 69 Bus system	2013

[105]	Ant Lion Optimizer	IEEE 33 bus system	2022
[106]	Artificial gorilla troops optimization	IEEE – 33 & 69 Bus system	2023
[107]	Moth Flame Optimization	--	2019
[108]	Manta ray foraging optimization	IEEE 118, 15, 51 bus system	2021

2.2 Research Gap from the literature

"In most of authors Solved DG allocation problems effectively in RDS and produced some results but they have certain limitations such as

1. Several researchers state that Distributed Generation (DG) serves as an active power generation source in Radial Distribution Systems (RDS). From an operational perspective, these sources also supply reactive power in wind energy systems. However, many studies have not considered the placement of DG units that inject both active and reactive power, which could yield better results by reducing power losses. [51]-[72]
2. Most researchers have not addressed the uncertainties associated with solar and wind-based DG in RDS. [102]-[108]
3. The majority of the studies have been conducted on standard IEEE test systems. However, there has been limited research on Indian real-time test systems. [51]-[108]
4. The studies primarily focus on linear loads, with only some addressing nonlinear loads. Different load types, such as residential, commercial, and industrial loads, have not been separately analyzed. [51]-[108]
5. Researchers have mainly concentrated on solar-based DG systems and have not focused on the integration of solar and wind DG systems to achieve reduced power losses, minimized voltage deviations, and improved voltage stability. [102]-[108]
6. Researchers have not extensively explored the reduction of harmonics in RDS through proper DG allocation. [51]-[108]

7. Total Harmonic Distortion (THD) has not been calculated for Indian real-time test systems in many studies. [51][108]

2.3 Research Objectives:

To do this, we took up several different kinds of DERs to the DS and analyse how they function together.

1. The study models the uncertainty associated with solar and wind-based sources. Several DS-related restrictions are also considered. A detailed stochastic mathematical model is constructed to take into consideration the load's unknowns and the intermittent nature of renewable energy sources like wind and solar. A stochastic optimisation approach and mandatory buffers are employed to deal with the unpredictability.
2. The optimal placement of solar-powered DGs in DS is proposed to cut down on power loss, voltage swings, and THD.
3. Power loss, voltage variation, and total harmonic distortion are all reduced with optimal integration of wind-based DGs in DS. By analysing the predicted operational costs and system security of a reference microgrid, we find that DER coordination leads to significant savings. More can be done to lessen the impact of the unfavourable outcomes associated with the anticipated power dispatch of controllable generators and hourly unserved electricity by concerted probabilistic efforts.
4. Solar and wind power, as well as other renewable energy sources, can be integrated into the DS in a way that minimises power loss, voltage variation, and total harmonic distortion."

2.4 Research Methodology:

A distributed generation system can enhance the voltage profile of a distribution network and reduce power losses. It can also boost the amount of power that the cables and transformers can deliver. When deployed, these generators utilize reactive power to address power losses. However, distribution networks need to be carefully planned for when it comes to the placement and size of distributed generation (DG) installations. The fundamental objective of this work is to optimise the voltage profile and minimise real power losses by deciding where and how much distributed generation should be put. Installing distributed generation units in less-than-ideal locations, or with smaller

capacities than necessary, can cause a number of complications. The costs of doing business are impacted by problems including voltage flicker, voltage state degradation, system losses, harmonics, and power system stability.

Recent studies have shown that the use of an optimization technique can help in the design and construction of power systems by identifying the optimal location and amount of distributed generation to be installed in a given distribution network. Artificial bees, ant colonies, and particle swarm optimization are some of the algorithms that seek to mimic the intelligence of insects in nature. The appropriate capacity and location of DG have been the subject of extensive research efforts on a global scale, employing a wide variety of optimisation techniques. The Firefly Algorithm was shown to offer promise in reducing system-wide power losses on an IEEE 28 bus test system by improving the size and position of DG. In simulations, the proposed method resulted in less power loss.

In this work Particle Swarm Optimization with Differential Velocities (PSODV) algorithm is proposed. The proposed algorithm is implemented on a Indian 28 and IEEE 85 bus system considering solar DG, wind DG, hybrid solar - wind DG and residential, commercial, industrial loads. The optimal bus location, size of DG are calculated and the performance evaluation parameters P_{loss} (kW), V_{min} (p.u.), VSI_{min} (p.u.), % Reduction P_{loss} are evaluated in all the cases. The effectiveness of the proposed Particle Swarm Optimization with Differential Velocities (PSODV) algorithm is evaluated in comparison with Firefly (FF) algorithm and Gorilla Troops Optimizer (GTO) algorithm.

2.5 Organization of Thesis:

Chapter 3: This chapter discusses the Mathematical modelling of solar irradiation and wind turbine speed. This chapter focuses on the development of mathematical models for accurately predicting solar irradiation and wind turbine speed, which are critical for the effective integration of solar and wind Distributed Generations (DGs) in Radial Distribution Systems (RDS)

Chapter 4: In this chapter problem formulation optimization algorithms are presented. This chapter introduces the problem formulation and the optimization techniques used to enhance the integration of solar and wind DGs into RDS. The problem is formulated

as a multi-objective optimization task aimed at minimizing power losses, improving voltage profiles, and reducing Total Harmonic Distortion (THD)

Chapter 5: This chapter presents a comprehensive analysis of the results obtained after integrating solar and wind DGs into RDS. The outcomes are evaluated based on key performance metrics, including power loss reduction, voltage stability, and harmonic distortion minimization.

Chapter 6: This chapter summarizes the key findings of the research and provides insights into the broader implications of integrating solar and wind DGs into RDS. It emphasizes the effectiveness of the proposed mathematical models and optimization techniques in achieving significant power loss reduction, improved voltage profiles, and reduced harmonics.

2.6 Chapter Summary

In chapter detailed literature review on optimal placement of distributed generators in the distribution system is presented. Optimal placement of solar PV in the distribution system is discussed. Optimal placement of wind in the distribution system is discussed. Combined optimal placement of solar PV & wind in the distribution system is discussed. Research gap and objectives are presented.

CHAPTER 3

SOLAR IRRADIATION AND WIND SPEED MATHEMATICAL MODELLING

3.1 Solar Irradiance Load Profiling and Modelling

3.1.1Solar Irradiance Load Profiling

The proposed method uses the load profiles of factories, households, and businesses to simulate the load profile. The load behaviour is described using the consumption curves are presented in Fig. 3.1.

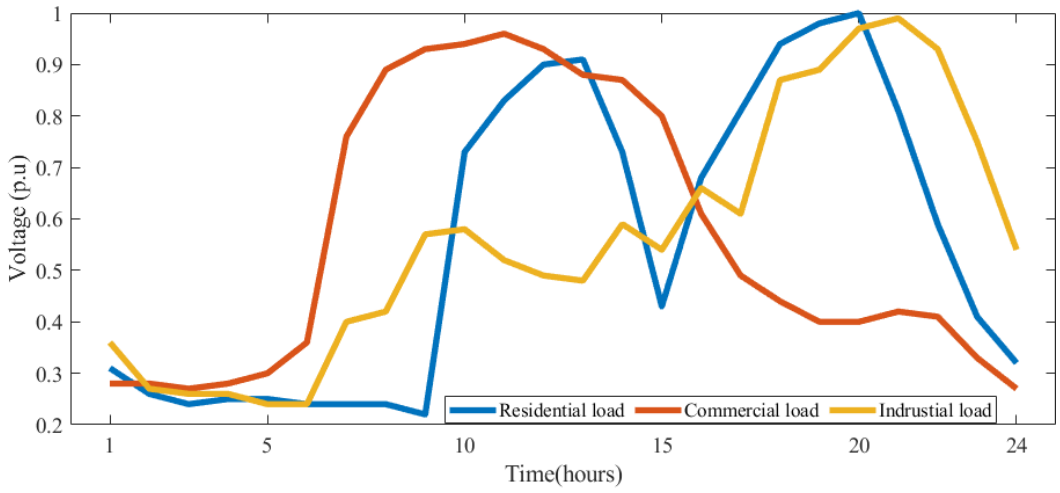

Fig 3.1Load Pattern

3.1.2Solar Irradiance Modelling

The efficiency of solar panels is also affected by their intermittent nature. Compared to other forms of energy, they perform better in bright environments. A quick search for the Beta PDF function revealed its usefulness in calculating solar radioactivity. We used hourly data to compare its standard deviation and average to historical readings[109]–[112].With this solar irradiance is expressed as:

$$f_b(s) = \{\frac{\Gamma(\alpha+\beta)}{\Gamma(\alpha)\Gamma(\beta)} s^{(\alpha-1))}(1-s)^{(\beta-1)} \quad 0 \le s \le 1, \alpha, \beta$$

$$\geq 0 \qquad otherwise$$

$$\beta = (1-\mu)\left(\frac{\mu(1-\mu)}{\sigma^2} - 1\right) \qquad \propto = \frac{\mu\beta}{1-\mu} \qquad (3.1)$$

where gamma is a function and s is solar irradiation (in kilowatts per square metre). Mean () and standard deviation () of s can be used to determine the shape parameters (and). The maximum output can be determined using the formula:

$$P_0(s) = N * FF * V_y * I_y \quad (3.2)$$

PV module output (Po) at solar irradiance (S) is proportional to the square of the number of PV modules (N).

$$FF = \frac{V_{MPPT} * I_{MPPT}}{V_{OC} * I_{SC}} \quad (3.3)$$

$$V_y = V_{OC} - K_v * T_{cy} \quad (3.4)$$

$$I_y = s[I_{sc} + K_v(T_{cy} - 25)] \quad (3.5)$$

$$T_{cy} = T_A + s(\frac{N_{OT} - 20}{0.8}) \quad (3.6)$$

Fill factor (FF), open-circuit voltage (VOC), short-circuit current (ISC), and PV module operating temperature (NOT). T_y is cell temperature, T_A is the ambient temperature.

3.1.3 Solar PV Specifications

The Solar PV Specifications are tabulated in Table 3.1

Table 3.1 Solar PV Specifications

Specifications	Ratings
Solar Panel	220W
Ambient Temperature (Ts)	30.76˚C
Normal Cell operating temperature (N ot)	43˚C
Open circuit Voltage	36.96V
Short circuit current (Isc)	8.38A
Voltage Max. Power point voltage (Vmppt)	28.36V
Current Max. Power point (Imppt)	7.76A
current temperature coefficient (Ki)	0.00545 A/˚C
Voltage temperature coefficient (Kv)	0.1278 V/˚C

3.1.4 Mean and standard deviations of solar irradiance (Kw/m^2) for study period

The Mean and standard deviations of solar irradiance (Kw/m^2) for study period is tabulated in Table 3.2.

Table 3.2 Mean and standard deviations of solar irradiance (Kw/m^2)

Hours	Summer		Autumn		Winter	
	u_s	σ_s	u_s	σ_s	u_s	σ_s
1	0	0	0	0	0	0
2	0	0	0	0	0	0
3	0	0	0	0	0	0
4	0	0	0	0	0	0
5	0.0032	0.0045	0	0	0	0
6	0.1278	0.0406	0.0707	0.0299	0.03	0.0417
7	0.2538	0.0714	0.2177	0.0433	0.1623	0.0463
8	0.3824	0.1189	0.3988	0.0803	0.3741	0.0669
9	0.4908	0.1388	0.5465	0.1121	0.4732	0.0669
10	0.568	0.1659	0.6442	0.1336	0.5831	0.0998
11	0.6164	0.1445	0.6827	0.1492	0.6463	0.1219
12	0.599	0.1175	0.6645	0.1452	0.6496	0.1262
13	0.5614	0.0995	0.5923	0.1282	0.5921	0.1117
14	0.4672	0.0788	0.4731	0.0999	0.4786	0.0838
15	0.3548	0.055	0.3121	0.0635	0.3228	0.0515
16	0.2228	0.041	0.1402	0.0309	0.1609	0.0382
17	0.103	0.0276	0.0057	0.0112	0.0269	0.0372
18	0	0	0	0	0	0
19	0	0	0	0	0	0
20	0	0	0	0	0	0
21	0	0	0	0	0	0
22	0	0	0	0	0	0
23	0	0	0	0	0	0
24	0	0	0	0	0	0

The Expected Output of solar irradiance level for 7, 11, 15 hours at summer, autumn, winter, spring are presented from Fig. 3.2 to Fig. 3.5.

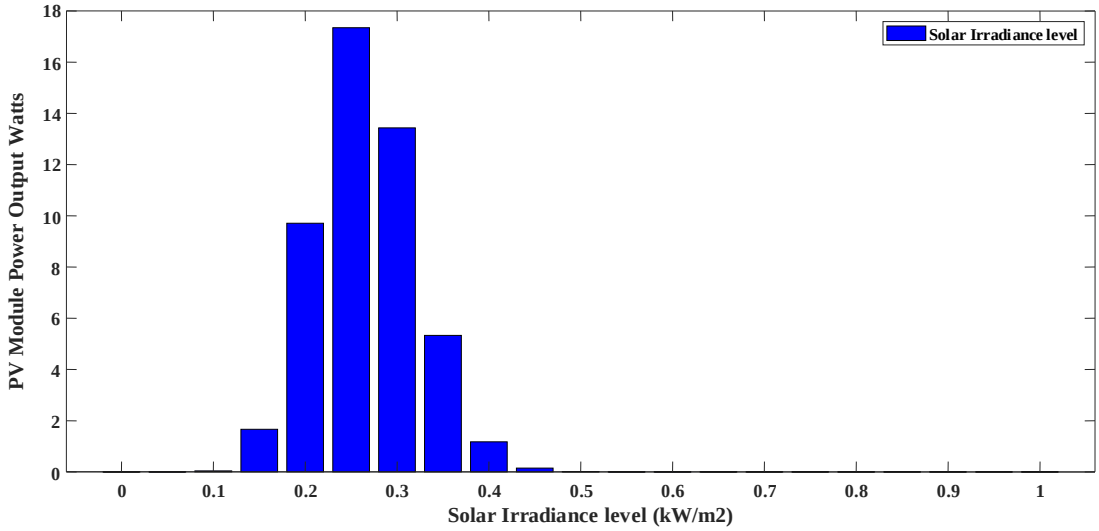

Fig. 3.2 Expected Output of solar irradiance level for 7 hours (summer)

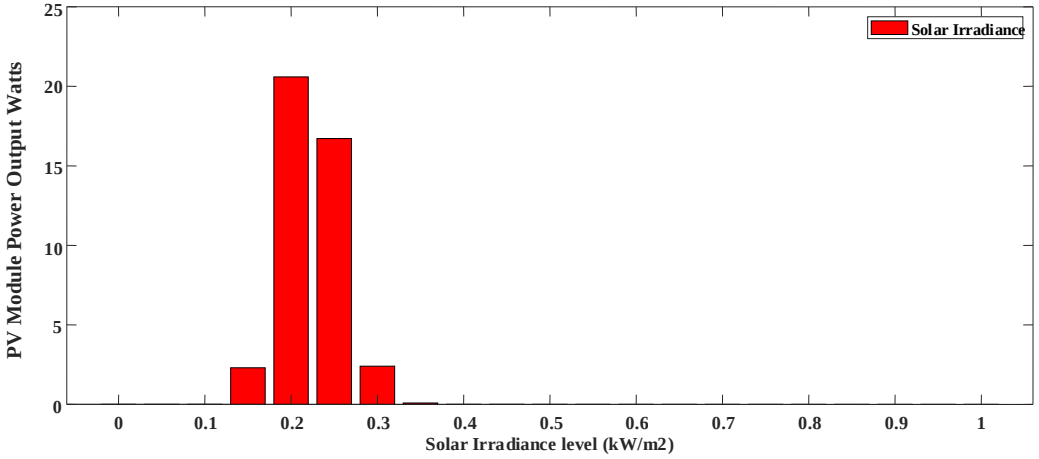

Fig. 3.3 Expected Output of solar irradiance level for 7 hours (Autumn)

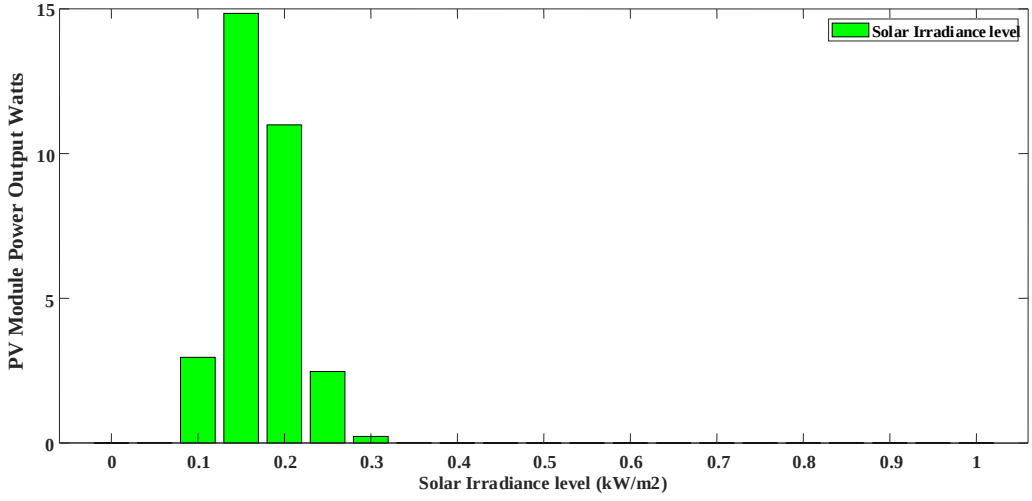

Fig. 3.4 Expected Output of solar irradiance level for 7 hours (Winter)

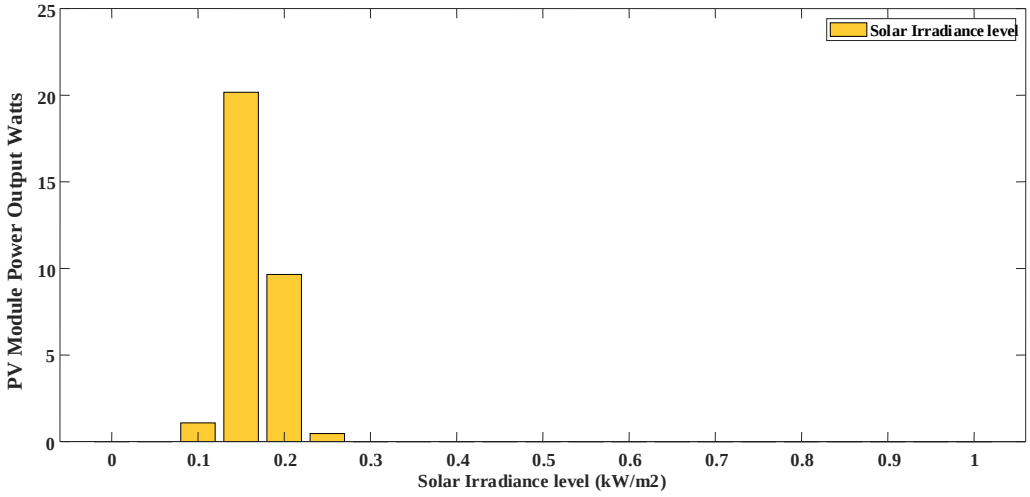

Fig. 3.5 Expected Output of solar irradiance level for 7 hours (Spring)

3.2Modeling of wind speed

In order To explain the uncertain nature of wind speed over a certain time period is selected from liturature[113]–[117]. wind speed segment can be expressed as

$$f_v^t = \frac{k^t}{c^t} * (\frac{v^t}{c^t})^{k^t-1} * exp(-(\frac{v^t}{c^t})^{k^t-1}) \qquad for\ c^t > 1; k^t > 0 \tag{3.7}$$

The values of k^t, c^t are find the below equation

$$k^t = (\frac{\sigma^t}{\mu_v^t})^{-1.086} \tag{3.8}$$

$$c^t = \frac{\mu_v^t}{T(1+{}^1/_{k^t})} \tag{3.9}$$

$$\mu_v^t \ and\ \sigma_v^t \ \ are\ will\ found\ from\ mean\ and\ standard\ deviations$$

Average wind power $P_{WT}^t = \sum_{g=1}^{N_t} PG_{WTg} * P_v(v_g^t)$ (3.10)

Power generation of wind turbine power performance can be explained as

$$PG_{wtg}\begin{cases} 0 & v_{ag} < v_{cin} \quad or \quad v_{ag} > v_{cout} \\ (a * v_{ag}^3 + b * P_{rated}) & v_{cin} \le v_{ag} \le v_N \\ P_{rated} & v_N \le v_{ag} \le v_{cout} \end{cases} \tag{3.11}$$

$$P_{rated} = \ maximum\ power\ output\ \ and\ a, b\ are\ constants$$

$$v_{cin} \quad is\ cut\ in\ wind\ speed\ v_N\ normal\ wind\ spedd$$

3.2.1Specifications of wind

The Wind Specifications are tabulated in Table 3.3

Table 3.3 Wind Specifications

Description	Specifications	Ratings
Wind Turbine	Wind Turbine power rating	3000kw
	Cut -in speed	3.5m/s
	Cut-out Speed	25m/s
	Hub Height	66m
	Rated Speed	15m/s

3.2.2.Mean and standard deviations of Wind speed for study period

The Mean and standard deviations of wind speed for study period is tabulated in Table 3.4.

Table 3.4 Mean and standard deviations of wind speed

Hours	Summer		Autumn		Winter	
	u_s	σ_s	u_s	σ_s	u_s	σ_s
1	9.9	0.7937	3.9667	2.5146	2.1333	1.1676
2	9.3667	0.8021	3.8667	2.2301	2.2333	1.0693
3	9.1667	0.8505	3.8333	2.0648	2.5	1
4	9	0.8185	3.8	2.0075	2.7333	0.8021
5	8.7	0.755	3.7667	1.8717	2.9333	0.8021
6	8.6	1.0583	3.9	1.7776	2.9667	0.6807
7	9	1.1533	4.3333	2.0526	3.0667	0.6506
8	9.0333	1.1504	5	1.7059	3.8333	0.7095
9	9.3333	0.9504	5.5667	1.6073	5.1	0.8185
10	9.6	1.1533	5.8667	1.2423	5.5667	0.611
11	10.1333	1.0066	6.2333	1.6166	5.9333	0.3055
12	10.2667	0.8622	6.1667	1.5144	6.1	0.3606
13	7.9667	0.3786	5.3	0.8718	3.9333	0.3215
14	8	0.4583	5.2333	1.0116	3.8	0.5292
15	8	0.5	4.8667	1.0693	3.6	0.5292
16	7.7333	0.4509	4.3	1.1358	3	0.5568

17	6.9667	0.2309	3.3	1.5395	2.0667	0.9609
18	5.9667	0.3786	1.9333	1.2858	0.8333	0.5132
19	4.8333	0.3215	1.5667	1.0786	0.6333	0.2517
20	4.4333	0.3215	1.5	0.8718	0.7	0.3
21	4.3333	0.4163	1.5667	0.9074	0.8667	0.4509
22	4.1	0.2646	1.5	0.9644	0.9333	0.4041
23	4.0667	0.2082	1.5333	0.9292	0.9	0.3606
24	4	0.1732	1.5333	0.8386	0.9667	0.3215

The Wind turbine Expected output of wind speed for 1, 12, 23 hours at summer, autumn, winter, spring are presented from Fig. 3.6 to Fig. 3.9.

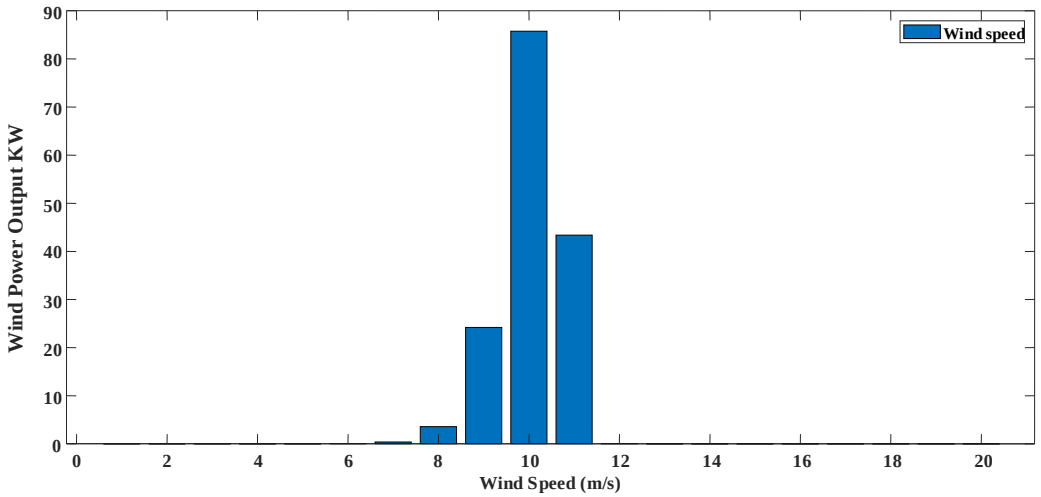

Fig. 3.6 Wind turbine Expected output of wind speed for 1 hours (Summer)

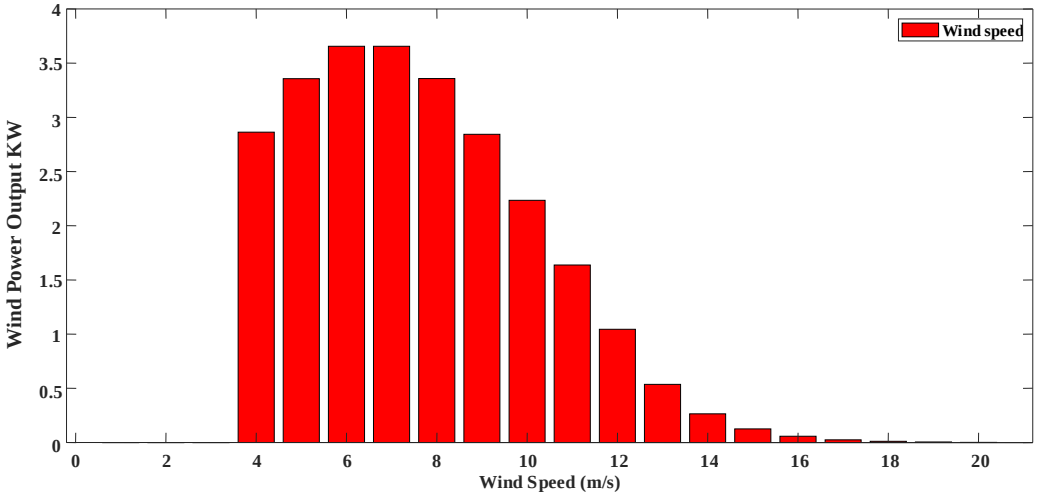

Fig. 3.7 Wind turbine Expected output of wind speed for 1 hours (Autumn)

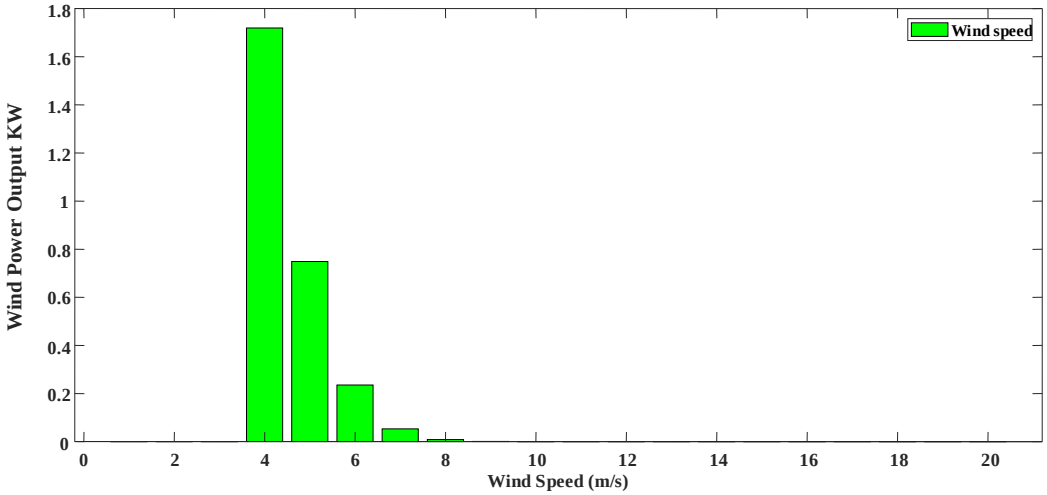

Fig. 3.8 Wind turbine Expected output of wind speed for 1 hours (Winter)

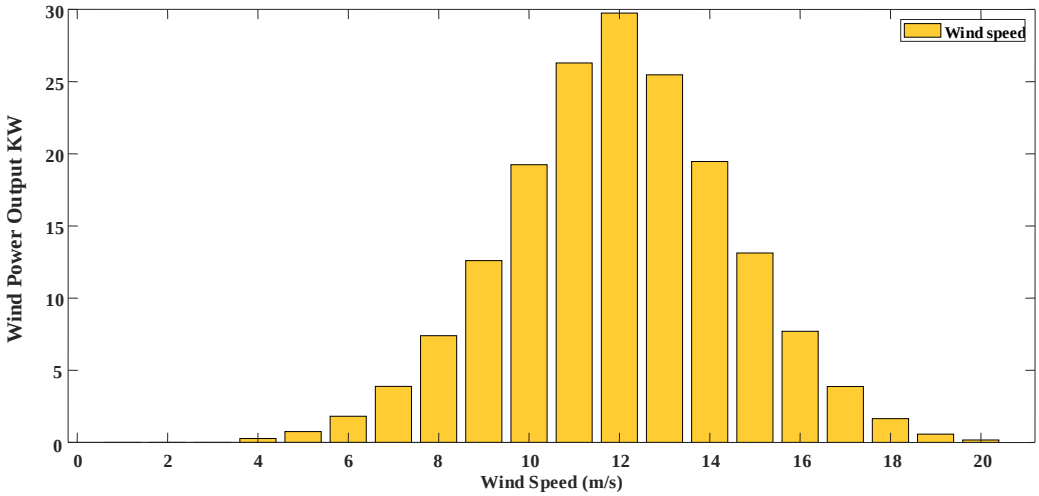

Fig. 3.9 Wind turbine Expected output of wind speed for 1 hour (Spring)

3.3 Chapter Summary

In this chapter mathematical modelling of solar and wind load profile is presented. Mean and standard deviations of solar PV and wind are tabulated. Load profiles of solar irradiance is presented. Solar PV specification and wind specification are presented.

CHATPER 4

PROBLEM FORMULATION OPTIMIZATION ALGORITHMS

4.1Problem Formulation

This research presents a method for optimising the placement of photovoltaic (PV) modules within the limitations of the distribution system to reduce power loss, increase the voltage stability margin, and improve the voltage profile. The graphic below reveals the competing VSI and power loss objective functions.

4.1.1 Voltage Stability Index Improvement

Unpredictable equipment failure, overloading, and other disruptions can affect the distribution network. These can cause fluctuations in the voltage, which can lead to a complete blackout. To prevent this, the system should maintain a steady voltage. The objective function of maintaining a stable voltage is the VSI:

$$f_1 = \mathrm{VSI} = |V_i|^4 - 4 * \{P_j x_{ij} - Q_j r_{ij}\}^2 - 4 * \{P_j r_{ij} - Q_j x_{ij}\}^2 * |V_s|^2 \quad (4.1)$$

The voltage stability index is calculated by taking into account the various factors that affect the transmission of electricity, such as the voltage on the bus, the active load, the reactive load, and the resistance between the lines i and j. It can be used to determine the optimal bus stops for PV installation. To get the best possible value, we rank the various bus stops according to their respective values.

4.1.2 Power Loss Minimization

After identifying suitable locations for photovoltaic installations, it is important to minimize power loss. This can be done by implementing an objective function in the distribution networks:

$$f_2 = \sum_{b=1}^{n_b} |I_b|^2 R_b \quad (4.2)$$

I_b = Branch Current, R_b = Branch Resistance, and n_b = Number of Branches.

The distribution network's constraints can be used to solve the multi-objective optimization problem:

“Voltage constraints

$$|V_{min}| \leq |V_k| \leq |V_{max}| \quad (4.3)$$

Thermal constraints

$$I_{ij} \leq I_{ij}^{max} \quad (4.4)$$

DG capacity constraints

$$P_{DG,min} \leq P_{DG,k} \leq P_{DG,max} \quad (4.5)$$

Power balance consraints

Generation= Demand +Losses

$$P_{slack} + \sum_{k=1}^{N_{DG}} P_{DG,k} = \sum_{k=1}^{N_L} P_{D,k} + \sum_{k=1}^{n_b} P_{loss,k} \quad (4.6)$$

It is not feasible to estimate and identify line flows using a radial network with a high R/X. This setting aims to analyze the flow of electricity through a forward-backward sweep load distribution. The results of the investigations support the findings of distributed generation systems that utilize the PSODE algorithm. The amount of solar radiation that a system can receive must also be determined using the previous data.

Fitness is given as

F= P_{Loss}

$$F = \sum_{b=1}^{n_b} | I_b |^2 R_b \quad (4.7)$$

Subjected to constrains

Voltage Stability index

$$V_t^{min} \leq | V_t | \leq V_t^{max} \quad (4.8)$$

$where\ V_t^{min}\ and\ V_t^{max}$

DG capacity constrains

$$P_{DG,min} \leq P_{DG,k} \leq P_{DG,max} \quad (4.9)$$

Thermal constraints

$$I_{ij} \leq I_{ij}^{max} \quad (4.10)$$

4.1.3 Total Harmonic Distortion

The term THD, which stands for total harmonic distortion, refers to the ratio of the power of the various harmonic components to the fundamental frequency of a signal. It is often used as a synonym for distortion factor. THD is calculated as follows

$$THD_i = \frac{\sqrt{V_2^2+V_3^2+V_4^2+\cdots}}{V_1} (4.11)$$

4.2 Firefly Algorithm

The optimization process can be carried out through the use of the firefly algorithm. This method is a metaheuristic approach that is inspired by nature[118]–[122].The rules of this algorithms as follows:

1. The firefly attraction does not have a gender difference.
2. The brightness of fireflies changes depending on their proximity to one another. When two or more fireflies are around, the insects will glow brightly.
3. Changes in FF brightness are directly proportional to objective function values in maximisation problems, but they are inversely proportional to objective function values in minimization problems.

The firefly algorithm (FA) can be written in pseudo code using these techniques. The Pesudo code is as follows:

$Objective\ function\ \boldsymbol{f(X)}, \boldsymbol{X} = [\boldsymbol{X_1}, \ldots\ldots \boldsymbol{X_d}]^{\boldsymbol{T}}$

$Generate\ intial\ population\ of\ fire\ flies, \boldsymbol{X_i}\ (\boldsymbol{i} = \boldsymbol{1}, \boldsymbol{2}, \ldots\ldots, \boldsymbol{n})$

Light intensity $\boldsymbol{I_i}$ at $\boldsymbol{X_i}$ is determined by **f(X$_i$)**

Define light absorption coefficient

While(t< Max Generation)

for i=1:n all n firefiles

for j=1:i all n fire flies

if **(Ij > If**), Move firefly i towards j in d-dimension;end if

Attractiveness varies with distance r via exp[-γr]

Evaluate new solution and update light intensity

end for j

end for i

Rank the fireflies and find the current best

end while

Post process results visualization

4.2.1 Steps to solve PV module allocation problem using FA

The steps to solve PV module allocation problem using FA is presented below

1. After gathering information about the system, some FA defaults were set
2. Load data from several PVAs and create a generation load model with this information.
3. Make sure that the distribution is simple.
4. By ranking the buses according to their VSI, you can find suitable locations where PV panels can be installed.
5. FA is calculate as

$$\beta(r) = \beta_0 e^{-\gamma r^2} \tag{4.12}$$

The separation of the firefly species is represented by r, and the value of 0 indicates its attractiveness. The distance between them is computed by using the formula:

$$r_{ij} = \|x_i - x_j\| = \sqrt{\sum_{k=1}^{d}(x_{i,k} - x_{j,k})^2} \tag{4.13}$$

6. The optimal value for PV modules that can be placed at a potential site depends on the brightness of the fireflies:

$$x_i = x_i + \beta_0 e^{-\gamma r_{ij}^2}(x_j - x_i) + \alpha\,(\text{rand} - \frac{1}{2}) \tag{4.14}$$

The Second value, i.e.,$\beta_0 e^{-\gamma r_{ij}^2}(x_j - x_i)$

7. The power loss of the PV modules is calculated by comparing the values from the previous generation with the current state.
8. Repeat steps 5 if convergence fails after the highest number of repetitions.

4.3 Gorilla troops optimizer(GTO) algorithm

The gorilla's social dynamics are modeled through the use of the Gorilla Troops Optimizer, a swarm-inspired algorithm. This animal is regarded as one of the most sociable primates on the planet. Its male counterpart is referred to as a silverback due to the hairs covering his back. A gorilla family is composed of a male, several females, and their offspring. The dominant male member of the group is responsible for leading his group to food and protecting their territory. Studies have shown that the behavior of females and males could differ significantly from one another. Male gorillas tend to leave their groups in order to find more attractive females. They will then start to form new groups with these females. Doing so allows them to establish territories that can grow. Female gorillas also tend to stay away from male gorillas. This is because they don't have the same social dynamics. The profit and discovery phases of the algorithm are focused on exploring and finding. The algorithm uses five operators to simulate the actions of a gorilla during its exploration. It can be used to find the animal in various locations, such as going somewhere new, going with other gorillas, or going somewhere familiar. During the exploitation phase, two operators are used to improve the search efficiency. One of them follows the silverback, while the other one is focused on attracting the female gorillas[123]–[127].

The behaviours of gorillas are influenced by the social cues that they receive from their groups. For instance, GTO learns when it's best to join other gorillas or move to a new region. In Fig.4.1(a) GTO process and4.1(b) flow chart is presented.

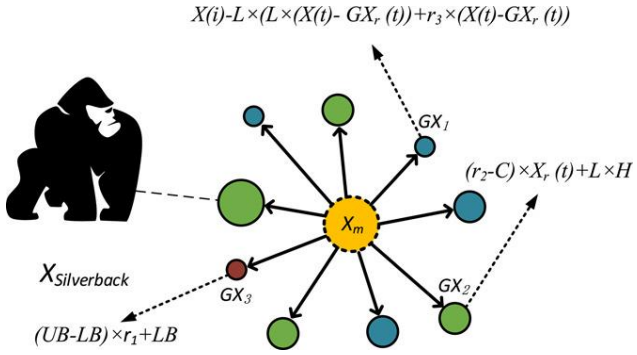

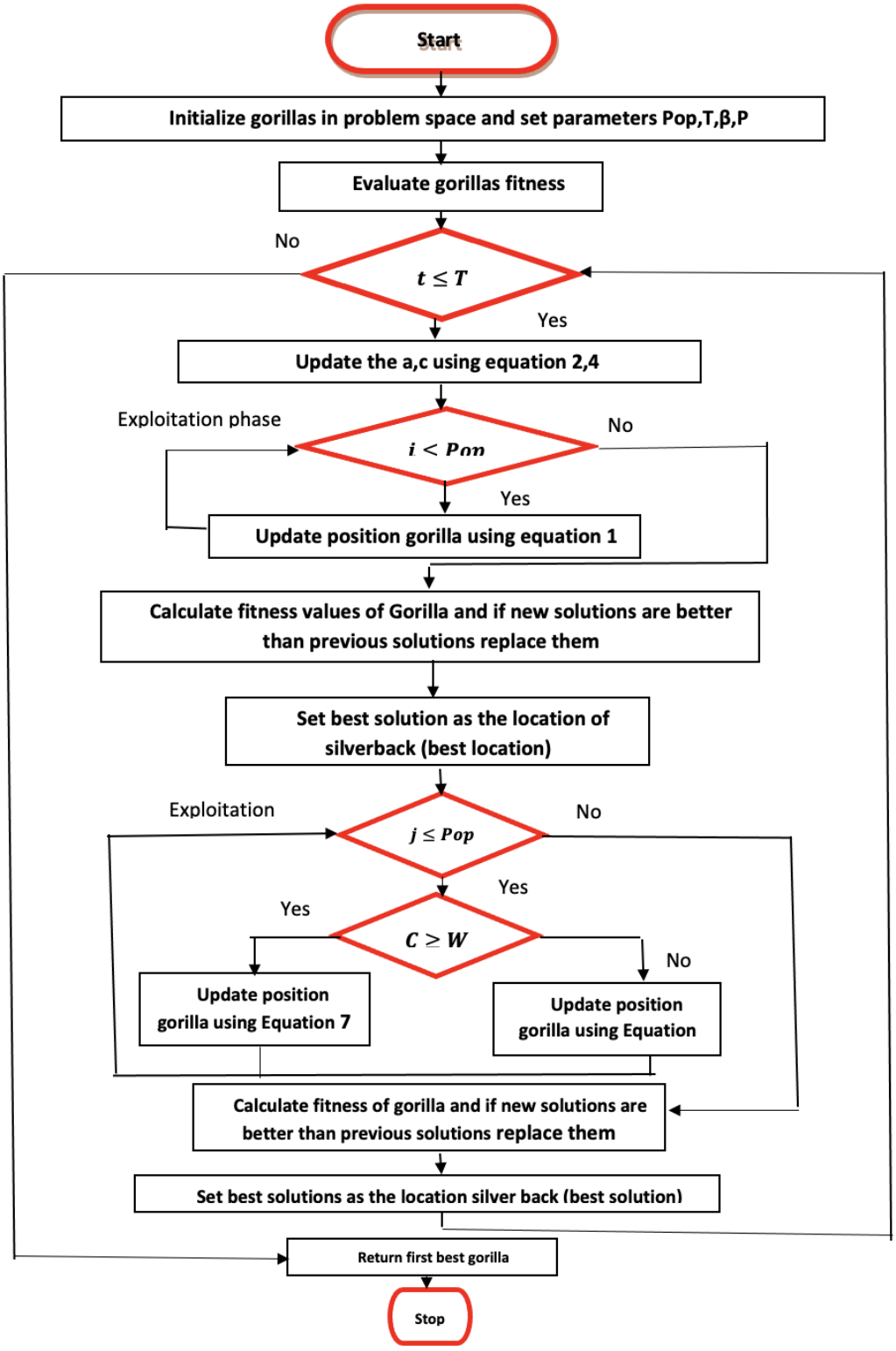

Fig. 4.1(a) GTO Process 4.1 (b) Flowchart.

4.3.1 Exploration

The three mechanisms that are part of the exploratory phase are presented by Equation 4.17. The first one is the migration mechanism that will be used to find the unknown location. For simplicity, the choice will be between the two procedures: the first involves traveling towards the other gorillas and the second involves migration to a fixed location. If the rand is less than half, the second procedure will be chosen.

This section describes the various steps involved in an optimization project's exploratory phase. It's widely believed that a silverback gorilla has the authority to make decisions for its group. The animal is known to go to unusual locations in its natural habitat. At each stage of the optimization process, the silverback solution is identified as the best candidate. Three mechanisms are then presented to explain how they work.

GX(t+1)=

$$\begin{cases} (uB - LB) \times r_1 + LB & rand < p \\ (r_2 - c) \times X_r(t) + L \times H & rand \geq 0.5 \\ X(i) - L \times \left(L \times \left(X(t) - GX_r(t)\right)\right) & rand < 0.5 \end{cases} \quad (4.15)$$

where X(t) is the current position vector of the gorilla and GX(t+1) is a potential new position vector. Random numbers from 0 to 1 are symbolised by the symbols r1, r2, and rand. The symbols UB and LB stand for the extremes of the variables.

$$C = F \times \left(1 - \frac{It}{MaxIt}\right) \quad (4.16)$$

The MaxIt is the maximum value that may be used in an iteration. At the beginning, the variation values are generated over a vast range, but as the optimization process progresses, this will narrow down to a manageable range. The F is formulated as follows:

$$F=\cos(2 \times r_4) + 1 \quad (4.17)$$

L is given as

$$L = C \times l \quad (4.18)$$

In addition, the value of l can be obtained by taking into account the silverback's stance. This is done through the use of Equation 4.20. The silverback gorillas face a critical

situation in order to gain food and form a group, but they can only learn how to lead by experience.:

$$H = Z \times X(t) \tag{4.19}$$

$$Z = [-C, C] \tag{4.20}$$

The silverback is the most likely choice due to its lower cost.

4.3.2 Exploitation

During the exploitation stage of the GTO algorithm, two behaviors must be adopted to maintain the group's cohesion. One of these is to keep up with the silverback, while the other is to compete with the females for their attention. As indicated by the C value, adult males can choose to follow the silverback or go head-to-head with other males. The optimization parameter W must be set first to ensure that C meets the necessary requirements.

4.3.2.1 Following the Silverback

The gorillas are known to be at their best when they are young. For instance, male gorillas can easily follow the silverback. Everyone within the group also has the ability to influence the behavior of the others. This method can be demonstrated by using the equation 4.22:

$$GX(t+1) = L \times M \times (X(t) - X_{silverback}) + X(t) \tag{4.21}$$

The XSilverback algorithm presents the optimal solution by mapping the silverback vector to the given value:

$$M = (\left|\frac{1}{N}\sum_{i=1}^{N} GX_i\,(t)\right| \text{^} g)^{\frac{1}{g}} \tag{4.22}$$

4.4 PSODV (Particle swarm optimization with Differential velocities algorithm)

The DE calculations' differential administrator is responsible for coordinating the updates of the PSO and other functions, which are referred to as "PSODV." It is recommended that the administrator does not make the chemical of their choice. To ensure that the calculations are correct, the administrator has compressed the selection procedure into all the parts of the issue[118]–[122]. Step by step algorithm is as follows:

Stage 1: Initialize the parameters randomly.

$V_i^0 = V_{i,min} + rand\ 0.\left(V_{i,max} - V_{i,min}\right), i = 1,2, \ldots\ldots, n_p$ (4.23)

Stage 2: During the assessment phase, the administrator should also include the data collected by the foundation program for MATLAB in the discussion. This will help in identifying the various factors that affect the force quality.

Stage 3: The provided multipliers can be used to speed up the interaction and increase the synergy.

Stage 4: The evaluation process continues to identify and evaluate innovative individuals.

Stage 5: The position is updated as follows:

$$\overrightarrow{\delta} = \overrightarrow{X_k} - \overrightarrow{X_j}$$

The i^{th} focus on molecule's d^{th} (1< d < n) speed part is refreshed as

$V_{id}(\mathrm{t}+1) = \{\omega V_{id}(t) + \beta\delta_d + C_2\psi_2\left(P_{gd} - X_{id}(t)\right), if\ rand\ (0,1) \leq$

$CR\ \ V_{id}(t)\ other\ wise$ (4.24)

Where CR: Statistical Likelihood of a Crossover Occurring

δ_d : Scaling factor ranging from 0 to 1 (everything else is the same as previously analysed). Difference vector of ith centering on dth portion of molecule.

When $CR \leq 1$the DE administrator and the PSO update rate plot are in agreement, further avenues of investigation open up . Even after being sped up to that extent, their original qualities remain unchanged.

$\vec{T}_{ri}$is given as

$$\vec{T}_{ri} = \vec{X}_i(t) + \vec{V}_i(t+1) \quad (4.25)$$

To improve the fit's intrinsic value, the molecule is relocated. Subsequently for the target work $f(\vec{X})$, the molecule migration is done as follows:

$$\underset{X_i}{\rightarrow}(t+1) = \underset{T_{ri}}{\rightarrow} \; if \; f\left(\underset{T_{ri}}{\rightarrow}\right) \leq f\left(\underset{X_i}{\rightarrow}(t)\right)$$

$$\underset{X_i}{\rightarrow}(t+1) = \underset{X_i}{\rightarrow}(t) \; otherwise \tag{4.26}$$

$$if \; \underset{X_i}{\rightarrow}(t) = \underset{X_i}{\rightarrow}(t+1) = \underset{X_i}{\rightarrow}(t+2) = \cdots . = \underset{X_i}{\rightarrow}(t+N) \quad then \; for \; r = 1,2,3 \ldots . , n$$

$$X_{ir}(t+N+1) = X_{min} + rand_r(0,1)(X_{max} - X_{min}) \tag{4.16}$$

$X_{\max} and X_{min}$ are upper and lower bounds on the search space, while f is the amount of frequency.

Step 6: Repeat steps 2–5 until the final measure is achieved, that is, the best possible solution for a speculative measure.

The iterative process of PSODE computation is shown as a flowchart in Fig.4.2

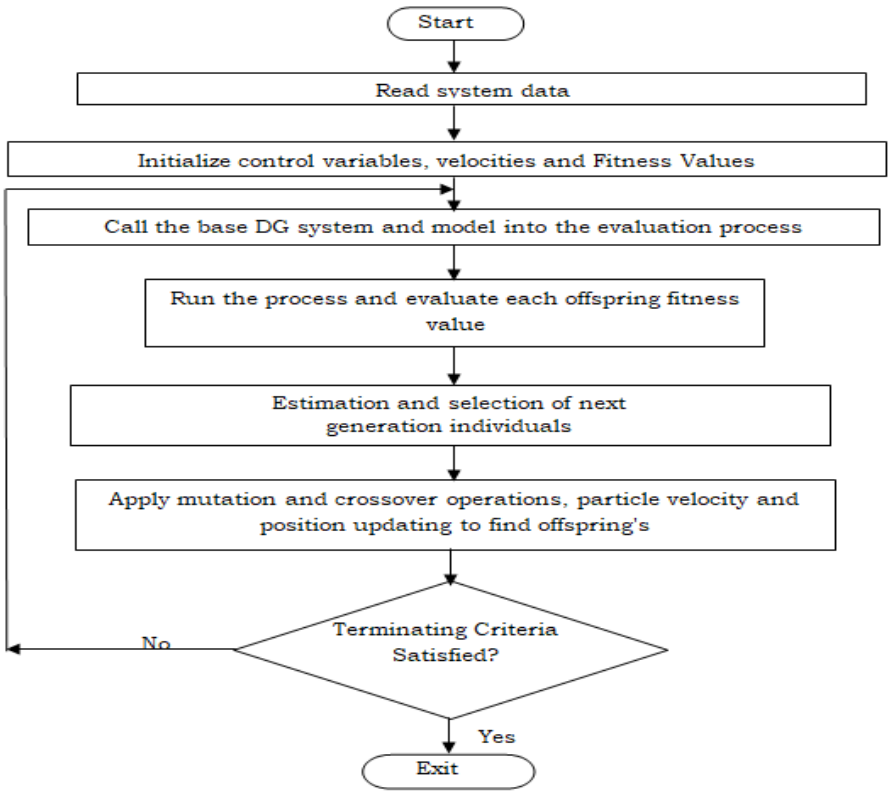

Fig. 4.2 PSODV algorithm Flowchart

4.5 Chapter Summary

In this chapter problem formulation is presented. Algorithm steps and flowcharts for firefly, particle swarm and gorilla troops optimization are presented in this chapter.

CHAPTER 5

RESULTS AND DISCUSSION

In this work proposed Particle Swarm Optimization with Differential Velocities (PSODV) algorithm is implemented on a Indian 28 and IEEE 85 bus system considering solar DG, wind DG, hybrid solar - wind DG and residential, commertial, industrial loads under the following cases.

- Optimal Location of DER Considering Solar DG
- Optimal Location of DER Considering Wind DG
- Optimal Location of DER Considering Hybrid Solar-Wind DG

The optimal bus location, size of DG are calculated and the performance evaluation parameters P_{loss}(kW), V_{min}(p.u.), VSI_{min}(p.u.), % Reduction $P_{loss}$are evaluated in all the cases. The effectiveness of the proposed Particle Swarm Optimization with Differential Velocities (PSODV) algorithm is evaluated in comparison with Firefly (FF) algorithm and Gorilla Troops Optimizer (GTO) algorithm.

5.1 Optimal Location of DER Considering Solar DG

In this case optimal location of DER with the solar DG is considered. The proposed PSODV algorithm is implemented under residential, commertial, industrial loads on the following bus

- Optimal Location of DER on Indian 28 RDS
- Optimal Location of DER on IEEE 85 RDS

The optimal bus location, size of DG are calculated and the performance evaluation parameters P_{loss}(kW), V_{min}(p.u.), VSI_{min}(p.u.), % Reduction $P_{loss}$are evaluated in all the cases. The effectiveness of the proposed Particle Swarm Optimization with Differential Velocities (PSODV) algorithm is evaluated in comparison with Firefly (FF) algorithm and Gorilla Troops Optimizer (GTO) algorithm.The block diagram for thesolarDG in RDS is presented in Fig. 5.1.

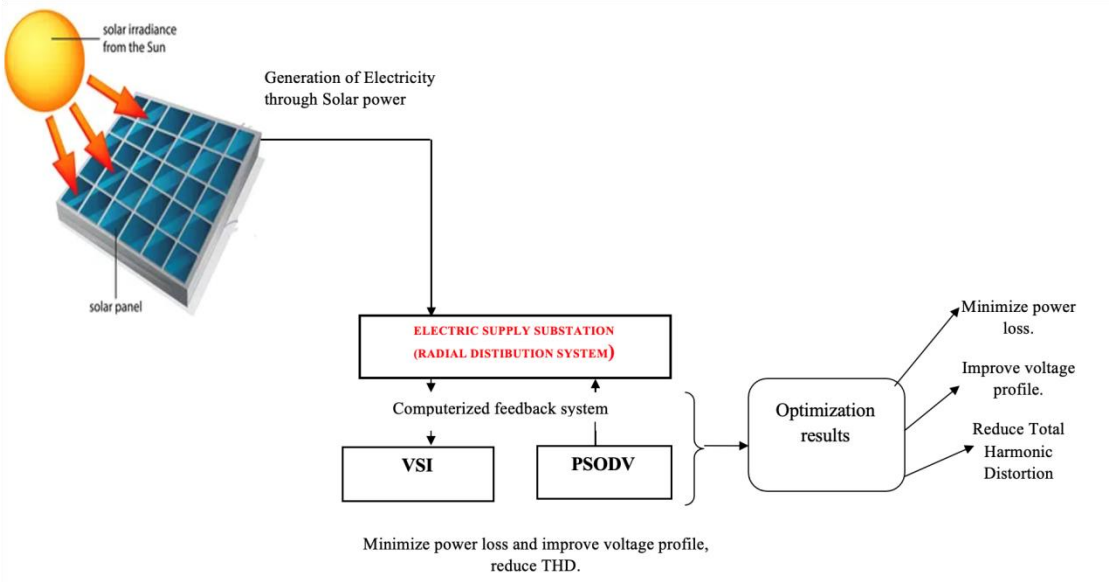

Fig 5.1Solar DG in RDS

5.1.1 Optimal Location of DER on Indian28 RDS

In this optimal Location of DER Considering Solar DG is implemented on IEEE 28 RDS considering 1 solar DG, 2 solar DGs, 3 solar DGs under the following cases.

- Optimal Location of DER on Indian 28 RDS with Residential Load
- Optimal Location of DER onIndian28 RDS with Commertial Load
- Optimal Location of DER onIndian28 RDS with Industrial Load

5.1.1.1 Optimal Location of DER on Indian 28 RDS with Residential Load

In this case optimal location of DER on Indian 28 RDS with residential load is implemented using the proposed Particle Swarm Optimization with Differential Velocities (PSODV) algorithm. The hourly power loss of residential load is presented in Table 5.1.

Table 5.1 Hourly Power loss of Residential Load

Time (Hr.)	P_{loss} (kW) (Base case)	Case 1 1 SDG P_{loss} (kW)	Case 2 2 SDG P_{loss} (kW)	Case 3 3 SDG P_{loss} (kW)
1	5.92	4.55	3.323	3.23
2	4.1354	3.18014	2.330156	2.18429
3	3.51349	2.70354	1.98246	1.8532

4	3.81789	2.93687	2.15273	2.152116
5	3.81789	2.93687	2.15273	2.152116
6	3.51349	2.70354	1.98246	1.8532
7	3.51349	2.70354	1.98246	1.8532
8	3.51349	2.70354	1.98246	1.8532
9	2.943826	2.2665779	1.71185	1.665
10	35.038159	26.515143	19.05358	17.79182
11	46.048648	34.712	24.8309181	23.7140605
12	54.78727	41.182117	29.36317	27.705677
13	56.107273	42.156859	30.0439524	28.009509
14	35.038159	26.515143	19.05358	17.79182
15	11.59909	8.871448	6.456787	6.30445
16	30.158	22.8649	16.4669	15.9932
17	43.7101	32.9754	23.6103	21.9596
18	60.1769	45.1579	32.1367	29.8518
19	65.8628	49.3405	35.0457	34.6618
20	**68.8189**	**51.5105**	**38.3096**	**36.6885**
21	43.7101	32.9754	23.6103	21.9596
22	22.3811	17.0243	12.3084	11.913
23	10.5135	8.0465	7.6406	7.1317
24	6.3194	4.8505	4.5256	3.3377

The peak value are recorded at 20th hour. The P_{loss}(kW) is 68.8189 kW, V_{min}(p.u.) is 0.9123p.u., VSI_{min}(p.u.) is 0.6927. The system performance with the optimal allocation of 1 solar DG, 2 solar DGs, 3 solar DGs are tabulated in Table 5.2.

Table 5.2 System Performance for 28 RDS

Scenario	Location Of Bus	Sizes of DG (kW)	Power Losses (P_{loss}) kW	Voltage Minimum (V_{min}) P. U.	Voltage Stability Index (VSI_{min}) P. U.	Reduction of Losses (%)

BC	-	-	68.8189	0.9123	0.6927	-
1 SDG	12	450.4790	51.5105	0.9299	0.7477	25.150
2 SDG	12 23	265.7509 373.6920	36.5513	0.9575	0.8396	46.885
3 SDG	12 23 27	228.6116 204.3185 245.6731	34.0480	0.9613	0.8539	50.51

In 1 solar DG case DG is optimally placed on bus 12 with 450.4790 kW size. The P_{loss}(kW) is 51.5105 kW, V_{min}(P. U.) is 0.9299P. U., VSI_{min}(P. U.) is 0.7477, % Reduction of P_{loss} is 25.15 %. In 2 solar DGs case DGs is optimally located at buses 12, 23 with sizes of 265.7509 kW, 373.620 kW. The P_{loss}(kW) is 36.5513 kW, V_{min}(P. U.) is 0.9575P. U., VSI_{min}(P. U.) is 0.8396, % Reduction of P_{loss} is 46.885%. In 3 solar DGs case DGs is optimally located at buses 12, 23, 27 with sizes of 228.6116 kW, 204.3185 kW, 245.6731 kW. The P_{loss}(kW) is 34.0480 kW, V_{min}(P. U.) is 0.9613P. U., VSI_{min}(P. U.) is 0.8539, % Reduction of P_{loss} is 50.51%.

The power loss comparision of all the cases for 24 hour profile and 28 RDS are presented in Fig. 5.2 and Fig. 5.3 respectively.

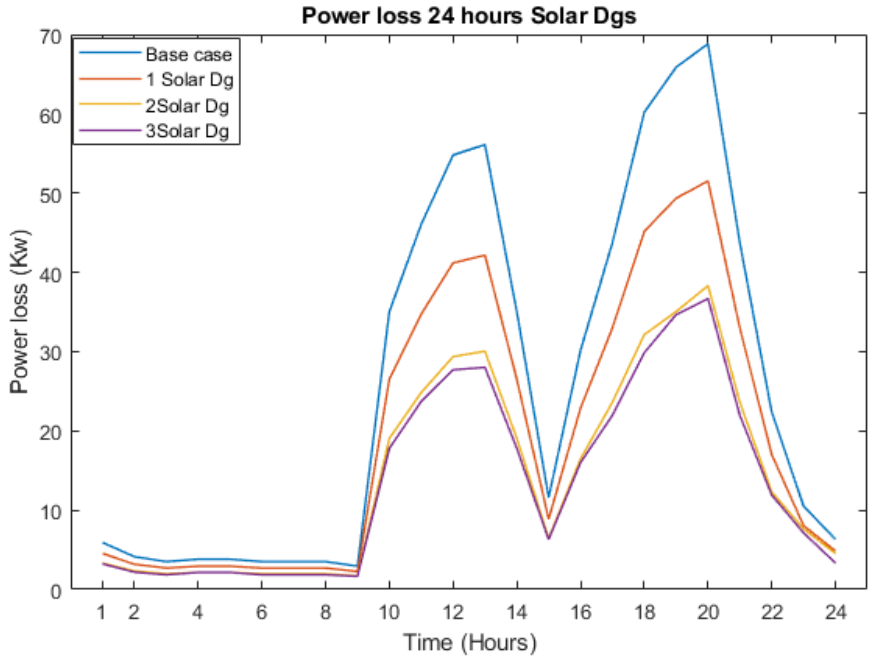

Fig. 5.2 Power Loss for 24 hour Profile

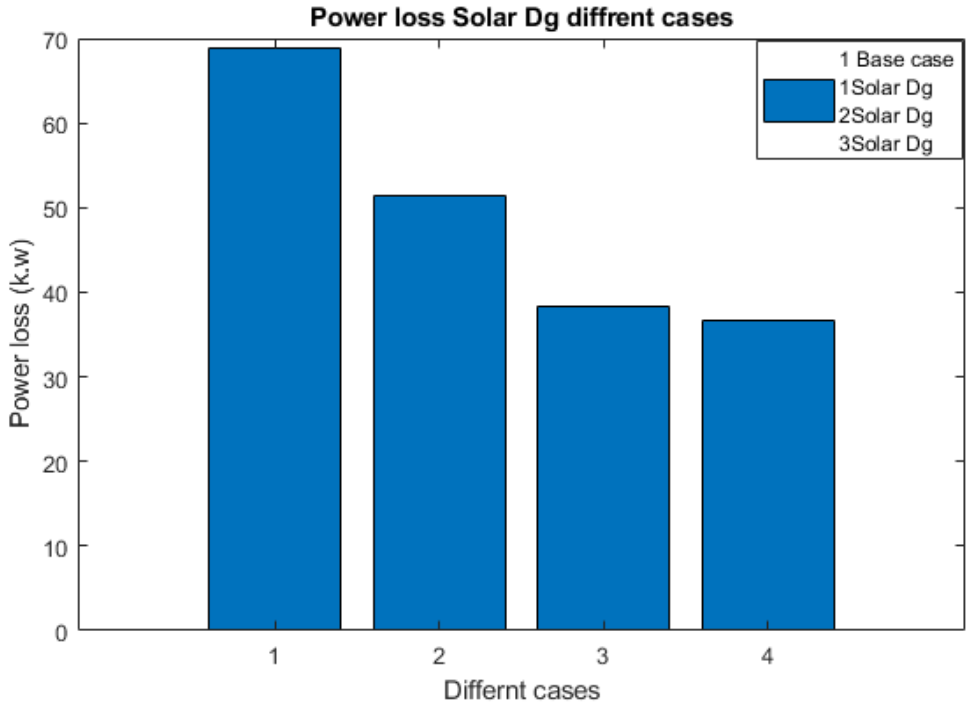

Fig. 5.3 Power Loss for 28 RDS System

From the above the peak power loss is recorded at 20th hour and the power loss P_{loss}(kW) is decreased from 68.8189 kW→34.0480kW. The voltage profile V_{min} (p.u.) is presented in Fig. 5.4.

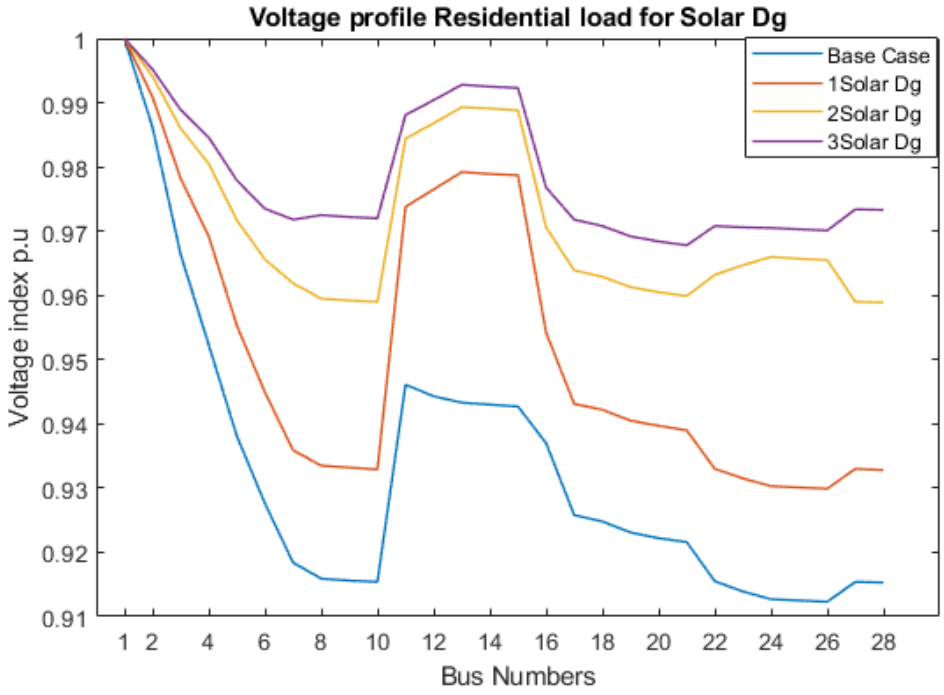

Fig. 5.4 Voltage Profile

From the above the The voltage profile V_{min} (p.u.) is enhanced@0.9123 (p. u)→ 0.9613(p.u). The VSI_{min} (p.u.) is presented in Fig. 5.5

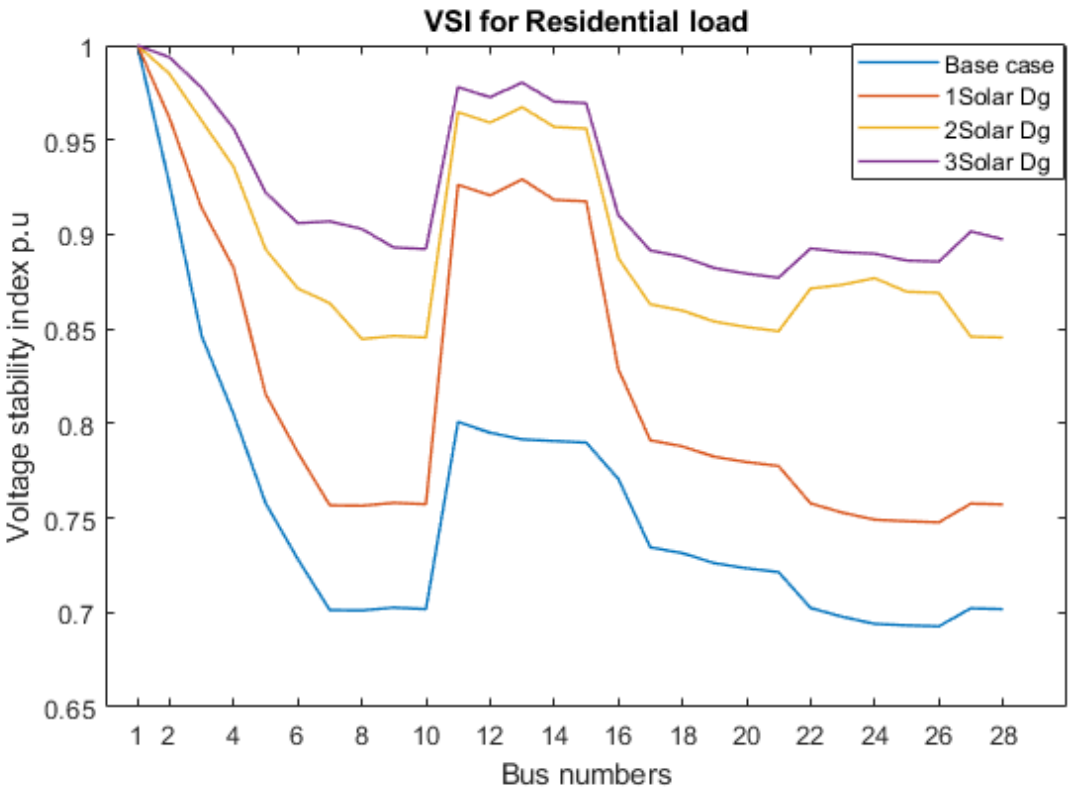

Fig. 5.5 Voltage Stability Index

From the above the VSI_{min} (p.u.) is enhanced@0.6927(p.u.)→ 0.8539(p.u.). The effectiveness of the proposed Particle Swarm Optimization with Differential Velocities (PSODV) algorithm is evaluated in comparison with Firefly (FF) algorithm and Gorilla Troops Optimizer (GTO) algorithm and presented in Table 5.3.

Table 5.3 Performance Comparision 28 RDS

Method	Case Type	Power Losses (P_{loss}) kW	Voltage Minimum (V_{min}) P. U.	Voltage Stability Index (VSI_{min}) P. U.	Reduction of Losses (%)
Base case		68.8189	0.9123	0.6927	NA
	1 SDG	51.5105	0.9299	0.7477	25.150
	2 SDG	36.5513	0.9575	0.8396	46.885

Proposed PSODV Algorithm	3 SDG	34.0480	0.9613	0.8539	50.51
GTO Algorithm	1 SDG	51.0066	0.9215	0.7545	25.88
	2 SDG	35.8397	0.9572	0.8395	47.92
	3 SDG	33.6501	0.9633	0.8611	51.10
FF Algorithm	1 SDG	50.995	0.9281	0.7398	25.8997
	2 SDG	36.3512	0.9542	0.8332	47.178
	3 SDG	33.9388	0.9614	0.8542	50.68

From the above the proposed Particle Swarm Optimization with Differential Velocities (PSODV) algorithm exhibited the best performance i.e., the power loss P_{loss}(kW) is decreased from 68.8189 kW→34.0480 kW, The voltage profile V_{min} (p.u.) is enhanced@0.9123(p.u.)→ 0.9613 (p.u,)the VSI_{min} (p.u.) is enhanced@0.6927(p.u.)→ 0.8539 (p.u.).

5.1.1.2 Optimal Location of DER on Indian 28 RDS with Commertial Load

In this case optimal location of DER on IEEE 28 RDS with commertialload is implemented using the proposed Particle Swarm Optimization with Differential Velocities (PSODV) algorithm. The hourly power loss of residential load is presented in Table 5.4.

Table 5.4 Hourly Power loss of Commertial Load

Time (Hr.)	P_{loss} (kW) (Base case)	Case 1 1 SDG P_{loss} (kW)	Case 2 2 SDG P_{loss} (kW)	Case 3 3 SDG P_{loss} (kW)
1	4.8101	3.6967	2.7065	2.5781
2	4.8101	3.6967	2.7065	2.5781
3	4.4661	3.4334	2.5147	2.3571
4	4.8101	3.6967	2.7065	2.5781
5	5.5379	4.2534	3.1117	2.916
6	8.0453	6.1675	4.5014	4.2163
7	38.1638	28.8474	20.7017	19.3257

8	53.4854	40.2201	28.6908	26.7528
9	58.802	44.1447	31.4307	29.297
10	60.1769	45.1579	32.1367	29.8518
11	**62.9824**	**47.2231**	**33.5742**	**31.2864**
12	58.802	44.1447	31.4307	29.297
13	52.2015	39.2707	28.0267	26.136
14	50.9355	38.334	27.371	25.5268
15	42.5668	32.1255	23.0123	21.4752
16	23.9996	18.2424	13.1778	12.3178
17	15.1998	11.6021	8.4235	7.8816
18	12.1632	9.2998	6.7658	6.3332
19	9.9919	7.6498	5.5744	5.2196
20	9.9919	7.6498	5.5744	5.2196
21	11.0492	8.4537	6.1552	5.7626
22	10.5135	8.0465	5.8611	5.4877
23	6.7304	5.1644	3.7738	3.5356
24	4.4661	3.4334	2.5147	2.3571

The peak value are recorded at 11th hour. The P_{loss}(kW) is 62.9824 kW, V_{min}(p.u.) is 0.9161p.u., VSI_{min}(p.u.) is 0.7044. The system performance with the optimal allocation of 1 solar DG, 2 solar DGs, 3 solar DGs are tabulated in Table 5.5.

Table 5.5 System Performance for 28 RDS

Scenario	Location Of Bus	Sizes of DG (kW)	Power Losses (P_{loss}) kW	Voltage Minimum (V_{min}) P. U.	Voltage Stability Index (VSI_{min}) P. U.	Reduction of Losses (%)
BC	-	-	62.9824	0.9161	0.7044	-
1 SDG	12	430.8526	47.2231	0.9329	0.7574	25.021
2 SDG	12 23	254.4227 358.1321	33.5742	0.9592	0.8459	46.69

3 SDG	12 23 27	218.8719 195.9363 235.4333	31.2864	0.9629	0.8597	50.325

In 1 solar DG case DG is optimally placed on bus 12 with 430.8526 kW size. The P_{loss}(kW) is 47.2231 kW, V_{min}(p.u.) is 0.9329(p.u.), VSI_{min}(p.u.) is 0.7574, % Reduction of P_{loss} is 25.021%. In 2 solar DGs case DGs is optimally located at buses 12, 23 with sizes of 254.4227 kW, 358.1321 kW. The P_{loss}(kW) is 33.5742 kW, V_{min}(p.u.) is 0.9592(p.u.), VSI_{min}(p.u.) is 0.8459, % Reduction of P_{loss} is 46.69%. In 3 solar DGs case DGs is optimally located at buses 12, 23, 27 with sizes of 218.8719 kW, 195.9363 kW, 235.4333 kW. The P_{loss}(kW) is 31.2864 kW, V_{min}(p.u.) is 0.9629(p.u.), VSI_{min}(p.u.) is 0.8597, % Reduction of P_{loss} is 50.325%.

The power loss comparision of all the cases for 24 hour profile and 28 RDS are presented in Fig. 5.6 and Fig. 5.7 respectively.

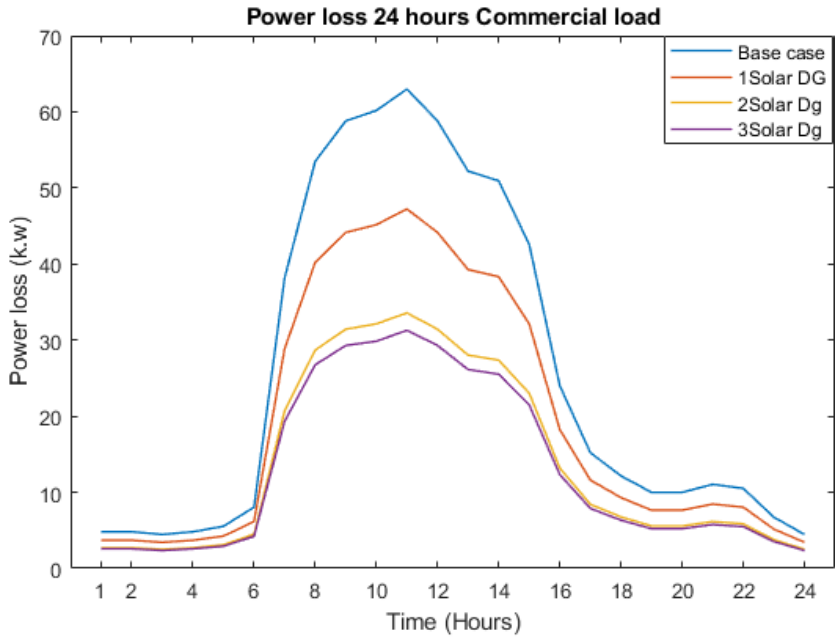

Fig. 5.6 Power Loss for 24 hour Profile

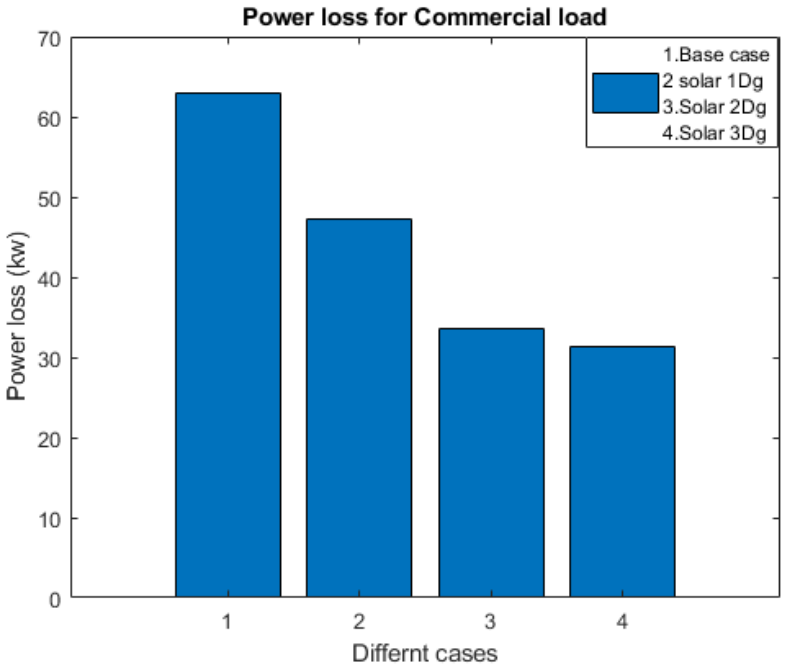

Fig. 5.7 Power Loss for 28 RDS System

From the above the peak power loss is recorded at 11th hour and the power loss P_{loss}(kW) is decreased from 62.9824 kW→31.2864kW. The voltage profile V_{min} (p.u.) is presented in Fig. 5.8.

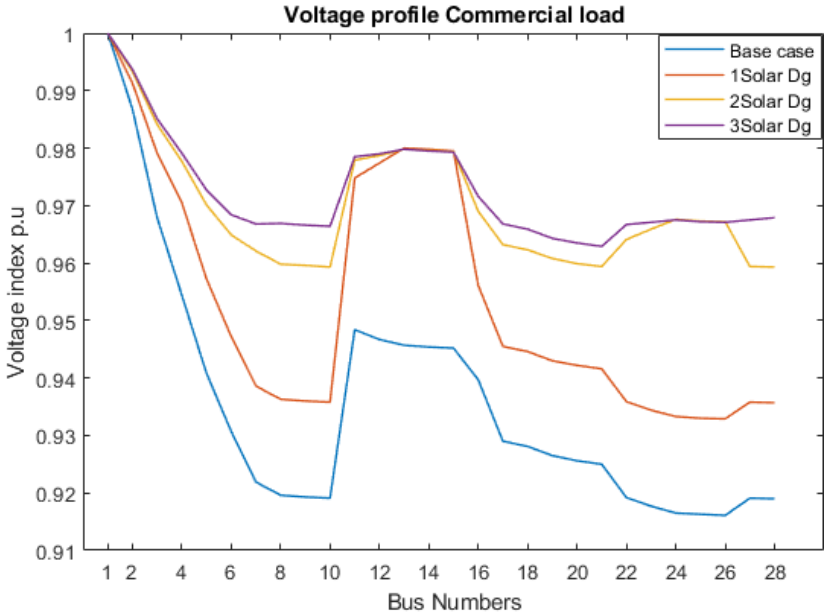

Fig. 5.8 Voltage Profile

From the above the The voltage profile V_{min} (p.u.) is enhanced@0.9161(p.u.)→ 0.9629(p.u.)The VSI_{min} (p.u.) is presented in Fig. 5.9

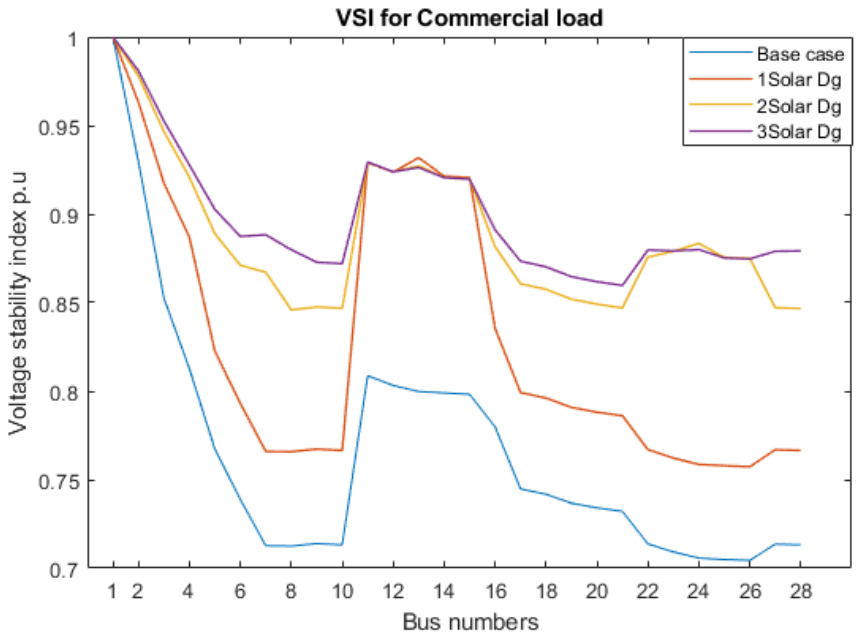

Fig. 5.9 Voltage Stability Index

From the above the VSI_{min} (p.u.) is enhanced@0.7044(p.u.)→ 0.8597(p.u.). The effectiveness of the proposed Particle Swarm Optimization with Differential Velocities (PSODV) algorithm is evaluated in comparison with Firefly (FF) algorithm and Gorilla Troops Optimizer (GTO) algorithm and presented in Table 5.6.

Method	Case Type	Power Losses (P_{loss}) kW	Voltage Minimum (V_{min}) P. U.	Voltage Stability Index (VSI_{min}) P. U.	Reduction of Losses (%)
Base case		62.9824	0.9161	0.7044	NA
Proposed PSODV Algorithm	1 SDG	47.2231	0.9329	0.7574	25.021
	2 SDG	33.5742	0.9592	0.8459	46.69
	3 SDG	31.2864	0.9629	0.8597	50.325
GTO Algorithm	1 SDG	47.0066	0.9151	0.7545	25.36
	2 SDG	35.8397	0.9572	0.8395	47.90
	3 SDG	33.6501	0.9633	0.8611	50.09
FF Algorithm	1 SDG	50.955	0.9281	0.7398	25.89

	2Solar DGs	36.3512	0.9542	0.8332	47.17
	3Solar DGs	33.9388	0.9614	0.8542	50.6

Table 5.6 Performance Comparision 28 RDS

From the above the proposed Particle Swarm Optimization with Differential Velocities (PSODV) algorithm exhibited the best performance i.e., the power loss P_{loss}(kW) is decreased from 62.9824 kW to 31.2864kW, The voltage profile V_{min} (p.u.) is enhanced from 0.9161 (p.u.)→ 0.9629 (p.u.), the VSI_{min} (p.u.) is enhanced@0.7044 (p.u.)→ 0.8597 (p.u.).

5.1.1.3 Optimal Location of DER on Indian 28 RDS with Industrial Load

In this case optimal location of DER on IEEE 28 RDS with industrialload is implemented using the proposed Particle Swarm Optimization with Differential Velocities (PSODV) algorithm. The hourly power loss of residential load is presented in Table 5.7.

Table 5.7 Hourly Power loss of Industrial Load

Time (Hr.)	P_{loss} (kW) (Base case)	Case 1 1 SDG P_{loss} (kW)	Case 2 2 SDG P_{loss} (kW)	Case 3 3 SDG P_{loss} (kW)
1	8.0453	6.1675	4.5014	4.2163
2	4.4661	3.4334	2.5147	2.3571
3	4.1354	3.1801	2.3302	2.1843
4	4.1354	3.1801	2.3302	2.1843
5	3.5135	2.7035	1.9825	1.8587
6	3.5135	2.7035	1.9825	1.8587
7	9.9919	7.6498	5.5744	5.2196
8	11.0492	8.4537	6.1552	5.7626
9	20.8242	15.8512	11.47	10.7251
10	21.595	16.4321	11.8854	11.1125
11	17.1971	13.1131	9.5087	8.8949
12	15.1998	11.6021	8.4235	7.8816

13	14.5635	11.1201	8.0769	7.558
14	22.3811	17.0243	12.3084	11.5071
15	18.6028	14.1752	10.2702	9.6057
16	28.3192	21.4866	15.4879	14.471
17	23.9996	18.2424	13.1778	12.3178
18	50.9355	38.334	27.371	25.5268
19	53.4854	40.2201	28.6908	26.7528
20	64.4132	48.2753	34.3057	31.9651
21	**67.3313**	**50.4189**	**35.7942**	**33.3459**
22	58.802	44.1447	31.4307	29.297
23	37.1053	28.058	20.1442	18.807
24	18.6028	14.1752	10.2702	9.6057

The peak value are recorded at 21th hour. The P_{loss}(kW) is 67.3313 kW, V_{min}(p.u.) is 0.9133 (p.u.), VSI_{min}(p.u.) is 0.6957. The system performance with the optimal allocation of 1 solar DG, 2 solar DGs, 3 solar DGs are tabulated in Table 5.8.

Table 5.8 System Performance for 28 RDS

Scenario	Location Of Bus	Sizes of DG (kW)	Power Losses (P_{loss}) kW	Voltage Minimum (V_{min}) P. U.	Voltage Stability Index (VSI_{min}) P. U.	Reduction of Losses (%)
BC	NA	NA	67.3313	0.9133	0.6957	NA
1 SDG	12	445.5571	50.4189	0.9306	0.7501	25.118
2 SDG	12 23	262.9233 369.7970	35.7942	0.9579	0.8412	46.83
3 SDG	12 23 27	226.1697 202.2404 243.1040	33.3459	0.9617	0.8554	50.47

In 1 solar DG case DG is optimally placed on bus 12 with 445.5571 kW size. The P_{loss}(kW) is 50.4189 kW, V_{min}(p.u.) is 0.9306 p.u., VSI_{min}(p.u.) is 0.7501, %

Reduction of P_{loss} is 25.118%. In 2 solar DGs case DGs is optimally located at buses 12, 23 with sizes of 262.9233 kW, 369.7970 kW. The P_{loss}(kW) is 35.7942 kW, V_{min}(p.u.) is 0.9579p.u., VSI_{min}(p.u.) is 0.8412, % Reduction of P_{loss} is 46.83%. In 3 solar DGs case DGs is optimally located at buses 12, 23, 27 with sizes of 226.1697 kW, 202.2404 kW, 243.1040 kW. The P_{loss}(kW) is 33.3459 kW, V_{min}(p.u.) is 0.9617 p.u., VSI_{min}(p.u.) is 0.8554, % Reduction of P_{loss} is 50.47%.

The power loss comparision of all the cases for 24 hour profile and 28 RDS are presented in Fig. 5.10 and Fig. 5.11 respectively.

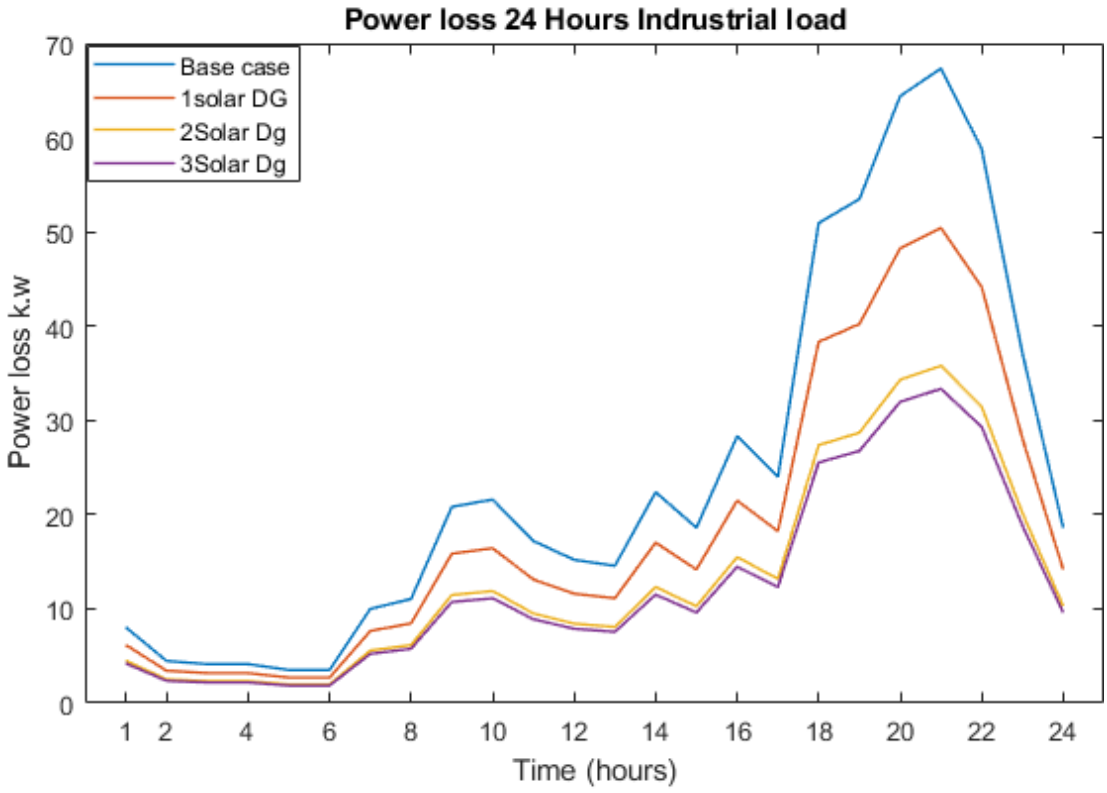

Fig. 5.10 Power Loss for 24 hour Profile

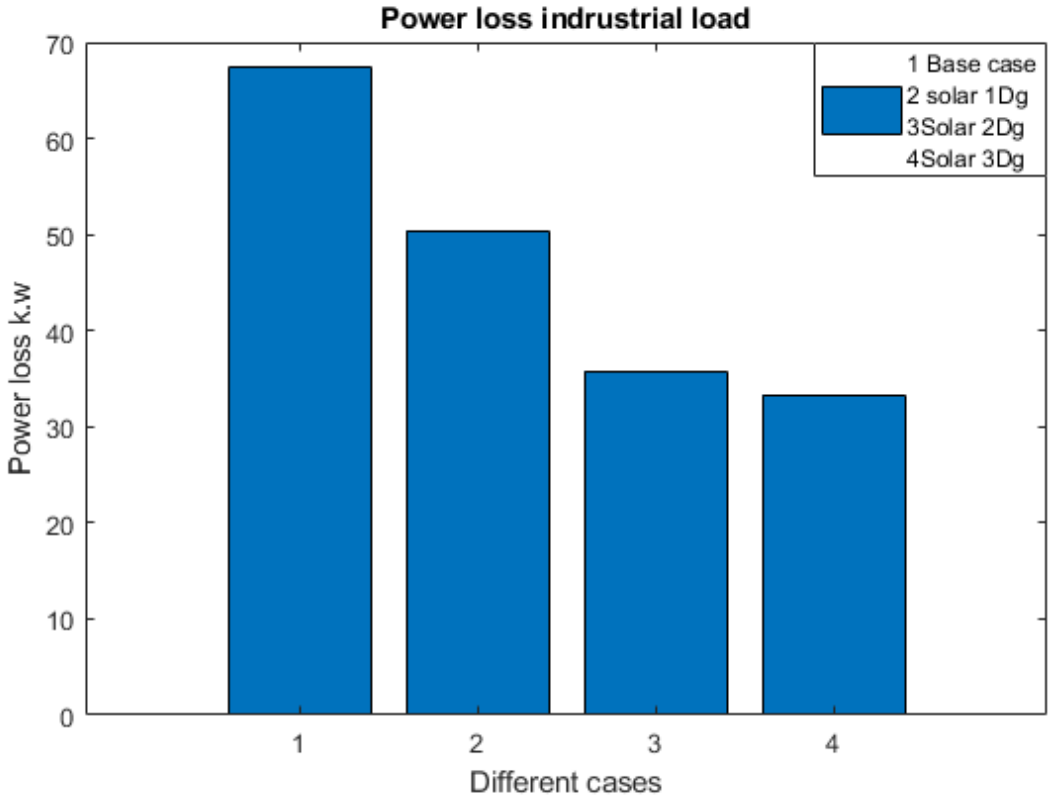

Fig. 5.11 Power Loss for 28 RDS System

From the above the peak power loss is recorded at 21th hour and the power loss P_{loss}(kW) is decreased from 67.3313 kW→33.3459kW. The voltage profile V_{min} (p.u.) is presented in Fig. 5.12.

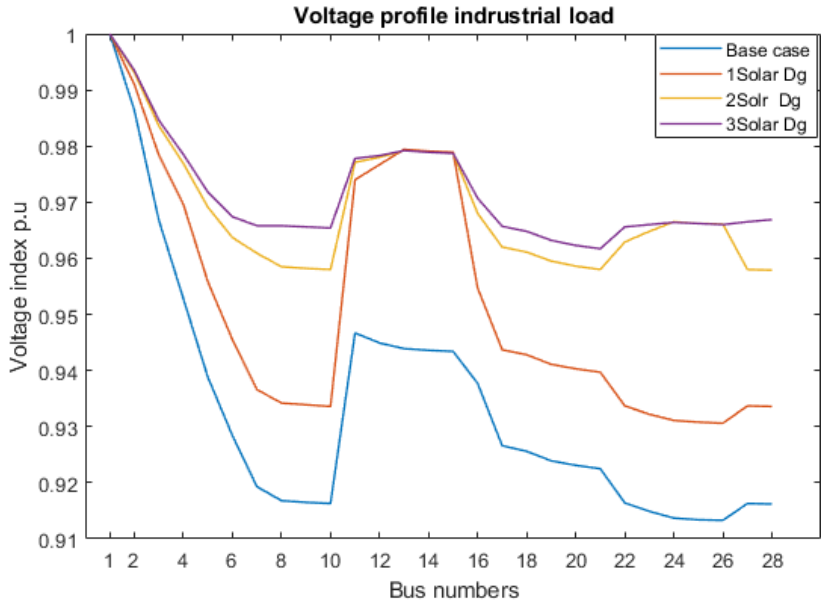

Fig. 5.12 Voltage Profile

From the above the The voltage profile V_{min} (p.u.) is enhanced@0.9133 p.u. → 0.9617 p.u. The VSI_{min} (p.u.) is presented in Fig. 5.13

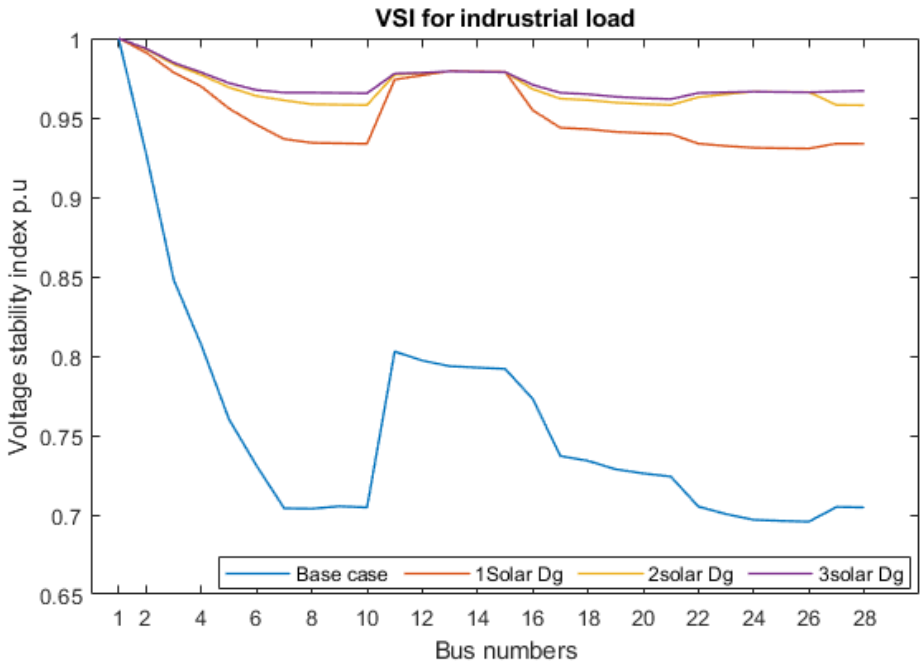

Fig. 5.13 Voltage Stability Index

From the above the VSI_{min} (p.u.) is enhanced@0.6957 p.u. → 0.8554 p.u. The effectiveness of the proposed Particle Swarm Optimization with Differential Velocities (PSODV) algorithm is evaluated in comparison with Firefly (FF) algorithm and Gorilla Troops Optimizer (GTO) algorithm and presented in Table 5.9.

Table 5.9 Performance Comparision 28 RDS

Method	Case Type	Power Losses (P_{loss}) kW	Voltage Minimum (V_{min}) P. U.	Voltage Stability Index (VSI_{min}) P. U.	Reduction of Losses (%)
Base case		67.3313	0.9133	0.6957	NA
Proposed PSODV Algorithm	1 SDG	50.4189	0.9306	0.7501	25.118
	2 SDG	35.7942	0.9579	0.8412	46.838
	3 SDG	33.3459	0.9617	0.8554	50.474
	1 SDG	50.061	0.9315	0.7545	25.64

GTO Algorithm	2 SDG	35.8397	0.9572	0.8395	47.90
	3 SDG	33.6501	0.9633	0.8611	50.09
FF Algorithm	1 SDG	50.955	0.9281	0.7398	25.89
	2 SDG	36.3512	0.9542	0.8332	47.17
	3 SDG	33.9388	0.9614	0.8542	50.6

From the above the proposed Particle Swarm Optimization with Differential Velocities (PSODV) algorithm exhibited the best performance i.e., the power loss P_{loss}(kW) is decreased from 67.3313 kW→33.3459kW, The voltage profile V_{min} (p.u.) is enhanced@0.9133 p.u. → 0.9617 p.u., the VSI_{min} (p.u.) is enhanced@0.6957 p.u. → 0.8554 p.u.

5.1.2 Optimal Location of DER on IEEE 85 RDS

In this optimal Location of DER Considering Solar DG is implemented on IEEE 85 RDS considering 1 solar DG, 2 solar DGs, 3 solar DGs under the residential load condition. In this case optimal location of DER on IEEE 85 RDS with residential load is implemented using the proposed Particle Swarm Optimization with Differential Velocities (PSODV) algorithm. The hourly power loss of residential load is presented in Table 5.10.

Table 5.10 Hourly Power loss of Residential Load

Time (Hr.)	P_{loss} (kW) (Base case)	Case 1 1 SDG P_{loss} (kW)	Case 2 2 SDG P_{loss} (kW)	Case 3 3 SDG P_{loss} (kW)
1	25.6948	19.2883	17.8878	17.5846
2	17.8929	13.4652	12.4953	12.2854
3	15.1852	11.4388	10.6173	10.4395
4	16.5099	12.4306	11.5366	11.343
5	16.5099	12.4306	11.5366	11.343
6	15.1852	11.4388	10.6173	10.4395
7	15.1852	11.4388	10.6173	10.4395
8	15.1852	11.4388	10.6173	10.4395
9	12.7092	9.5828	8.8969	8.7485
10	156.2447	114.472	105.5397	103.6013
11	206.9298	150.5699	138.6001	136.0015
12	247.6163	179.2536	164.811	161.675

13	253.796	183.5888	168.7682	165.55
14	156.2447	114.472	105.5397	103.6013
15	50.6864	37.8097	35.0099	34.4034
16	133.9921	98.4886	90.8729	89.2206
17	196.1106	142.899	131.5818	129.125
18	272.904	196.9587	180.9651	177.4919
19	299.741	215.6483	197.9978	194.1644
20	313.758	225.3733	206.8495	202.8271
21	196.1106	142.899	131.5818	129.125
22	98.8171	73.0406	67.4812	66.2759
23	45.8867	34.2664	31.7374	31.1895
24	27.4352	20.5843	19.0872	18.7632

The peak value are recorded at 20thhour. The P_{loss}(kW) is 313.7580 kW, V_{min}(p.u.) is 0.871 p.u., VSI_{min}(p.u.) is 0.5756. The system performance with the optimal allocation of 1 solar DG, 2 solar DGs, 3 solar DGs are tabulated in Table 5.11.

Table 5.11 System Performance for 85 RDS

Scenario	Location Of Bus	Sizes of DG (kW)	Power Losses (P_{loss}) kW	Voltage Minimum (V_{min}) P. U.	Voltage Stability Index (VSI_{min}) P. U.	Reduction of Losses (%)
BC	-	-	313.7580	0.871	0.5756	-
1 SDG	53	909.1118	225.3733	0.9095	0.6842	28.169
2 SDG	53 47	115.7 1018.5	206.8495	0.9148	0.7004	34.073
3 SDG	53 47 35	115.7488 339.2598 736.4913	202.8271	0.9161	0.7045	35.355

In 1 solar DG case DG is optimally placed on bus 53 with 909.1118 kW size. The P_{loss}(kW) is 225.3733 kW, V_{min}(p.u.) is 0.9095 p.u., VSI_{min}(p.u.) is 0.6842 kW, % Reduction of P_{loss} is 28.169%. In 2 solar DGs case DGs is optimally located at buses 53, 47 with sizes of 115.7 kW, 1018.5 kW. The P_{loss}(kW) is 206.8495 kW, V_{min}(p.u.)is

0.9148 p.u., VSI_{min}(p.u.) is 0.7004, % Reduction of P_{loss} is 34.073%. In 3 solar DGs case DGs is optimally located at buses 53, 47, 35 with sizes of 115.7488 kW, 339.2598 kW, 736.4913 kW. The P_{loss}(kW) is 202.8271 kW, V_{min}(p.u.) is 0.9161 p.u., VSI_{min}(p.u.) is 0.7045, % Reduction of P_{loss} is 35.355%.

The power loss comparision of all the cases for 24 hour profile and 85 RDS are presented in Fig. 5.14 and Fig. 5.15 respectively.

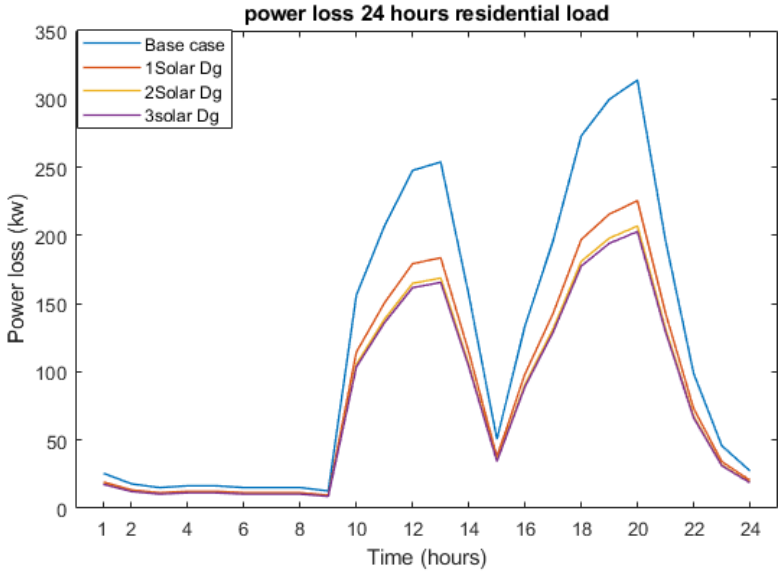

Fig. 5.14 Power Loss for 24 hour Profile

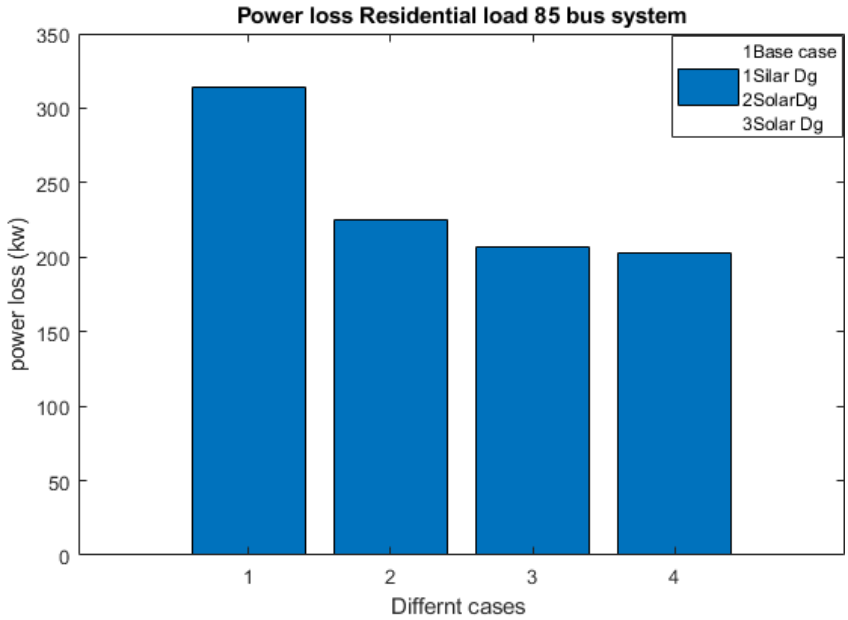

Fig. 5.15 Power Loss for 85 RDS System

From the above the peak power loss is recorded at 20th hour and the power loss P_{loss}(kW) is decreased from 313.7580 kW→202.8271kW. The voltage profile V_{min} (p.u.) is presented in Fig. 5.16.

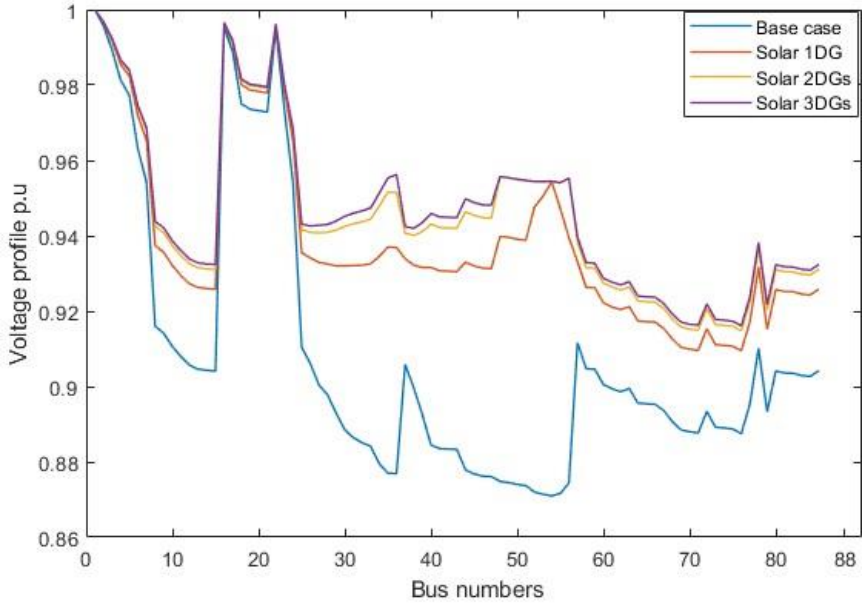

Fig. 5.16 Voltage Profile

From the above the The voltage profile V_{min} (p.u.) is enhanced@0.871 p.u. → 0.9161 p.u. The VSI_{min} (p.u.) is presented in Fig. 5.17

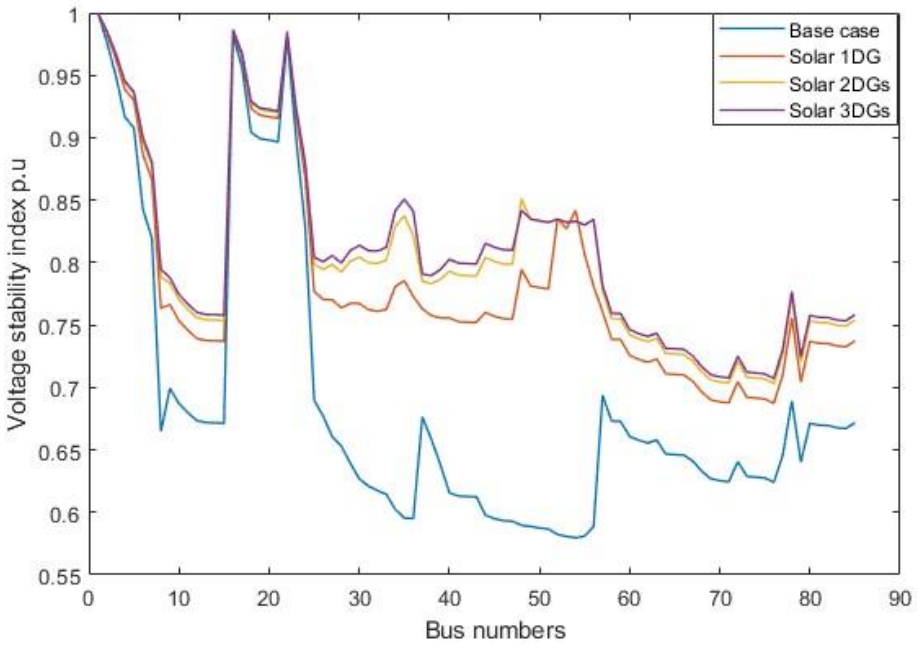

Fig. 5.17 Voltage Stability Index

From the above the VSI_{min} (p.u.) is enhanced@0.5767 p.u. → 0.7045 p.u. The effectiveness of the proposed Particle Swarm Optimization with Differential Velocities (PSODV) algorithm is evaluated in comparison with Firefly (FF) algorithm and Gorilla Troops Optimizer (GTO) algorithm and presented in Table 5.12.

Table 5.12 Performance Comparision 85 RDS

Method	Case Type	Power Losses (P_{loss}) kW	Voltage Minimum (V_{min}) P. U.	Voltage Stability Index (VSI_{min}) P. U.	Reduction of Losses (%)
Base case		313.7580	0.871	0.5756	NA
Proposed PSODV Algorithm	1 SDG	225.3733	0.9095	0.6842	28.169
	2 SDG	206.8495	0.9148	0.7004	34.073
	3 SDG	202.8271	0.9161	0.7045	35.355
GTO Algorithm	3 SDG	202.934	0.9091	0.7035	35.321
Fire fly Algorithm	3 SDG	202.051	0.9130	0.7012	35.60

From the above the proposed Particle Swarm Optimization with Differential Velocities (PSODV) algorithm exhibited the best performance i.e., the power loss P_{loss}(kW) is decreased from 313.7580 kW→202.8271kWkW, The voltage profile V_{min} (p.u.) is enhanced@0.871 p.u. → 0.9161 p.u, the VSI_{min} (p.u.) is enhanced@0.5767 p.u. → 0.7045 p.u.

5.2 Optimal Location of DER Considering Wind DG

In this case optimal location of DER with the solar DG is considered. The proposed Particle Swarm Optimization with Differential Velocities (PSODV) algorithm is implemented under residential, commertial, industrial loads on the following bus

- Optimal Location of DER on IEEE 28 RDS
- Optimal Location of DER on IEEE 85 RDS

The optimal bus location, size of DG are calculated and the performance evaluation parameters P_{loss}(kW), V_{min}(p.u.), VSI_{min}(p.u.), % Reduction $P_{loss}$are evaluated in all the cases. The effectiveness of the proposed Particle Swarm Optimization with Differential Velocities (PSODV) algorithm is evaluated in comparison with Firefly (FF) algorithm and Gorilla Troops Optimizer (GTO) algorithm. The block diagram for thewindDG in RDS is presented in Fig. 5.18.

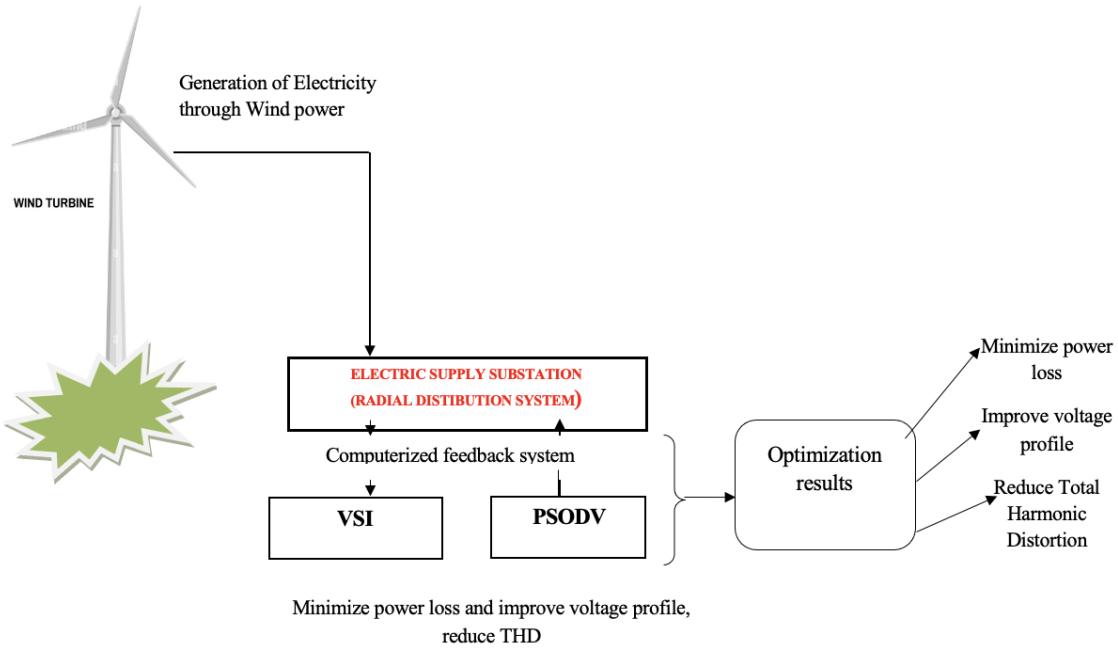

Fig 5.18Wind DG in RDS

5.2.1 Optimal Location of DER on IEEE 28 RDS

In this optimal Location of DER considering wind DG is implemented on IEEE 28 RDS considering 1 wind DG, 2 wind DGs, 3 wind DGs under the following cases.

- Optimal Location of DER on Indian 28 RDS with Residential Load
- Optimal Location of DER on Indian 28 RDS with Commertial Load
- Optimal Location of DER on Indian 28 RDS with Industrial Load

5.2.1.1 Optimal Location of DER on Indian 28 RDS with Residential Load

In this case optimal location of DER on IEEE 28 RDS with residential load is implemented using the proposed Particle Swarm Optimization with Differential Velocities (PSODV) algorithm. The peak value are recorded at 20^{th} hour. The P_{loss}(kW) is 68.8189 kW, V_{min}(p.u.) is 0.9123 p.u., VSI_{min}(p.u.) is 0.6927. The system

performance with the optimal allocation of 1 wind DG, 2 wind DGs, 3 wind DGs are tabulated in Table 5.13.

Table 5.13 System Performance for 28 RDS

Scenario	Location Of Bus	Sizes of DG (kW)	Power Losses (P_{loss}) kW	Voltage Minimum (V_{min}) P. U.	Voltage Stability Index (VSI_{min}) P. U.	Reduction of Losses (%)
BC	-	-	68.8189	0.9123	0.6927	-
1 WDG	12	437.7426	51.9385	0.9245	0.7306	24.528
2 WDG	12 23	264.3532 370.1155	36.5094	0.945	0.7876	46.94
3 WDG	12 23 27	227.1758 204.3472 246.1081	33.8018	0.9483	0.7985	50.88

In 1 wind DG case DG is optimally placed on bus 12 with 437.7426 kW size. The P_{loss}(kW) is 51.9385 kW, V_{min}(p.u.) is 0.9245 p.u., VSI_{min}(p.u.) is 0.7306, % Reduction of P_{loss} is 24.528%. In 2 wind DGs case DGs is optimally located at buses 12, 23 with sizes of 264.3532 kW, 370.1155 kW. The P_{loss}(kW) is 36.5094 kW, V_{min}(p.u.) is 0.945 p.u., VSI_{min}(p.u.) is 0.7876, % Reduction of P_{loss} is 46.94%. In 3 wind DGs case DGs is optimally located at buses 12, 23, 27 with sizes of 227.1758 kW, 204.3472 kW, 246.1081 kW. The P_{loss}(kW) is 33.8018 kW, V_{min}(p.u.) is 0.9483 p.u., VSI_{min}(p.u.) is 0.7985, % Reduction of P_{loss} is 50.88%.

The power loss comparision of all the cases for 24 hour profile and 28 RDS are presented in Fig. 5.19 respectively.

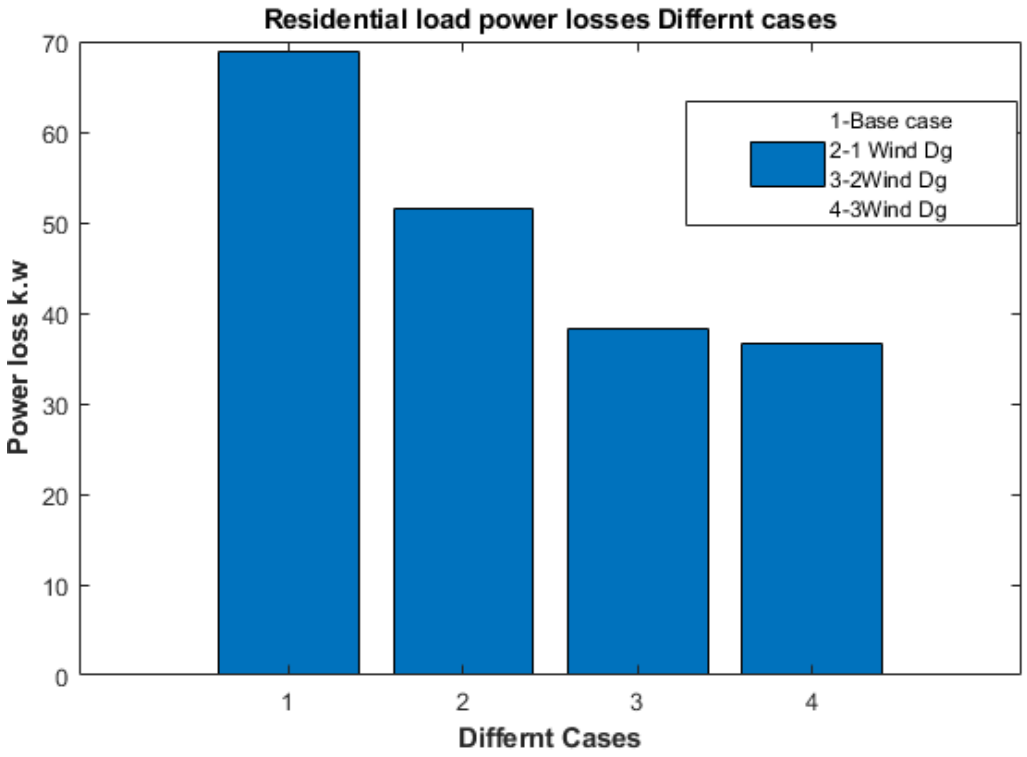

Fig. 5.19 Power Loss for 28 RDS System

From the above the peak power loss is recorded at 20th hour and the power loss P_{loss}(kW) is decreased from 68.8189 kW→33.8018kW. The voltage profile V_{min} (p.u.) is presented in Fig. 5.20.

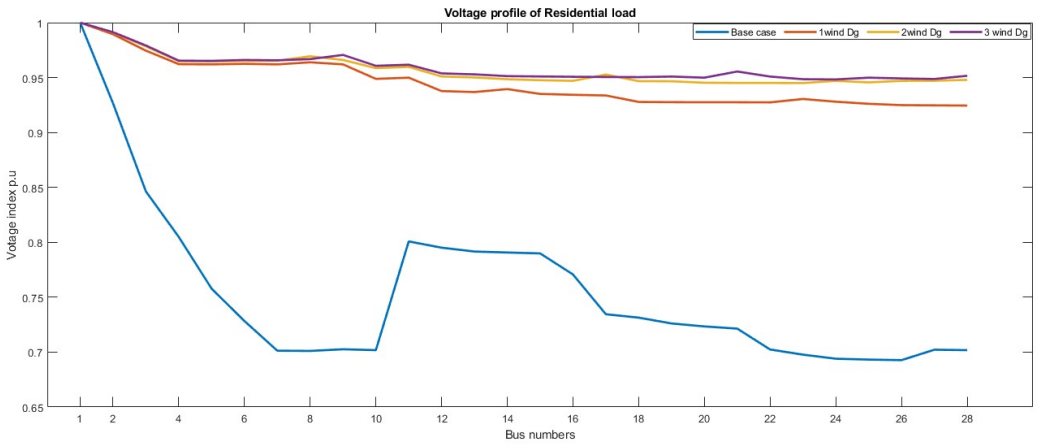

Fig. 5.20 Voltage Profile

From the above the The voltage profile V_{min} (p.u.) is enhanced@0.9123 p.u. → 0.9483 p.u. The VSI_{min} (p.u.) is presented in Fig. 5.21

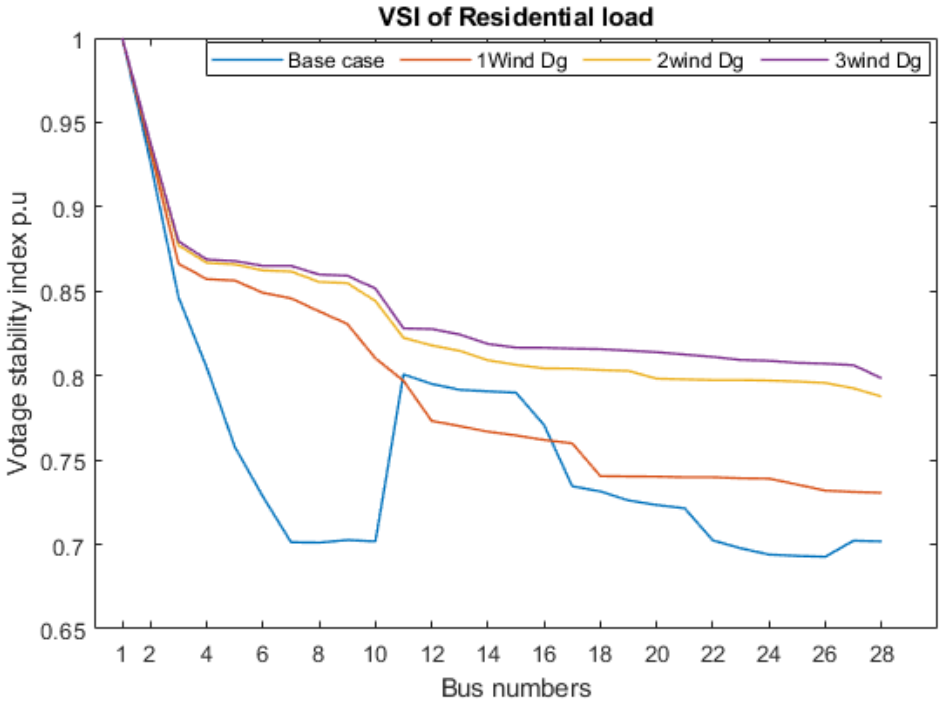

Fig. 5.21 Voltage Stability Index

From the above the VSI_{min} (p.u.) is enhanced@0.6927 p.u. → 0.7985 p.u. The effectiveness of the proposed Particle Swarm Optimization with Differential Velocities (PSODV) algorithm is evaluated in comparison with Firefly (FF) algorithm and Gorilla Troops Optimizer (GTO) algorithm and presented in Table 5.14.

Table 5.14 Performance Comparision 28 RDS

Method	Case Type	Power Losses (P_{loss}) kW	Voltage Minimum (V_{min}) P. U.	Voltage Stability Index (VSI_{min}) P. U.	Reduction of Losses (%)
Base case		68.8189	0.9123	0.6927	NA
Proposed PSODV Algorithm	1 WDG	51.9385	0.9245	0.7306	24.528
	2 WDG	36.5094	0.945	0.7876	46.948
	3 WDG	33.8018	0.9483	0.7985	49.117
GTO Algorithm	1 WDG	51.80	0.934	0.730	24.7299
	2 WDG	36.3361	0.941	0.7861	47.20
	3 WDG	33.6501	0.9439	0.8611	51.10

FF Algorithm	1 WDG	51.02	0.9231	0.7310	25.86
	2 WDG	36.2345	0.943	0.7872	47.348
	3 WDG	33.6513	0.9412	0.8413	51.1

From the above the proposed Particle Swarm Optimization with Differential Velocities (PSODV) algorithm exhibited the best performance i.e., the power loss P_{loss}(kW) is decreased from 68.8189 kW to 33.8018kW, The voltage profile V_{min} (p.u.) is enhanced@0.9123 p.u. → 0.983 p.u, the VSI_{min} (p.u.) is enhanced from 0.6927 p.u. → 0.7985 p.u.

5.2.1.2 Optimal Location of DER on Indian 28 RDS with Commertial Load

In this case optimal location of DER on IEEE 28 RDS with commertialload is implemented using the proposed Particle Swarm Optimization with Differential Velocities (PSODV) algorithm. The peak value are recorded at 11^{th} hour. The P_{loss}(kW) is 62.9824 kW, V_{min}(p.u.) is 0.9161 p.u., VSI_{min}(p.u.) is 0.7044. The system performance with the optimal allocation of 1 wind DG, 2 wind DGs, 3 wind DGs are tabulated in Table 5.15.

Table 5.15 System Performance for 28 RDS

Scenario	Location Of Bus	Sizes of DG (kW)	Power Losses (P_{loss}) kW	Voltage Minimum (V_{min}) P. U.	Voltage Stability Index (VSI_{min}) P. U.	Reduction of Losses (%)
BC	NA	NA	62.9824	0.9161	0.7044	NA
1 WDG	12	419.5841	47.5693	0.9278	0.7409	24.47
2 WDG	12 23	253.3407 355.1671	33.4898	0.9473	0.796	46.826
3 WDG	12 23 27	217.7411 196.0870 236.0546	31.0201	0.9505	0.8064	50.748

In 1 wind DG case DG is optimally placed on bus 12 with 419.5841 kW size. The P_{loss}(kW) is 47.5693 kW, V_{min}(p.u.) is 0.9278 p.u., VSI_{min}(p.u.) is 0.7409, % Reduction of P_{loss} is 24.47%. In 2 wind DGs case DGs is optimally located at buses 12, 23 with sizes of 253.3407 kW, 355.1671 kW. The P_{loss}(kW) is 33.4898 kW, V_{min}(p.u.) is 0.9473 p.u., VSI_{min}(p.u.) is 0.796, % Reduction of P_{loss} is 46.826%. In 3 wind DGs case DGs is optimally located at buses 12, 23, 27 with sizes of 217.7411 kW, 196.0870 kW, 236.0546 kW. The P_{loss}(kW) is 31.0201 kW, V_{min}(p.u.) is 0.9505 p.u., VSI_{min}(p.u.) is 0.8064, % Reduction of P_{loss} is 50.748%.

The power loss comparision of all the cases for 24 hour profile and 28 RDS are presented in Fig. 5.22.

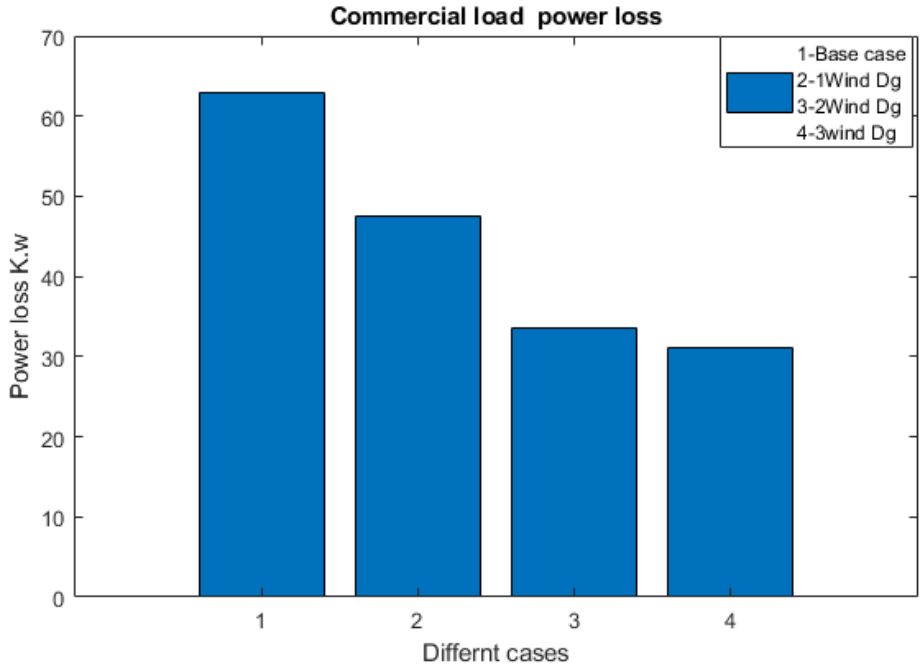

Fig. 5.22 Power Loss for 28 RDS System

From the above the peak power loss is recorded at 11^{th} hour and the power loss P_{loss}(kW) is decreased from 62.9824 kW→31.0201kW. The voltage profile V_{min} (p.u.) is presented in Fig. 5.23.

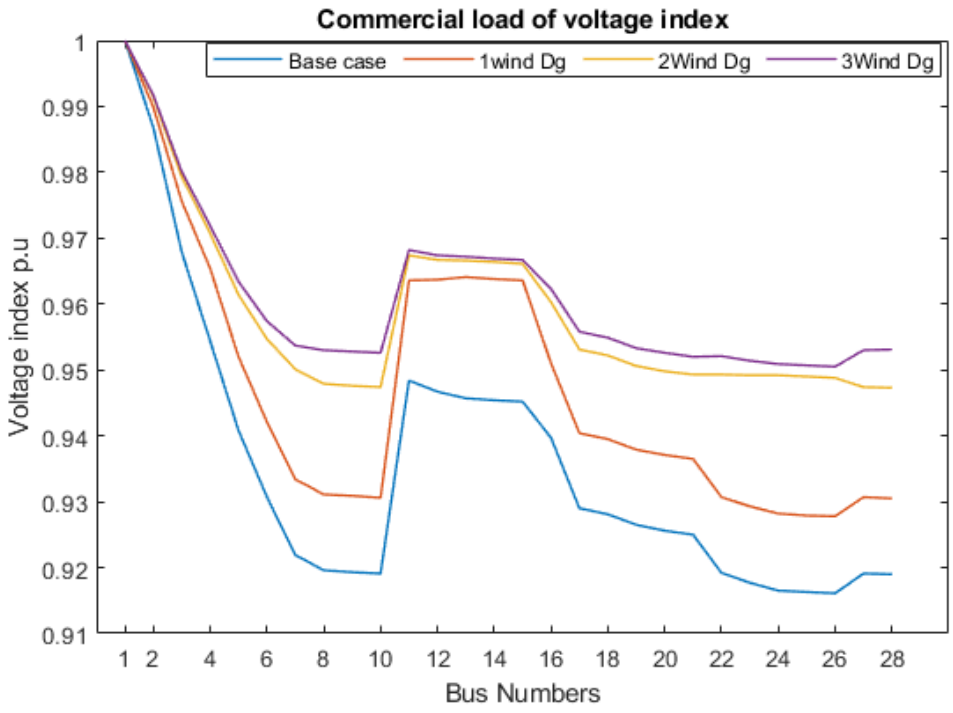

Fig. 5.23 Voltage Profile

From the above the The voltage profile V_{min} (p.u.) is enhanced@0.9161 p.u. → 0.9505 p.u. The VSI_{min} (p.u.) is presented in Fig. 5.24

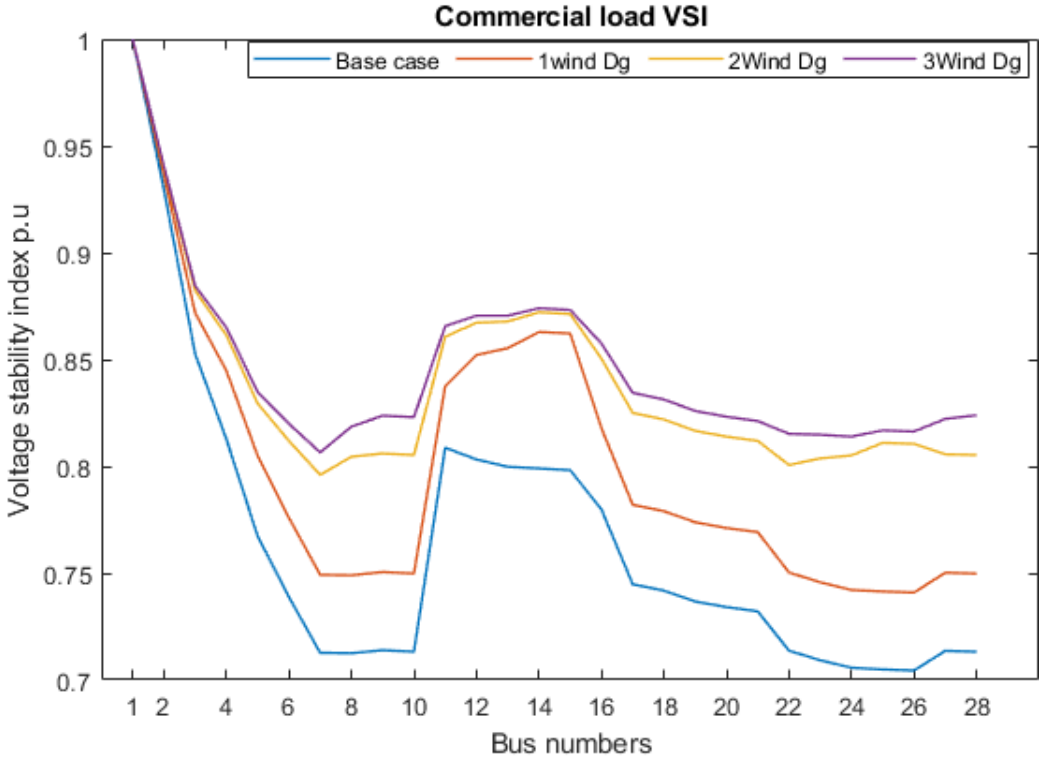

Fig. 5.24 Voltage Stability Index

From the above the VSI_{min} (p.u.) is enhanced@0.7044 p.u. → 0.8064 p.u. The effectiveness of the proposed Particle Swarm Optimization with Differential Velocities (PSODV) algorithm is evaluated in comparison with Firefly (FF) algorithm and Gorilla Troops Optimizer (GTO) algorithm. The proposed Particle Swarm Optimization with Differential Velocities (PSODV) algorithm exhibited the best performance i.e., the power loss P_{loss}(kW) is decreased from 62.9824 kW→31.0201kW, The voltage profile V_{min} (p.u.) is enhanced@0.9161 p.u. → 0.9505 p.u, the VSI_{min} (p.u.) is enhanced@0.7044 p.u. → 0.8064 p.u.

5.2.1.3 Optimal Location of DER on Indian 28 RDS with Industrial Load

In this case optimal location of DER on Indian 28 RDS with industrialload is implemented using the proposed Particle Swarm Optimization with Differential Velocities (PSODV) algorithm.The peak value are recorded at 21^{th} hour. The P_{loss}(kW) is 67.3313 kW, V_{min}(p.u.) is 0.9133 p.u., VSI_{min}(p.u.) is 0.6957. The system performance with the optimal allocation of 1 wind DG, 2 wind DGs, 3 wind DGs are tabulated in Table 516.

Table 5.16 System Performance for 28 RDS

Scenario	Location Of Bus	Sizes of DG (kW)	Power Losses (P_{loss}) kW	Voltage Minimum (V_{min}) P. U.	Voltage Stability Index (VSI_{min}) P. U.	Reduction of Losses (%)
BC	NA	NA	67.3313	0.9133	0.6957	NA
1 WDG	12	433.1962	50.8254	0.9253	0.7331	24.514
2 WDG	12 23	261.5905 366.3764	35.7409	0.9456	0.7897	48.40
3 WDG	12 23 27	224.8125 202.2946 243.5944	33.0940	0.9489	0.8005	50.849

In 1 wind DG case DG is optimally placed on bus 12 with 433.1962 kW size. The P_{loss}(kW) is 50.8254 kW, V_{min}(p.u.) is 0.9253 p.u., VSI_{min}(p.u.) is 0.7331, %

Reduction of P_{loss} is 24.514%. In 2 wind DGs case DGs is optimally located at buses 12, 23 with sizes of 261.5905 kW, 366.3764 kW. The P_{loss}(kW) is 35.7409 kW, V_{min}(p.u.) is 0.9456 p.u., VSI_{min}(p.u.) is 0.7897, % Reduction of P_{loss} is 48.40%. In 3 wind DGs case DGs is optimally located at buses 12, 23, 27 with sizes of 224.8125 kW, 202.2946 kW, 243.5944 kW. The P_{loss}(kW) is 33.0940 kW, V_{min}(p.u.) is 0.9489 p.u., VSI_{min}(p.u.) is 0.8005, % Reduction of P_{loss} is 50.849%.

The power loss comparision of all the cases for 24 hour profile and 28 RDS are presented in Fig. 5.25.

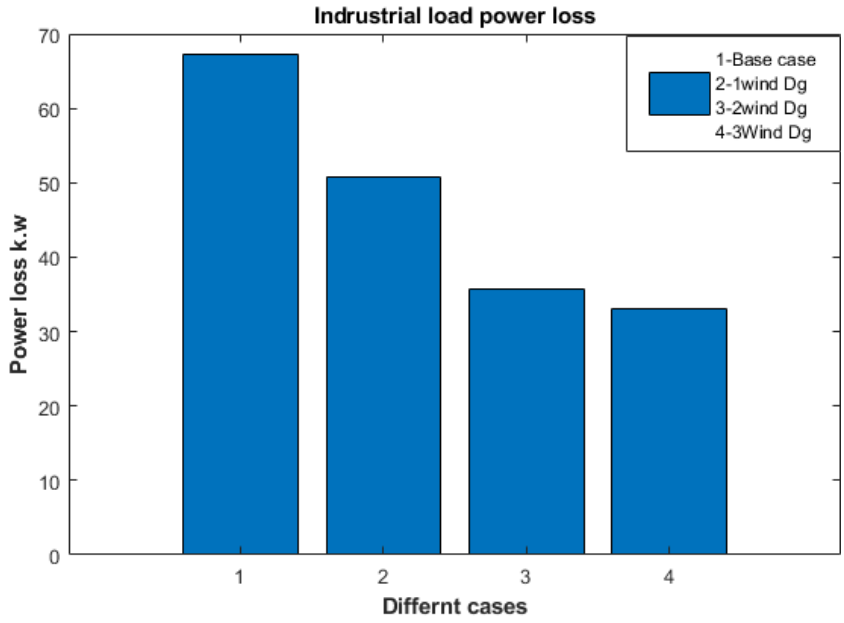

Fig. 5.25 Power Loss for 28 RDS System

From the above the peak power loss is recorded at 21th hour and the power loss P_{loss}(kW) is decreased from 67.3313 kW→33.0940kW. The voltage profile V_{min} (p.u.) is presented in Fig. 5.26.

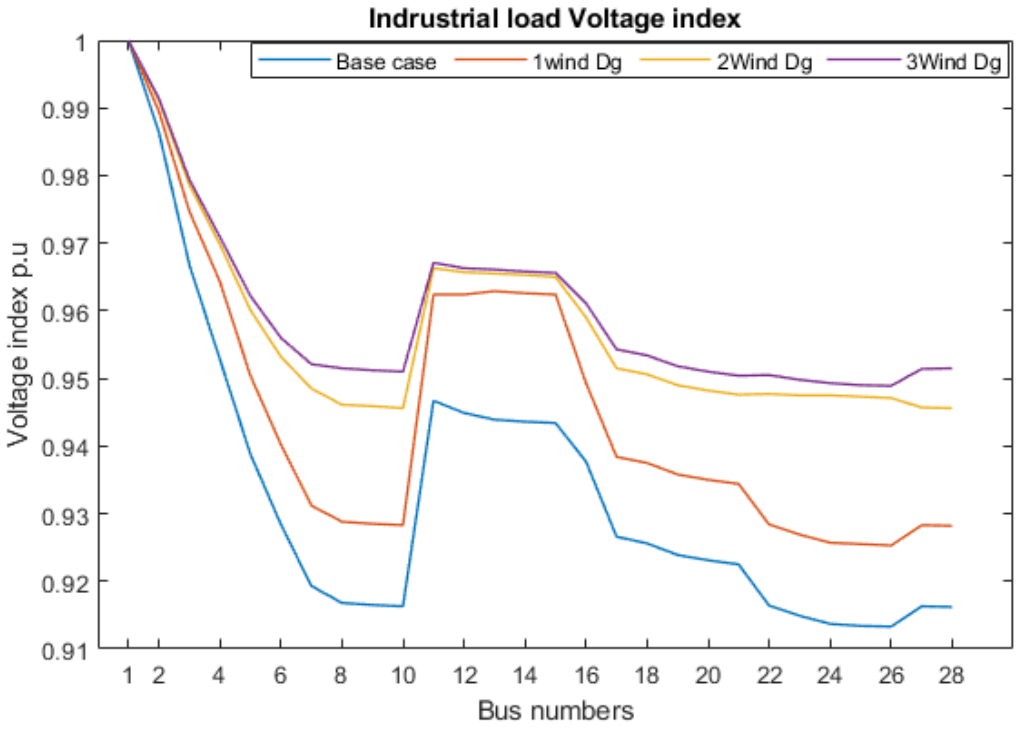

Fig. 5.26 Voltage Profile

From the above the The voltage profile V_{min} (p.u.) is enhanced@0.9133 p.u. →0.9489 p.u. The VSI_{min} (p.u.) is presented in Fig. 5.27

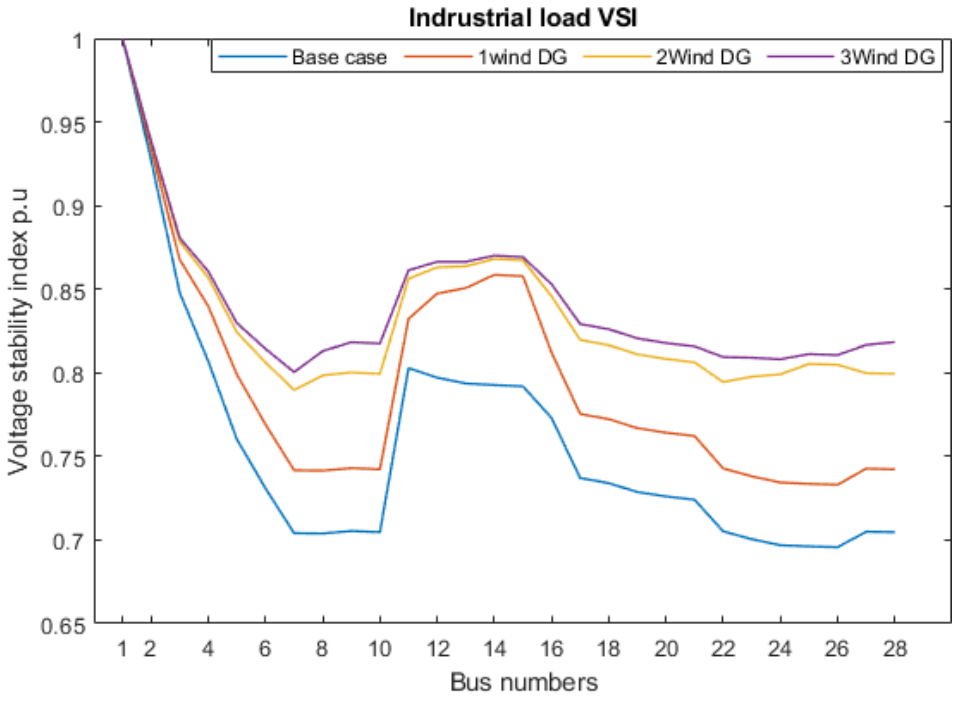

Fig. 5.27 Voltage Stability Index

From the above the VSI_{min} (p.u.) is enhanced@0.6957 p.u. →0.8005 p.u. The effectiveness of the proposed Particle Swarm Optimization with Differential Velocities (PSODV) algorithm is evaluated in comparison with Firefly (FF) algorithm and Gorilla Troops Optimizer (GTO) algorithm and presented in Table 5.17.

Table 5.17 Performance Comparision 28 RDS

Method	Case Type	Power Losses (P_{loss}) kW	Voltage Minimum (V_{min}) P. U.	Voltage Stability Index (VSI_{min}) P. U.	Reduction of Losses (%)
Base case		67.3313	0.9133	0.6957	NA
Proposed PSODV Algorithm	1 WDG	50.8254	0.9253	0.7331	24.51
	2 WDG	35.7409	0.9456	0.7897	46.91
	3 WDG	33.0940	0.9489	0.8005	50.84
GTO Algorithm	1 WDG	50.8354	0.9155	0.7321	24.49
	2 WDG	35.7219	0.9453	0.7834	46.94
	3 WDG	33.194	0.9480	0.801	50.7
FF Algorithm	1 WDG	50.9354	0.9143	0.731	24.34
	2 WDG	35.4215	0.9443	0.7842	47.392
	3 WDG	33.192	0.9460	0.7993	50.703

From the above the proposed Particle Swarm Optimization with Differential Velocities (PSODV) algorithm exhibited the best performance i.e., the power loss P_{loss}(kW) is decreased from 67.3313 kW→33.0940kW, The voltage profile V_{min} (p.u.) is enhanced@0.9489 p.u. → 0.9617 p.u., the VSI_{min} (p.u.) is enhanced@0.6957 p.u. → 0.8005 p.u.

5.2.2 Optimal Location of DER on IEEE 85 RDS

In this optimal Location of DER Considering Solar DG is implemented on IEEE 85 RDS considering 1 wind DG, 2 wind DGs, 3 wind DGs under the residential load condition. In this case optimal location of DER on IEEE 85 RDS with residential load is implemented using the proposed Particle Swarm Optimization with Differential

Velocities (PSODV) algorithm. The peak value are recorded at 20thhour. The P_{loss}(kW) is 313.7580 kW, V_{min}(p.u.) is 0.871 p.u., VSI_{min}(p.u.) is 0.5756. The system performance with the optimal allocation of 1 wind DG, 2 wind DGs, 3 wind DGs are tabulated in Table 5.18.

Table 5.18 System Performance for 85 RDS

Scenario	Location Of Bus	Sizes of DG (kW)	Power Losses (P_{loss}) kW	Voltage Minimum (V_{min}) P. U.	Voltage Stability Index (VSI_{min}) P. U.	Reduction of Losses (%)
BC	-	-	313.7580	0.871	0.5756	-
1 WDG	53	836.6005	230.3786	0.9025	0.6542	26.5744
2 WDG	53 47	117.8200 948.7168	211.2451	0.9065	0.6753	32.672
3 WDG	53 47 35	117.8159 325.4156 681.7519	207.1059	0.9075	0.6783	33.991

In 1 wind DG case DG is optimally placed on bus 53 with 836.6005 kW size. The P_{loss}(kW) is 230.3786 kW, V_{min}(p.u.) is 0.9025p.u., VSI_{min}(p.u.) is 0.6542 kW, % Reduction of P_{loss} is 26.5744%. In 2 wind DGs case DGs is optimally located at buses 53, 47 with sizes of 117.8200 kW, 948.7168 kW. The P_{loss}(kW) is 207.1059 kW, V_{min}(p.u.) is 0.9065 p.u., VSI_{min}(p.u.) is 0.6753, % Reduction of P_{loss} is 32.672%. In 3 solar DGs case DGs is optimally located at buses 53, 47, 35 with sizes of 117.8159 kW, 325.4156 kW, 681.7519 kW. The P_{loss}(kW) is 207.1059 kW, V_{min}(p.u.) is 0.9075 p.u., VSI_{min}(p.u.) is 0.6783, % Reduction of P_{loss} is 33.991%.

The power loss comparision of all the cases for and 85 RDS are presented in Fig. 5.28.

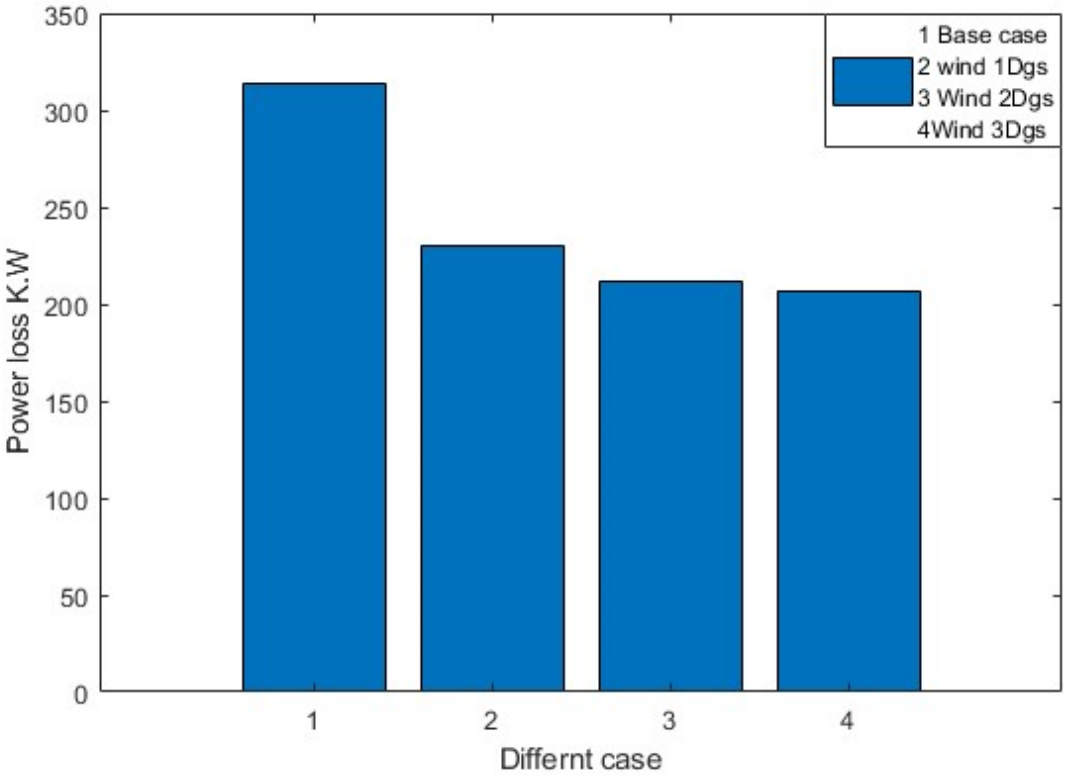

Fig. 5.28 Power Loss for 85 RDS System

From the above the peak power loss is recorded at 20th hour and the power loss P_{loss}(kW) is decreased from 313.7580 kW→207.1059kW. The voltage profile V_{min} (p.u.) is enhanced@0.871 p.u. → 0.9075 p.u. The VSI_{min} (p.u.) is enhanced@0.5767 p.u. →0.6783 p.u. The effectiveness of the proposed Particle Swarm Optimization with Differential Velocities (PSODV) algorithm is evaluated in comparison with Firefly (FF) algorithm and Gorilla Troops Optimizer (GTO) algorithm and presented in Table 5.19.

Table 5.19 Performance Comparision 85 RDS

Method	Case Type	Power Losses (P_{loss}) kW	Voltage Minimum (V_{min}) P. U.	Voltage Stability Index (VSI_{min}) P. U.	Reduction of Losses (%)
Base case		313.7580	0.871	0.5756	NA
	1 WDG	230.3786	0.9025	0.6542	26.574
	2 WDG	211.2451	0.9065	0.6753	32.67

Proposed PSODV Algorithm	3 WDG	207.1059	0.9075	0.6783	33.991

From the above the proposed Particle Swarm Optimization with Differential Velocities (PSODV) algorithm exhibited the best performance i.e., the power loss P_{loss}(kW) is decreased from 313.7580 kW to 207.1059kW kW, The voltage profile V_{min} (p.u.) is enhanced@0.871 p.u. →0.9075 p.u, the VSI_{min} (p.u.) is enhanced@0.5767 p.u. →0.6783 p.u.

5.3 Optimal Location of DER Considering Hybrid Solar-Wind DG

In this case optimal location of DER with the hybrid solar-wind DG is considered. The proposed Particle Swarm Optimization with Differential Velocities (PSODV) algorithm is implemented under residential, commertial, industrial loads on the following bus

- Optimal Location of DER on Indian 28 RDS
- Optimal Location of DER on IEEE 85 RDS

The optimal bus location, size of DG are calculated and the performance evaluation parameters P_{loss}(kW), V_{min}(p.u.), VSI_{min}(p.u.), % Reduction $P_{loss}$are evaluated in all the cases. The effectiveness of the proposed Particle Swarm Optimization with Differential Velocities (PSODV) algorithm is evaluated in comparison with Firefly (FF) algorithm and Gorilla Troops Optimizer (GTO) algorithm. The block diagram for thewindDG in RDS is presented in Fig. 5.29.

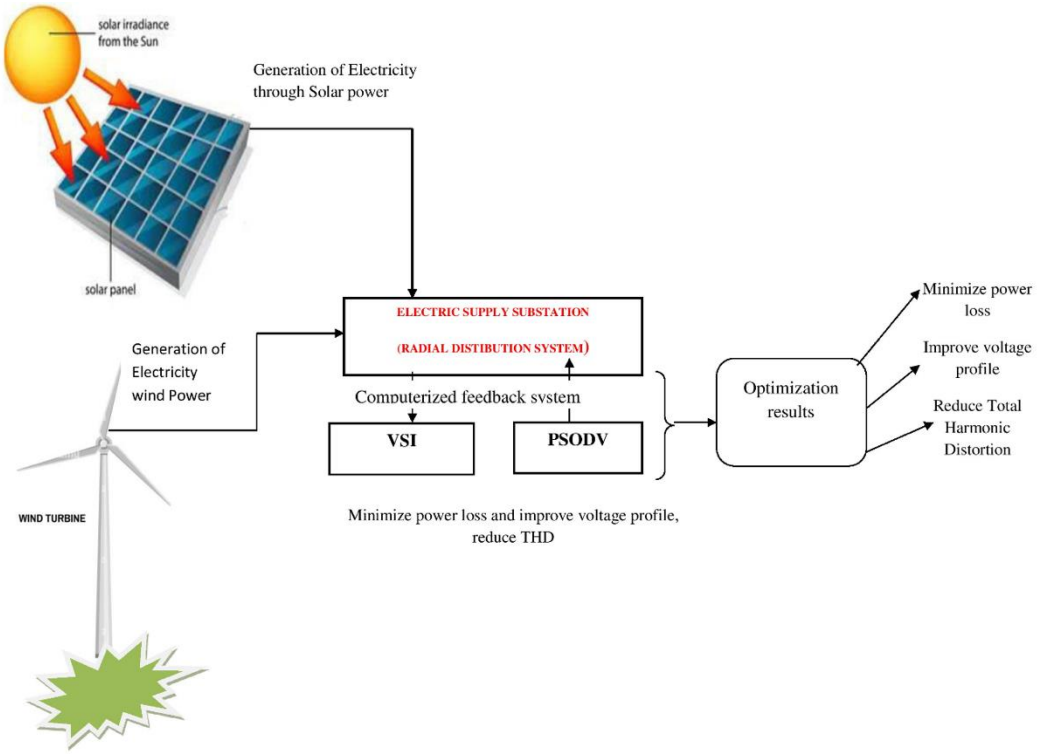

Fig 5.29Hybrid Solar-Wind DG in RDS

5.3.1 Optimal Location of DER on Indian 28 RDS

In this optimal Location of DER considering wind DG is implemented on IEEE 28 RDS considering 1 solar and 1 wind DGs under the following cases.

- Optimal Location of DER on Indian 28 RDS with Residential Load
- Optimal Location of DER onIndian28 RDS with Commertial Load
- Optimal Location of DER onIndian28 RDS with Industrial Load

5.3.1.1 Optimal Location of DER on Indian 28 RDS with Residential Load

In this case optimal location of DER on Indian 28 RDS with residential load is implemented using the proposed Particle Swarm Optimization with Differential Velocities (PSODV) algorithm. The hourly power loss of residential load is presented in Table 5.20.

Table 5.20 Hourly Power loss of Residential Load

Time (Hr.)	P_{loss} (kW) (Base case)	1 SDG & I WDG P_{loss} (kW)
1	5.9219	3.1571
2	4.1354	2.2099
3	3.51349	1.8793
4	3.81789	2.0412
5	3.81789	2.0412
6	3.51349	1.8793
7	3.51349	1.8793
8	3.51349	1.8793
9	2.943826	1.576
10	35.03816	18.2734
11	46.04865	23.8743
12	54.78727	28.2828
13	56.10727	28.946
14	35.03816	18.2734
15	11.59909	6.1476
16	30.158	15.7731
17	43.7101	22.6892
18	60.1769	30.9865
19	65.8628	33.8268
20	**68.8189**	**35.2987**
21	43.7101	22.6892
22	22.3811	11.7638
23	10.5135	5.5778
24	6.3194	3.3674

The peak value are recorded at 20^{th} hour. The P_{loss}(kW) is 68.8189 kW, V_{min}(p.u.) is 0.9123 p.u., VSI_{min}(p.u.) is 0.6927. The system performance with the optimal allocation of 1 Solar and 1 Wind DGs are tabulated in Table 5.21.

Table 5.21 System Performance for 28 RDS

Scenario	Location Of Bus	Sizes of DG (kW)	Power Losses (P_{loss}) kW	Voltage Minimum (V_{min}) P. U.	Voltage Stability Index (VSI_{min}) P. U.	Reduction of Losses (%)
Base case	NA	NA	68.8189	0.9123	0.6927	NA
1 SDG & I WDG	12 12	448.0347 844.3601	35.2997	0.9422	0.7881	48.70

In 1 Solar and 1 Wind DGs case is optimally placed on buses 12, 12 with 448.0347 kW, 844.3601 kW sizes. The P_{loss}(kW) is 35.2997 kW, V_{min}(p.u.) is 0.9422p.u., VSI_{min}(p.u.) is 0.7881, % Reduction of P_{loss} is 48.70%. The power loss for different cases are presented in Table 5.22

Table 5.22 Power loss for Different cases

Base case	**1 SDG**	**2 SDG**	**3 SDG**	**1 SDG, 1WDG**	**2 SDG, 1WDG**	**1 SDG, 2WDG**
68.819	51.511	38.31	36.689	35.2987	21.437	21.1011

The power loss comparision of all the cases for 24 hour profile and 28 RDS are presented in Fig. 5.30 and Fig. 5.31 respectively.

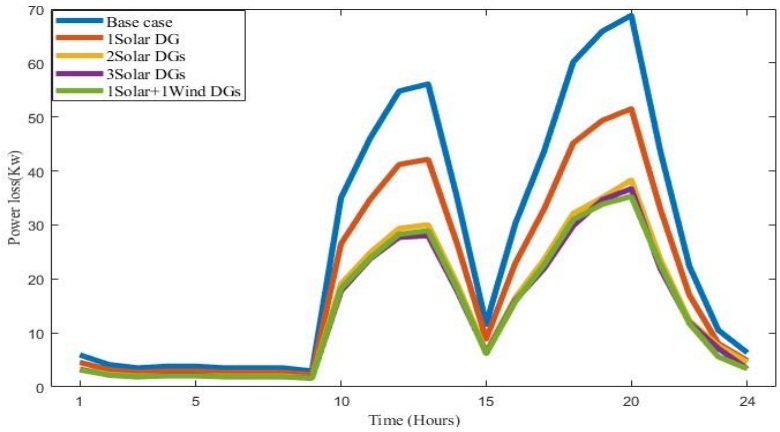

Fig. 5.30 Power Loss for 24 hour Profile

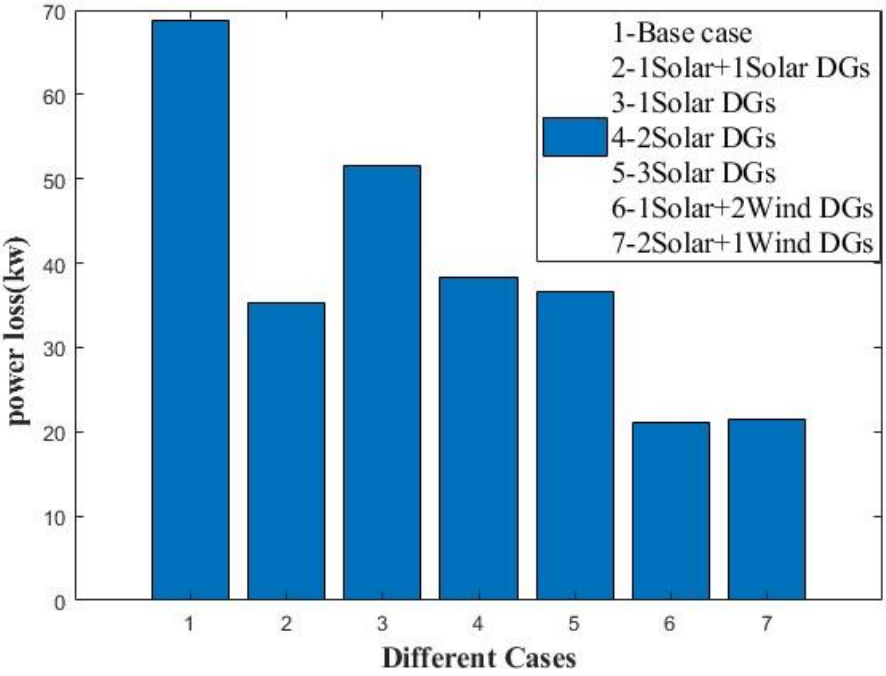

Fig. 5.31 Power Loss for 28 RDS System

From the above the peak power loss is recorded at 20th hour and the power loss P_{loss}(kW) is decreased from 68.8189 kW→35.2997kW. The voltage profile V_{min} (p.u.) is presented in Fig. 5.32&5.33

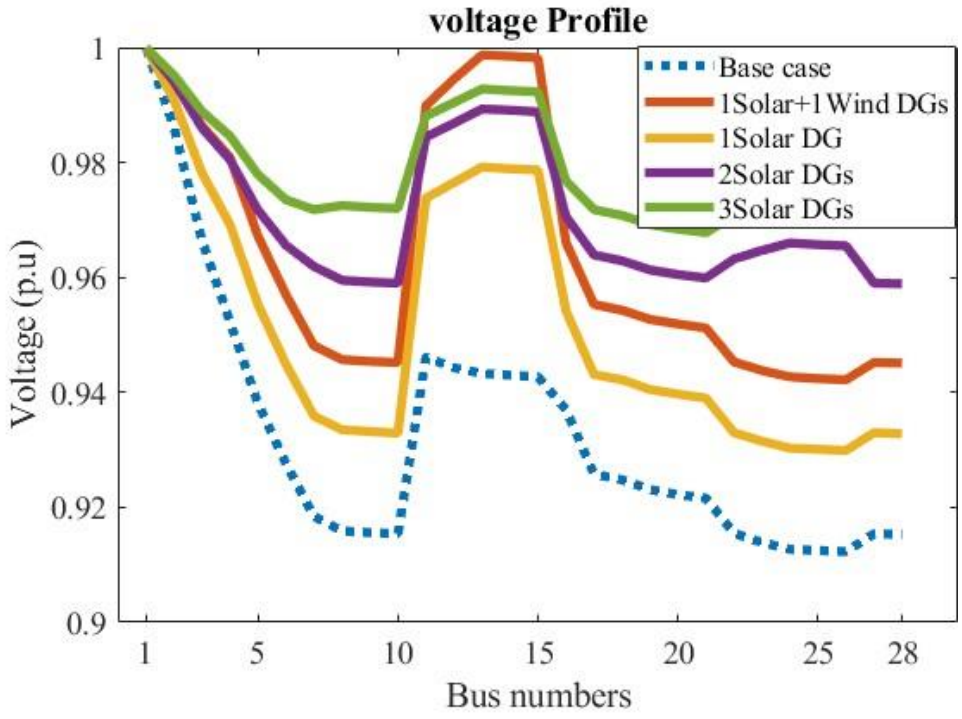

Fig. 5.32 Power Voltage profile for 28 RDS System

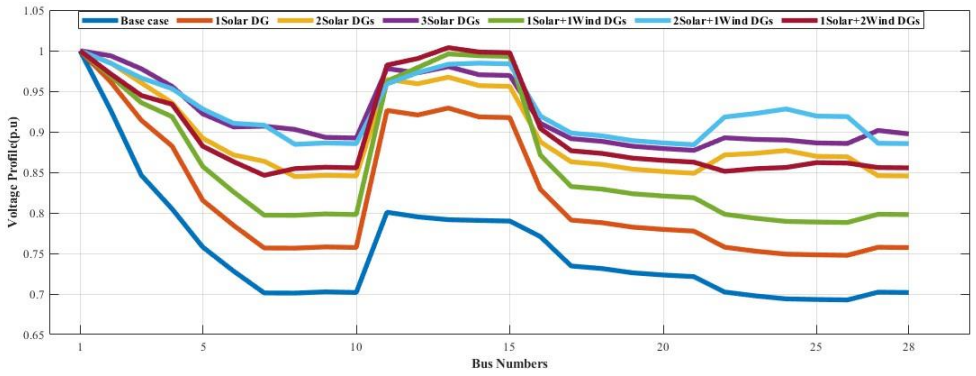

Fig. 5.33 Voltage Profile

From the above the The voltage profile V_{min} (p.u.) is enhanced@0.9123 p.u. → 0.9422 p.u. The VSI_{min} (p.u.) is presented in Fig. 5.34&5.35 respectively.

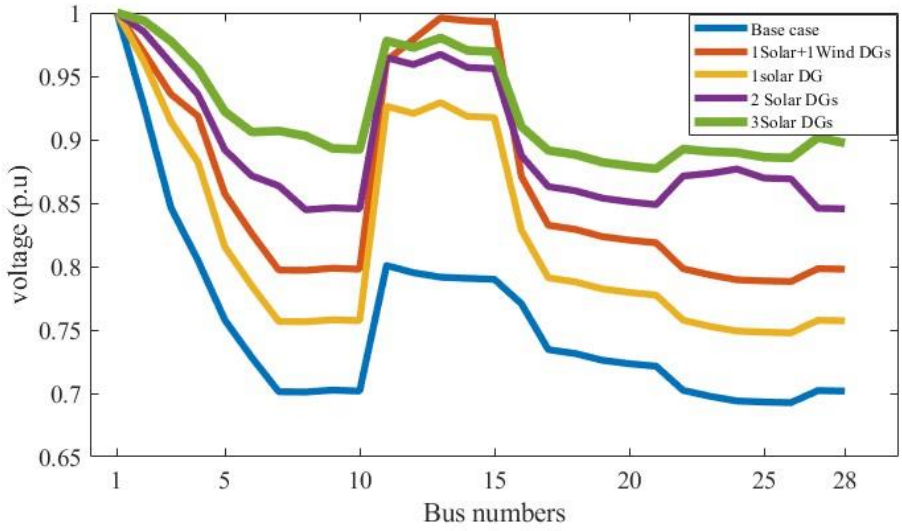

Fig 5.34 Voltage stability index

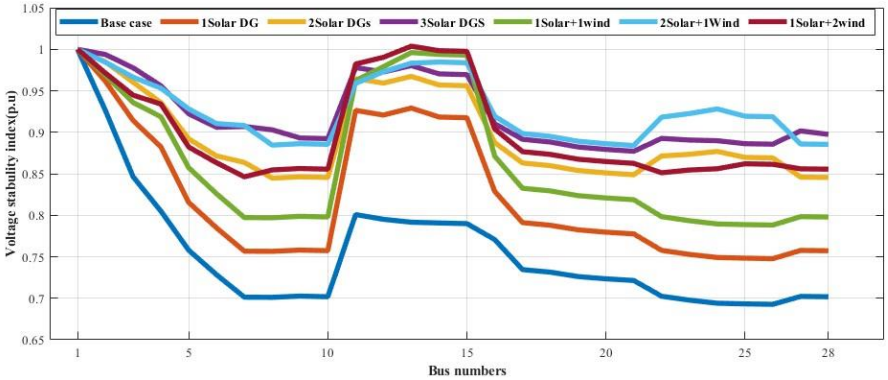

Fig. 5.35Voltage Stability Index

From the above the VSI_{min} (p.u.) is enhanced@0.6927 p.u. → 0.7881 p.u. The effectiveness of the proposed Particle Swarm Optimization with Differential Velocities (PSODV) algorithm is evaluated in comparison with Firefly (FF) algorithm and Gorilla Troops Optimizer (GTO) algorithm and presented in Table 5.23.

Table 5.23 Performance Comparision 28 RDS

Method	Case Type	Power Losses (P_{loss}) kW	Voltage Minimum (V_{min}) P. U.	Voltage Stability Index (VSI_{min}) P. U.	Reduction of Losses (%)
Base case		68.8189	0.9123	0.6927	NA
Proposed PSODV Algorithm	1 SDG & I WDG	35.2997	0.9422	0.7881	48.47
GTO Algorithm	1 SDG & I WDG	35.192	0.941	0.775	48.86
FF Algorithm	1 SDG & I WDG	35.023	0.940	0.774	49.10

From the above the proposed Particle Swarm Optimization with Differential Velocities (PSODV) algorithm exhibited the best performance i.e., the power loss P_{loss}(kW) is decreased @ 68.8189 kW→35.2997kW, The voltage profile V_{min} (p.u.) is enhanced@0.9123 p.u. → 0.9422 p.u, the VSI_{min} (p.u.) is enhanced from 0.6927 p.u. → 0.7881 p.u.

5.2.1.2 Optimal Location of DER on Indian 28 RDS with Commertial Load

In this case optimal location of DER on Indian 28 RDS with commertialload is implemented using the proposed Particle Swarm Optimization with Differential Velocities (PSODV) algorithm. The hourly power loss of residential load is presented in Table 5.24.

Table 5.24 Hourly Power loss of Commertial Load

Time (Hr.)	P_{loss} (kW) (Base case)	1 SDG & I WDG P_{loss} (kW)
1	4.8101	2.568
2	4.8101	2.568
3	4.4661	2.3855
4	4.8101	2.568
5	5.5379	2.9538
6	8.0453	4.2789
7	38.1638	19.8689
8	53.4854	27.628
9	58.802	30.2979
10	60.1769	30.9865
11	**62.9824**	**32.3895**
12	58.802	30.2979
13	52.2015	26.9816
14	50.9355	26.3435
15	42.5668	22.1089
16	23.9996	12.6009
17	15.1998	8.0315
18	12.1632	6.4434
19	9.9919	5.3037
20	9.9919	5.3037
21	11.0492	5.8591
22	10.5135	5.5778
23	6.7304	3.5847
24	4.4661	2.3855

The peak value are recorded at 11^{th} hour. The P_{loss}(kW) is 62.9824 kW, V_{min}(p.u.) is 0.9161 p.u., VSI_{min}(p.u.) is 0.7044. The system performance with the optimal allocation of 1 Solar and 1 Wind DGs are tabulated in Table 5.25.

Table 5.25 System Performance for 28 RDS

Scenario	Location Of Bus	Sizes of DG (kW)	Power Losses (P_{loss}) kW	Voltage Minimum (V_{min}) P. U.	Voltage Stability Index (VSI_{min}) P. U.	Reduction of Losses (%)
BC	NA	NA	62.9824	0.9161	0.7044	NA
1 SDG & I WDG	12 12	428.8391 802.1811	32.3902	0.9446	0.7962	48.5726

In 1 Solar and 1 Wind DGs case DGs are optimally located at buses 12, 12 with sizes of 428.8391 kW, 802.1811 kW. The P_{loss}(kW) is 32.3902 kW, V_{min}(p.u.) is 0.9446 p.u., VSI_{min}(p.u.) is 0.7962, % Reduction of P_{loss} is 44.33 %.

The power loss comparision of all the cases for 24 hour profile and 28 RDS are presented in Fig. 5.36 and Fig. 5.37 respectively.

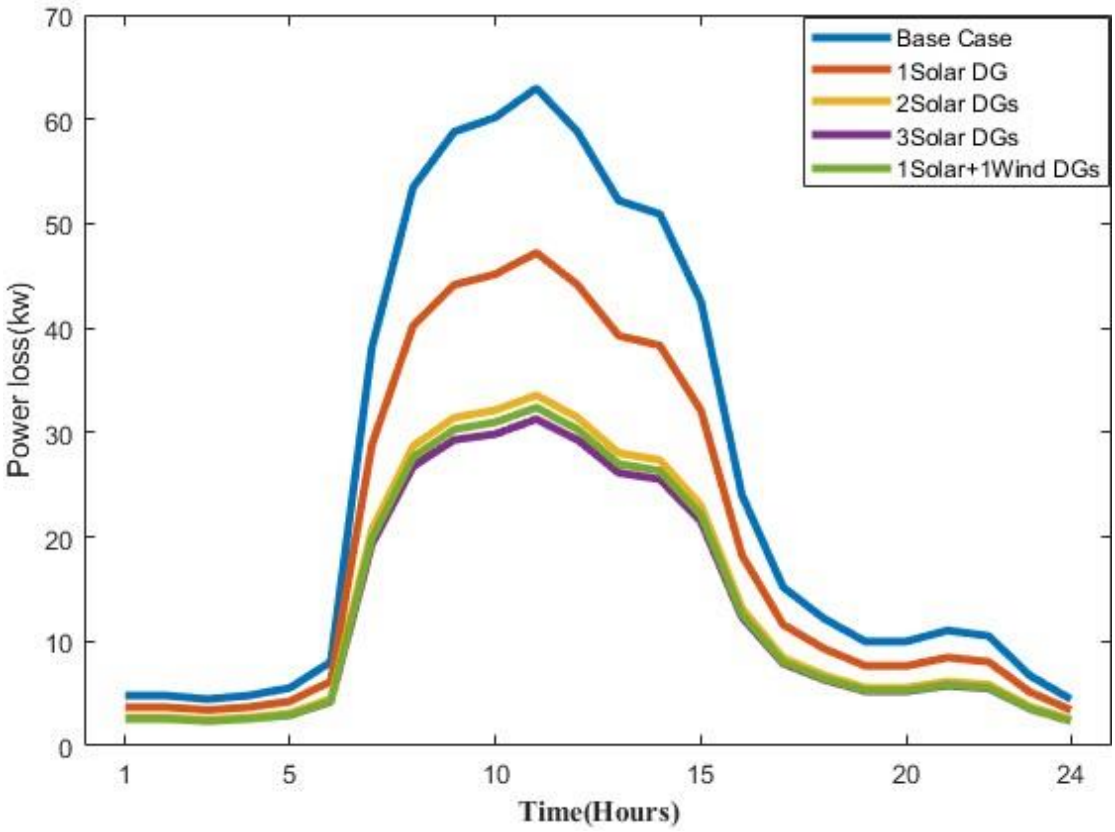

Fig. 5.36 Power Loss for 24 hour Profile

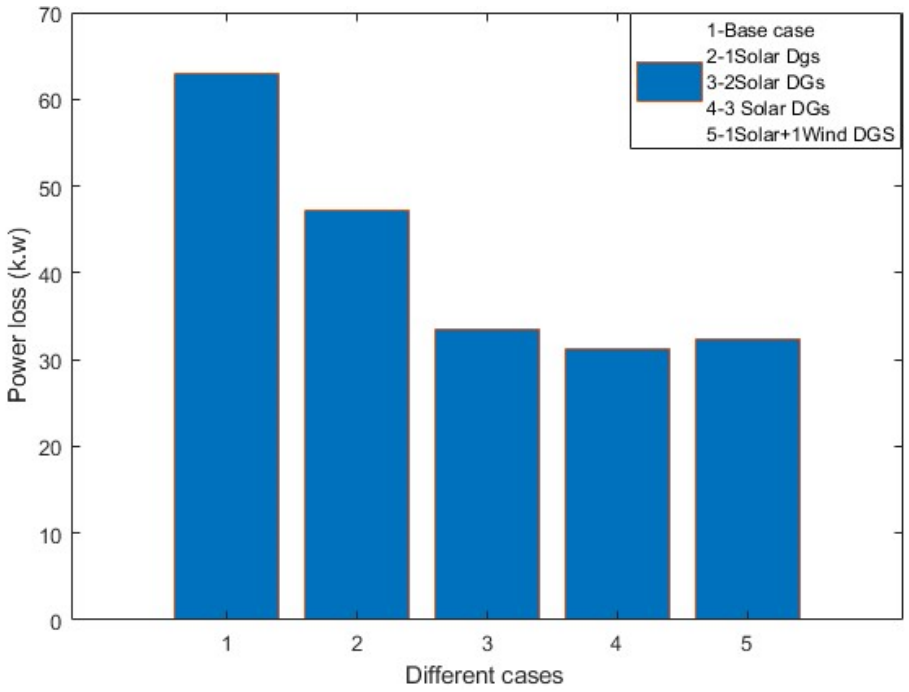

Fig. 5.37 Power Loss for 28 RDS System

From the above the peak power loss is recorded at 11th hour and the power loss P_{loss}(kW) is decreased @62.9824 kW→32.3902kW. The voltage profile V_{min} (p.u.) is presented in Fig. 5.38.

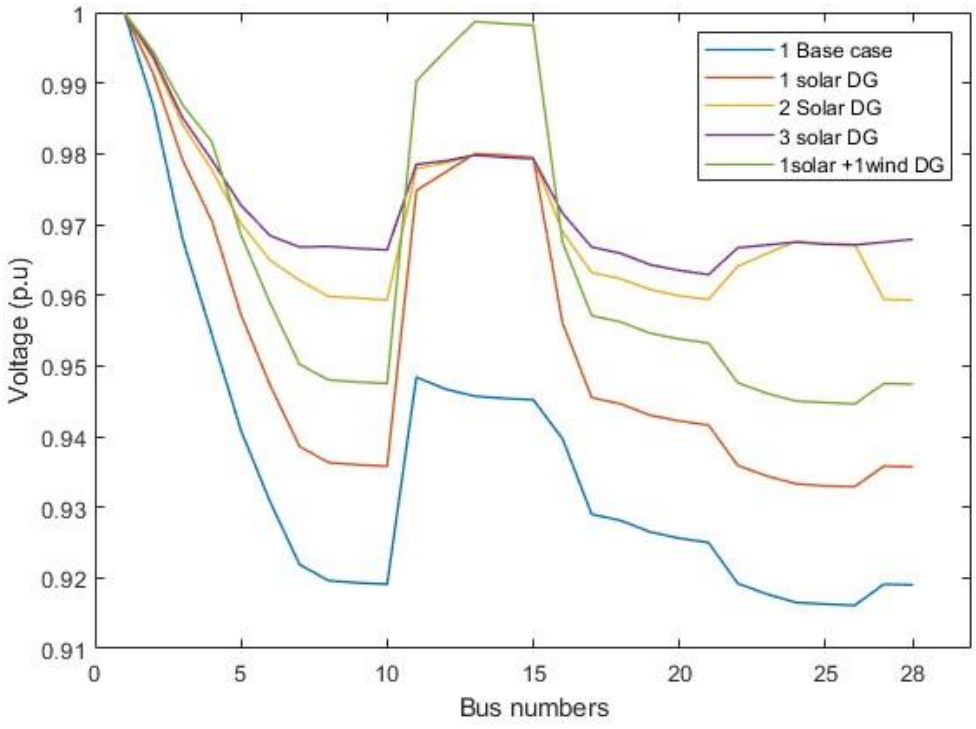

Fig. 5.38 Voltage Profile

From the above the The voltage profile V_{min} (p.u.) is enhanced@0.9161 p.u. →0.9446 p.u. The VSI_{min} (p.u.) is presented in Fig. 5.39

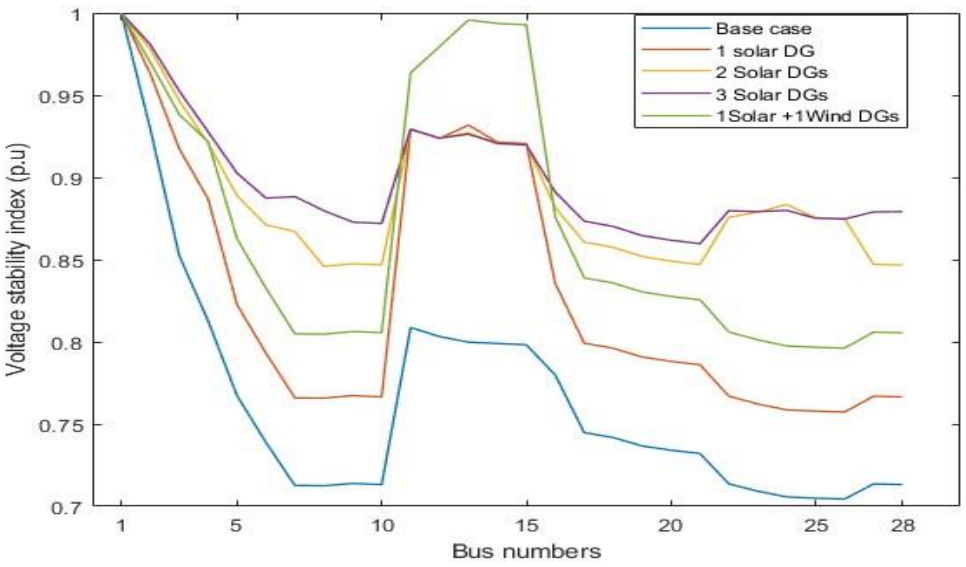

Fig. 5.39 Voltage Stability Index

From the above the VSI_{min} (p.u.) is enhanced@0.7044 p.u. →0.7962 p.u. The effectiveness of the proposed Particle Swarm Optimization with Differential Velocities (PSODV) algorithm is evaluated in comparison with Firefly (FF) algorithm and Gorilla Troops Optimizer (GTO) algorithm and presented in Table 5.26.

Table 5.26 Performance Comparision 28 RDS

Method	Case Type	Power Losses (P_{loss}) kW	Voltage Minimum (V_{min}) P. U.	Voltage Stability Index (VSI_{min}) P. U.	Reduction of Losses (%)
Base case		62.9824	0.9161	0.7044	NA
Proposed PSODV Algorithm	1 SDG & I WDG	32.3902	0.9446	0.7962	48.57
GTO Algorithm	1 SDG & I WDG	32.023	0.939	0.792	49.155
FF Algorithm	1 SDG & I WDG	31.992	0.9321	0.790	49.02

From the above the proposed Particle Swarm Optimization with Differential Velocities (PSODV) algorithm exhibited the best performance i.e., the power loss P_{loss}(kW) is decreased from 62.9824 kW→32.3902kW, The voltage profile V_{min} (p.u.) is enhanced@0.9161 p.u. →0.9446 p.u, the VSI_{min} (p.u.) is enhanced@0.7044 p.u. →0.7962 p.u.

5.3.1.3 Optimal Location of DER on Indian 28 RDS with Industrial Load

In this case optimal location of DER on Indian 28 RDS with industrialload is implemented using the proposed Particle Swarm Optimization with Differential Velocities (PSODV) algorithm. The hourly power loss of residential load is presented in Table 5.27.

Table 5.27 Hourly Power loss of Industrial Load

Time (Hr.)	P_{loss} (kW) (Base case)	1 SDG & I WDG P_{loss} (kW)
1	8.0453	4.2789
2	4.4661	2.3855
3	4.1354	2.2099
4	4.1354	2.2099
5	3.5135	1.8793
6	3.5135	1.8793
7	9.9919	5.3037
8	11.0492	5.8591
9	20.8242	10.9572
10	21.595	11.3568
11	17.1971	9.0727
12	15.1998	8.0315
13	14.5635	7.6992
14	22.3811	11.7638
15	18.6028	9.804
16	28.3192	14.828

17	23.9996	12.6009
18	50.9355	26.3435
19	53.4854	27.628
20	64.4132	33.1038
21	**67.3313**	**34.5584**
22	58.802	30.2979
23	37.1053	19.3291
24	18.6028	9.804

The peak value are recorded at 21th hour. The P_{loss}(kW) is 67.3313 kW, V_{min}(p.u.) is 0.9133 p.u., VSI_{min}(p.u.) is 0.6957. The system performance with the optimal allocation of 1 Solar and 1 Wind DGs are tabulated in Table 5.28.

Table 5.28 System Performance for 28 RDS

Scenario	Location Of Bus	Sizes of DG (kW)	Power Losses (P_{loss}) kW	Voltage Minimum (V_{min}) P. U.	Voltage Stability Index (VSI_{min}) P. U.	Reduction of Losses (%)
BC	NA	NA	67.3313	0.9133	0.6957	NA
1 SDG & I WDG	12 12	443.2239 618.0023	34.5593	0.9428	0.7901	48.672

In 1 Solar and 1 Wind DGs case DGs is optimally placed on buses 12, 12 with 443.2239 kW, 618.0023 kW sizes. The P_{loss}(kW) is 34.5593 kW, V_{min}(p.u.) is 0.9428 p.u., VSI_{min}(p.u.) is 0.7901, % Reduction of P_{loss} is 48.672%.

The power loss comparision of all the cases for 24 hour profile and 28 RDS are presented in Fig. 5.40 and Fig. 5.41 respectively.

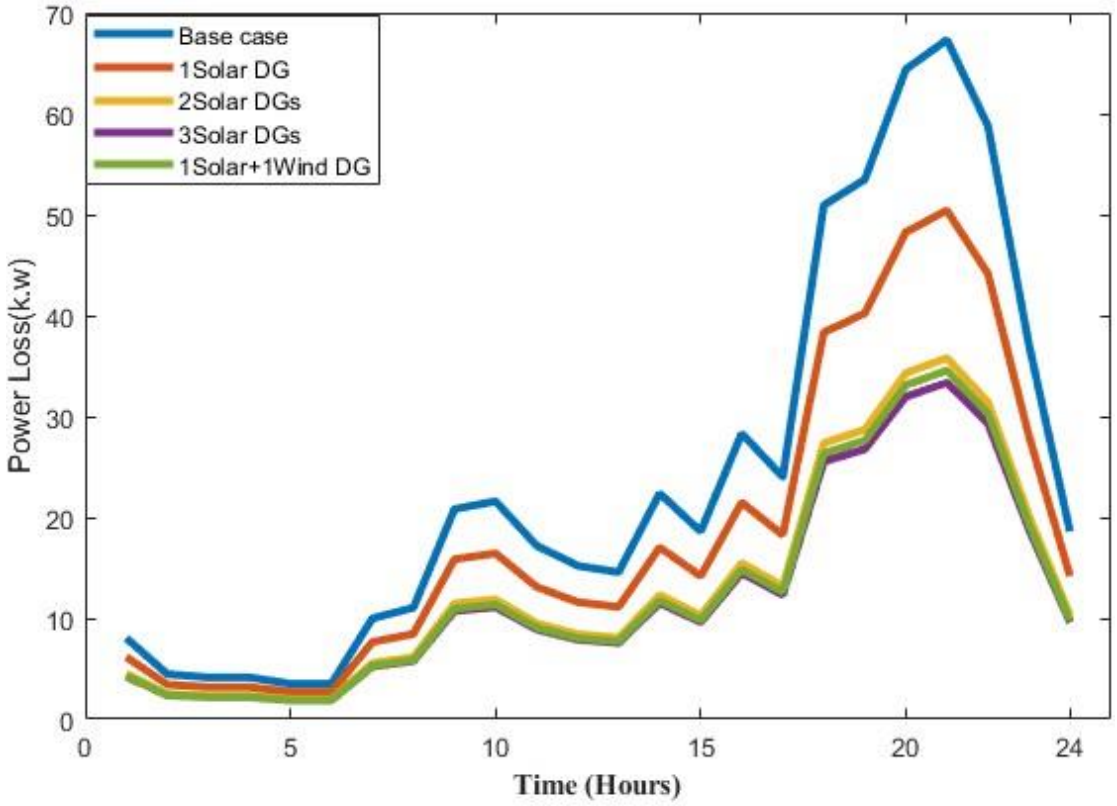

Fig. 5.40 Power Loss for 24 hour Profile

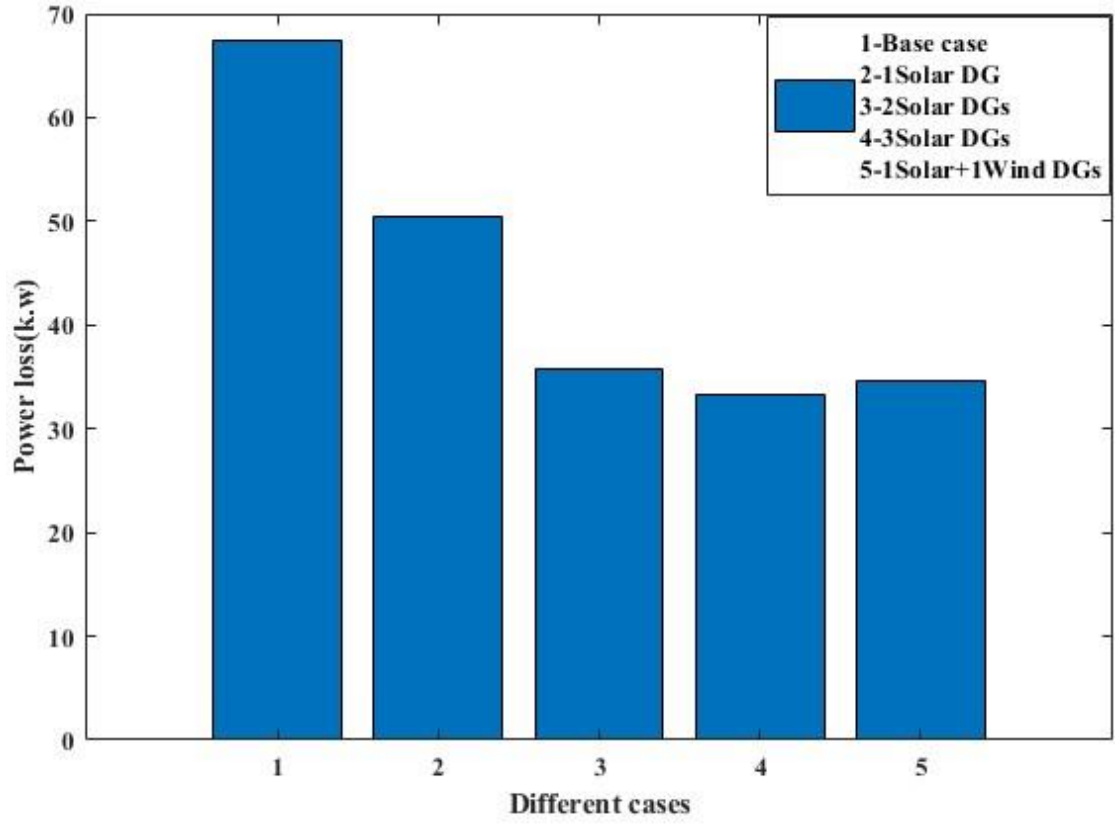

Fig. 5.41 Power Loss for 28 RDS System

From the above the peak power loss is recorded at 21th hour and the power loss P_{loss}(kW) is decreased abotut67.3313 kW→34.5593kW. The voltage profile V_{min} (p.u.) is presented in Fig. 5.42.

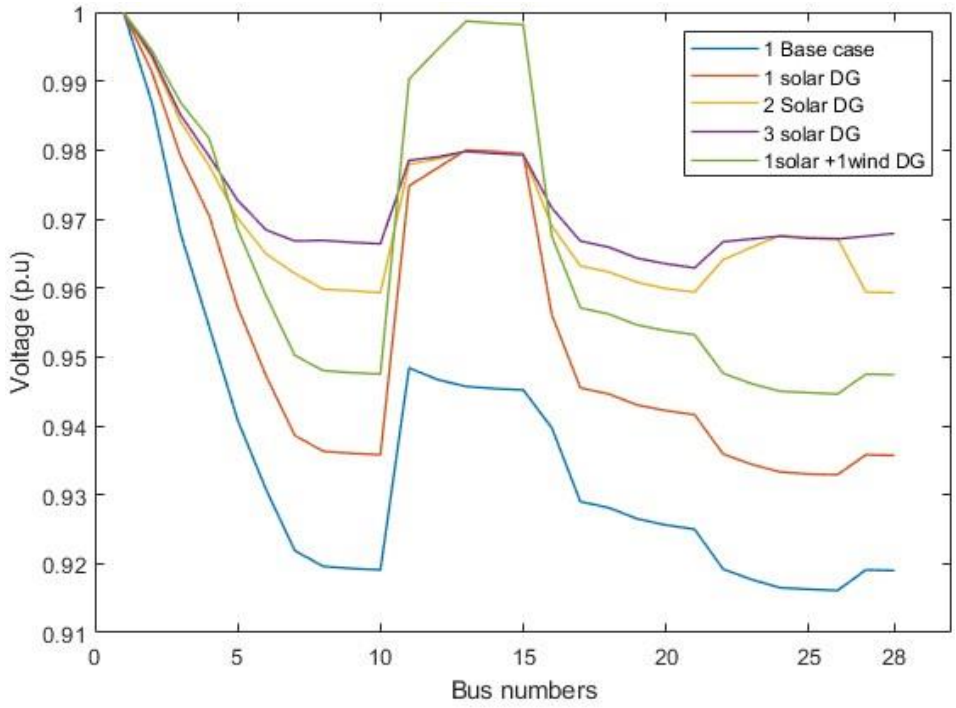

Fig. 5.42 Voltage Profile

From the above the The voltage profile V_{min} (p.u.) is enhanced@0.9133 p.u. to 0.9428 p.u. The VSI_{min} (p.u.) is presented in Fig. 5.43

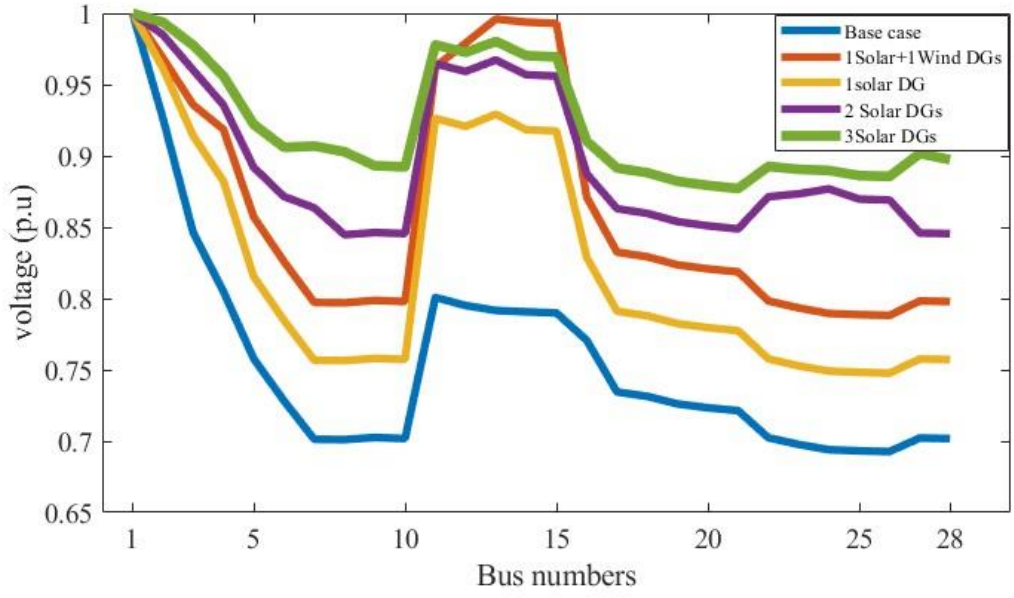

Fig. 5.43 Voltage Stability Index

From the above the VSI_{min} (p.u.) is enhanced@0.6957 p.u. to 0.7901 p.u. The effectiveness of the proposed Particle Swarm Optimization with Differential Velocities (PSODV) algorithm is evaluated in comparison with Firefly (FF) algorithm and Gorilla Troops Optimizer (GTO) algorithm and presented in Table 5.29.

Table 5.29 Performance Comparision 28 RDS

Method	Case Type	Power Losses (P_{loss}) kW	Voltage Minimum (V_{min}) P. U.	Voltage Stability Index (VSI_{min}) P. U.	Reduction of Losses (%)
Base case		67.3313	0.9133	0.6957	NA
Proposed PSODV Algorithm	1 SDG & I WDG	34.5593	0.9428	0.7901	48.67
GTO Algorithm	1 SDG & I WDG	34.359	0.943	0.792	48.97
FF Algorithm	1 SDG & I WDG	34.023	0.942	0.798	49.46

From the above the proposed Particle Swarm Optimization with Differential Velocities (PSODV) algorithm exhibited the best performance i.e., the power loss P_{loss}(kW) is decreased from 67.3313 kW→34.5593kW, The voltage profile V_{min} (p.u.) is enhanced@0.9428 p.u. → 0.9617 p.u., the VSI_{min} (p.u.) is enhanced@0.6957 p.u. → 0.7901 p.u.

5.3.2 Optimal Location of DER on IEEE 85 RDS

In this optimal Location of DER Considering Solar DG is implemented on IEEE 85 RDS considering 1 Solar and 1 Wind DGs under the residential load condition. In this case optimal location of DER on IEEE 85 RDS with residential load is implemented using the proposed Particle Swarm Optimization with Differential Velocities (PSODV) algorithm.

The peak value are recorded at 20thhour. The P_{loss}(kW) is 313.7580 kW, V_{min}(p.u.) is 0.871 p.u., VSI_{min}(p.u.) is 0.5756. The system performance with the optimal allocation of 1 wind DG, 2 wind DGs, 3 wind DGs are tabulated in Table 5.30.

Table 5.30 System Performance for 85 RDS

Scenario	Location Of Bus	Sizes of DG (kW)	Power Losses (P_{loss}) kW	Voltage Minimum (V_{min}) P. U.	Voltage Stability Index (VSI_{min}) P. U.	Reduction of Losses (%)
BC			313.7580	0.871	0.5756	
1 SDG & 1 WDG	53 53	919.9 1266	144.7022	0.9258	0.7347	53.8
2 SDG & 2 WDG	53 53 47 47	116.7 1012.7 922.4 1070.4	112.6950	0.9343	0.7619	64.08
3 SDG & 3 WDG	53 53 47 47 35 35	116.7 337.5 728.0 1192.7 1437.8 1321.7	105.8804	0.9364	0.7688	66.25

In 1 Solar and 1 Wind DGs case DGs is optimally placed on buses 53, 53 with 919.9 kW, 1266 kW sizes. The P_{loss}(kW) is 144.7022 kW, V_{min}(p.u.) is 0.9258 p.u., VSI_{min}(p.u.) is 0.7347, % Reduction of P_{loss} is 53.8%. For 2Solar 2Wind DGs power loss 112.6950kw,% Reduction of power loss 64.08%,& 3Solar,3Wind DGs power loss 105.8804kw,%Reduction 66.25%.

The power loss comparision of all the cases for 24 hour profile and 85 RDS are presented in Fig. 5.44 and Fig. 5.45 respectively.

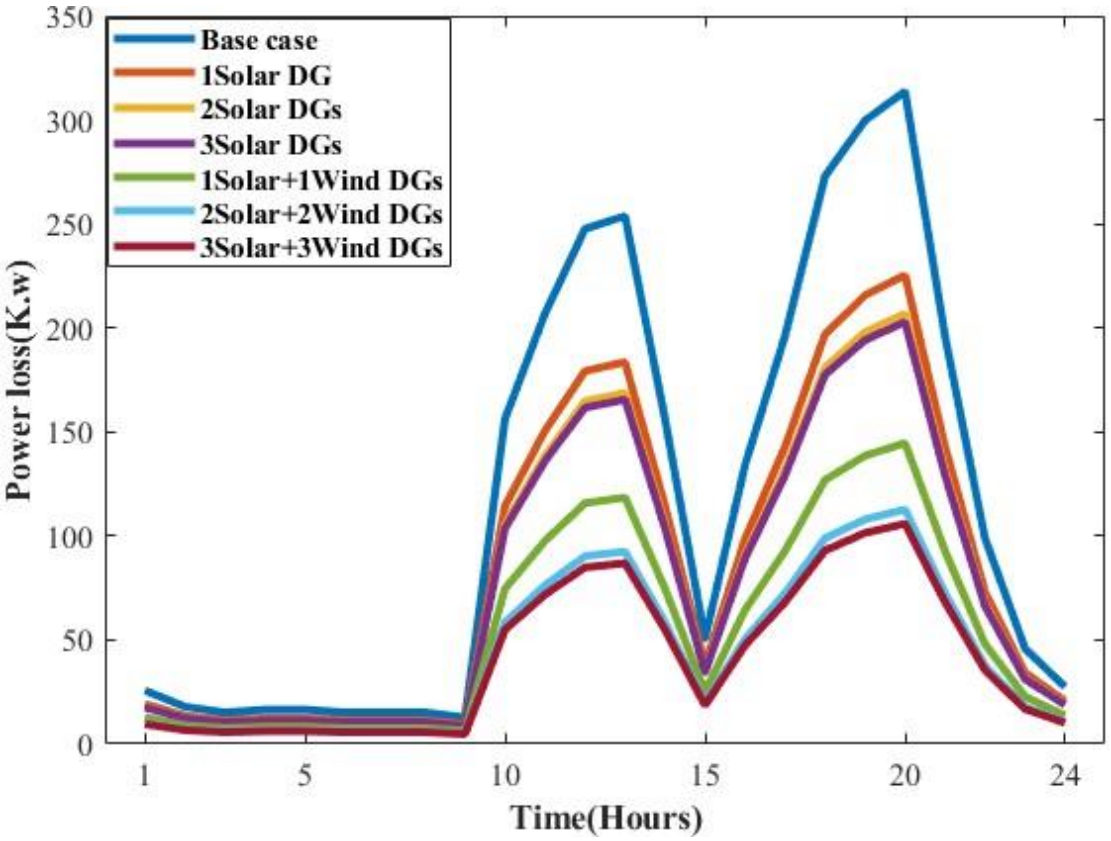

Fig. 5.44 Power Loss for 24 hour Profile

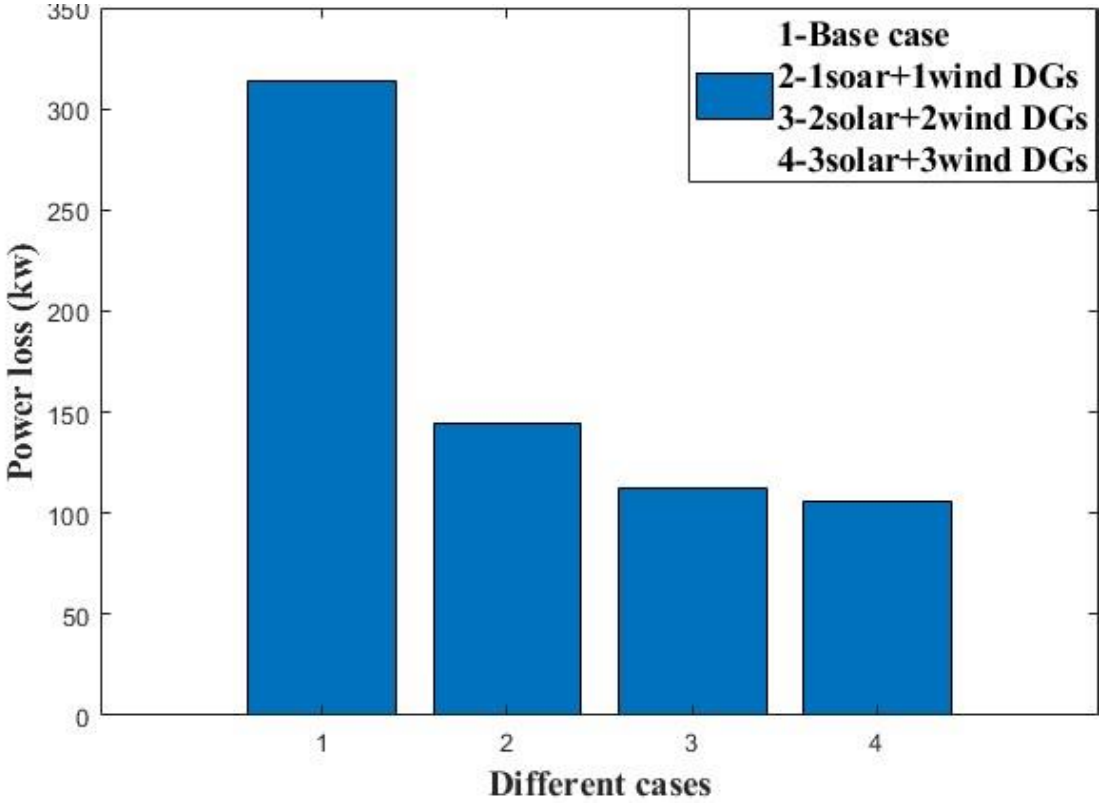

Fig. 5.45 Power Loss for 85 RDS System

From the above the peak power loss is recorded at 20th hour and the power loss P_{loss}(kW) is decreased @313.7580 kW→144.7022kW. The voltage profile V_{min} (p.u.) is presented in Fig. 5.46.

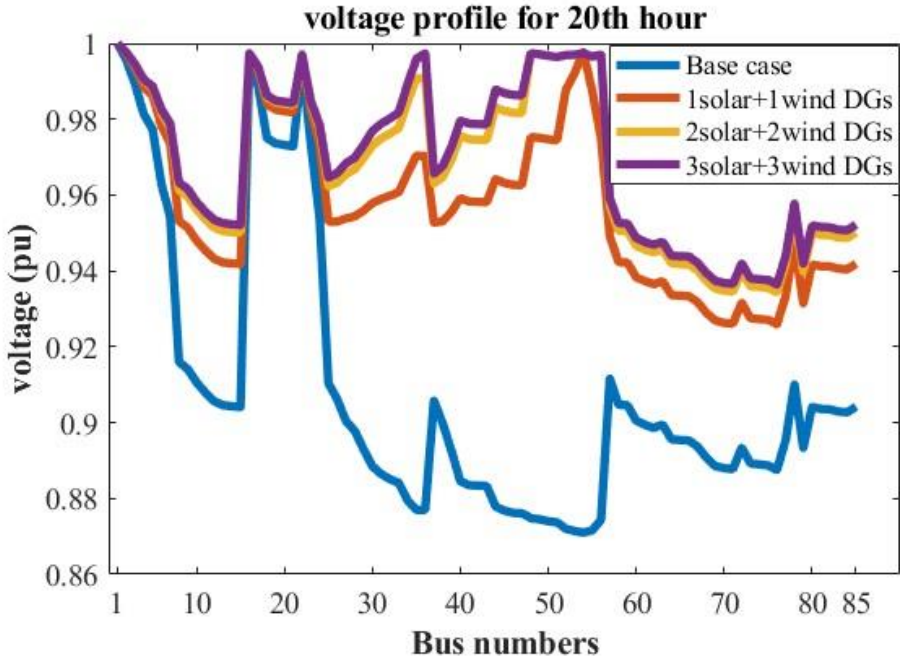

Fig. 5.46 Voltage Profile

From the above the The voltage profile V_{min} (p.u.) is enhanced@0.871 p.u. →0.9258 p.u. The VSI_{min}(p.u.) is presented in Fig. 5.47

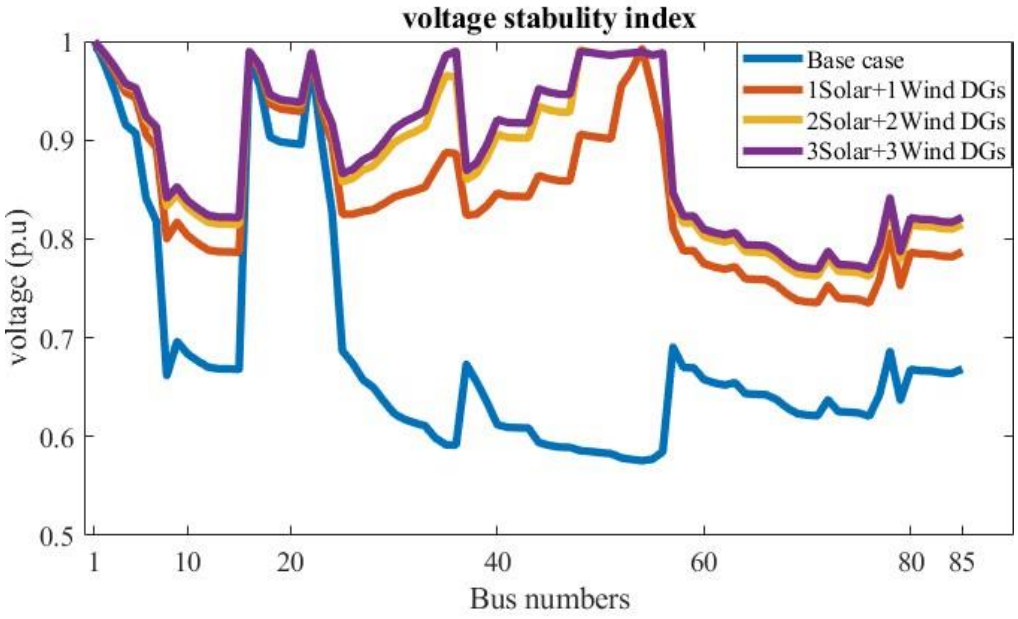

Fig. 5.47 Voltage Stability Index

From the above the VSI_{min} (p.u.) is enhanced from 0.5767 p.u. →0.7347 p.u. The effectiveness of the proposed Particle Swarm Optimization with Differential Velocities (PSODV) algorithm is evaluated in comparison with Firefly (FF) algorithm and Gorilla Troops Optimizer (GTO) algorithm and presented in Table 5.31.

Table 5.31 Performance Comparision 85 RDS

Method	Case Type	Power Losses (P_{loss}) kW	Voltage Minimum (V_{min}) P. U.	Voltage Stability Index (VSI_{min}) P. U.	Reduction of Losses (%)
BC		313.7580	0.871	0.5756	NA
Proposed PSODV Algorithm	1 SDG & 1 WDG	144.7022	0.9258	0.7347	53.8
	2 SDG & 2 WDG	112.6950	0.9343	0.7619	64.08
	3 SDG & 3 WDG	105.8804	0.9364	0.7688	66.25
GTO Algorithm	1 SDG & 1 WDG	145.6032	0.9260	0.735	53.59
FF Algorithm	1 SDG & 1 WDG	144.93	0.9250	0.7331	53.8

From the above the proposed Particle Swarm Optimization with Differential Velocities (PSODV) algorithm exhibited the best performance i.e., the power loss P_{loss}(kW) is decreased from 313.7580 kW→144.7022kW kW, The voltage profile V_{min} (p.u.) is enhanced@0.871 p.u. →0.9258 p.u, the VSI_{min} (p.u.) is enhanced@0.5767 p.u. →0.7347 p.u

5.4 Comparison Analysis

The proposed Particle Swarm Optimization with Differential Velocities (PSODV) algorithm is compared with results related to 28 bus system and tabulated in Table 5.32

Table 5.32Comparison Analysis data related 28 bus system

Method	Sizes of DG (kW)	Power Losses (P_{loss}) kW	Voltage Minimum (V_{min}) P. U.	Voltage Stability Index (VSI_{min}) P. U.
GOA	334.5567 230.4150 145.4057	33.650	0.9639	0.8615
WOA	182.5131 262.1375 265.0773	33.9388	0.9614	0.8542
DA	332.1821 235.1821 145.1592	33.6513	0.9634	0.8612
Proposed PSODV	222.0523 220.5258 256.781	33.1337	0.9633	0.8611
POA	228.6199 204.3446 245.6401	34.048	0.9653	0.8539

Similarly, The proposed Particle Swarm Optimization with Differential Velocities (PSODV) algorithm is compared with results related to 85 bus system and tabulated in Table 5.33

Table 5.33Comparison Analysis data related 85 bus system

	Base case	**PGS [22]**	**PSO [23]**	**MINLP [24]**	**BFOA [25]**	**Proposed PSODV**
Power loss (kW)	313.758	174.65	163.53	159.40	152.8	149.51
%Reductio	–	44.75	48.27	49.57	51.63	52.34

n in Power loss						
V_{min} (p.u)	0.8712	0.9091	0.9155	0.9175	0.9192	0.9213

The estimated values and convergence example of an 85-bus system generated by the proposed PSODV algorithm is presented in Fig. 5.48

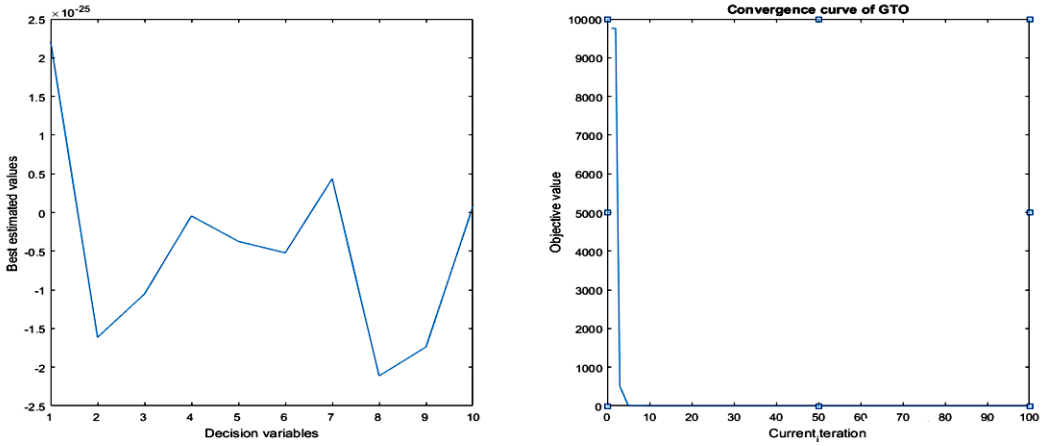

Fig.5.48The estimated values and convergence example of an 85-bus system generated by the GTO algorithm.

5.5 THD Analysis

The THD analysis for distorted IEEE 85-bus network considering the effects of linear load, non-linear load, and DG on % THDbusvolt using a CPL model are presented in Fig. 5.49

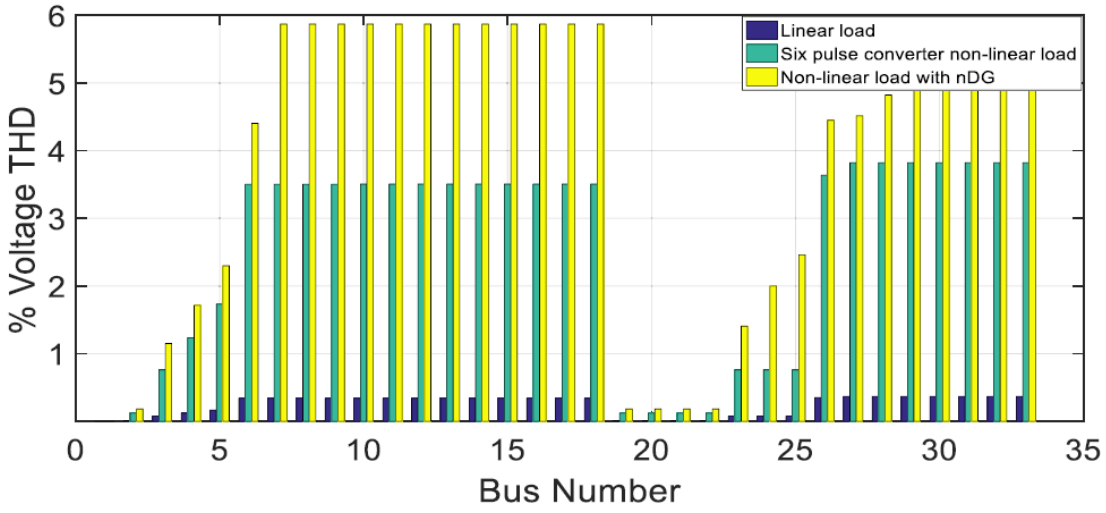

Fig. 5.49CPL Model THD analysis.

The CL model THD analysis is presented in Fig. 5.50

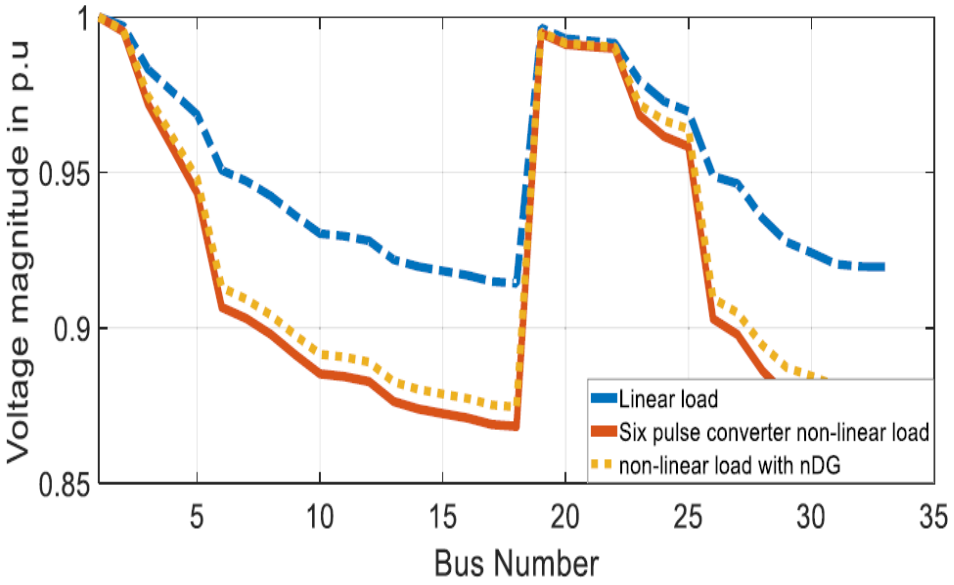

Fig. 5.50CL Model THD analysis

The 28-bus voltage profile is presented in Fig. 5.52, 28 bus THD analysis is presented in Fig. 5.53, THD busvolt in the CPL and CL Models as a Function of Loading are presented in Fig. 5.54. Influence of CPL and CL models on % THDbusvolt in a distorted IEEE 85-bus network is presented in Fig. 5.51.

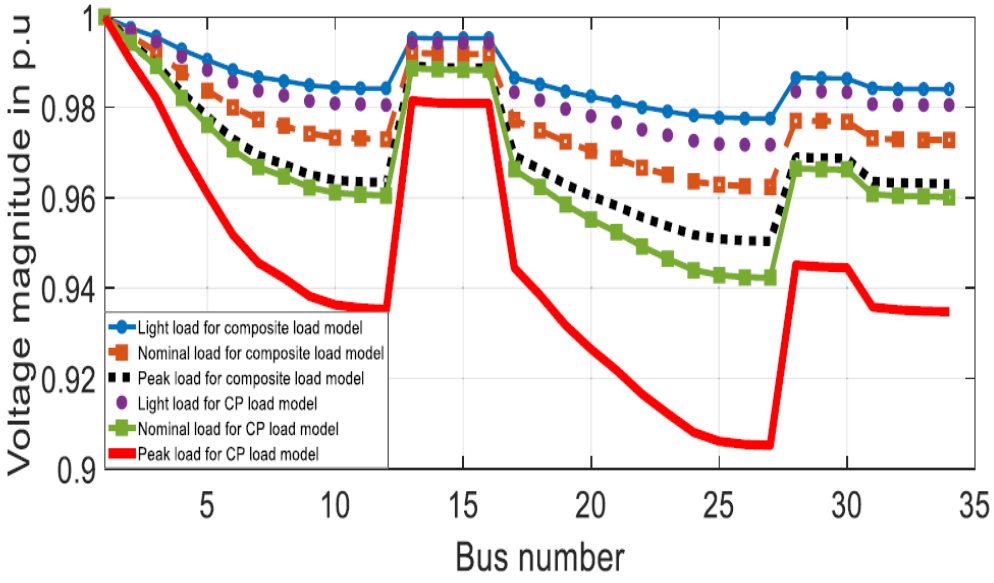

Fig. 5.51The 28-bus voltage profile.

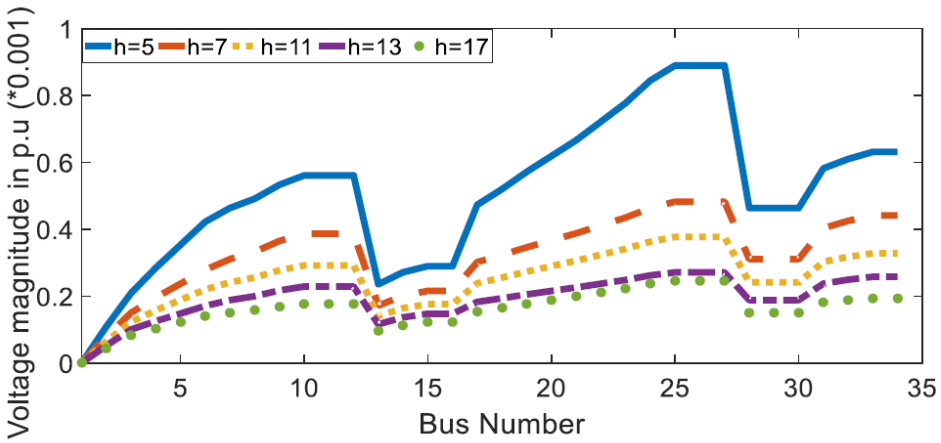

Fig. 5.5228 bus THD analysis

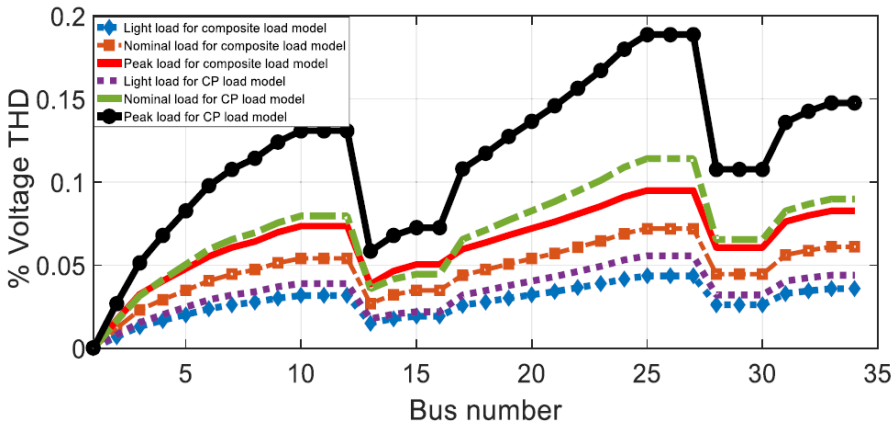

Fig. 5.53THD busvolt in the CPL and CL Models as a Function of Loading.

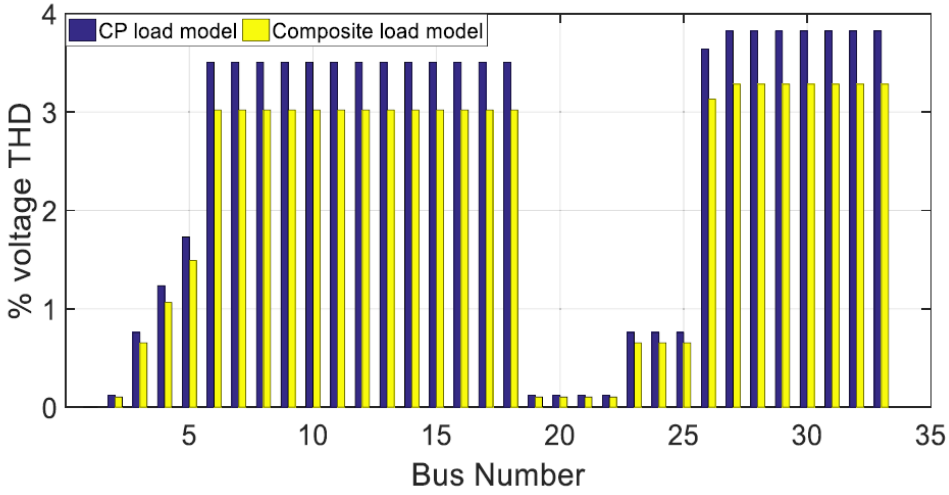

Fig. 5.54Influence of CPL and CL models on % THDbusvolt in a distorted IEEE 85-bus network.

The THD analysis of 85 bus is tabulated in Table 5.39. The CPL and CL model THD analysis is tabulated in Table 5.40. Impact of harmonics pollution on the nominal

load and CPL model performance of the IEEE 28-bus network is tabulated in Table 5.34.

Table 5.34The effects of distortion on an IEEE 85-bus network that is fully loaded with linear, non-linear, and nDG loads.

	Linear load		**Six-Pulse converter Non linear load**		**Six -Pulse converter nonlinear load and nDG**	
	CPL model	**CL model**	**CPL model**	**CL model**	**CPL model**	**CL model**
V_{min} (p.u)	0.9134	0.9143	0.8662	0.8683	0.8733	0.8745
THD Volt max (%)	0.3674	0.338	3.823	3.2833	5.87	4.9347
P_{loss} (kw)	201.59	194.59	567	550.76	506.86	492.59
Q_{loss} (kvar)	134.45	129.64	363.94	337.4	325.05	315.6

Table 5.35Harmonic sources of varying orders of the CPL model's (28-bus RDN) current injection are compared.

Harmonic order	**Harmonic current injection**					
	Projected method			**Shokhri and Zakaria**		
5	Bus 15 0.00166	Bus 25 0.00201	Bus 33 0.00127	Bus 15 0.00167	Bus 25 0.00202	Bus33 0.00127
7	0.00112	0.00072	0.00083	0.00112	0.00075	0.00083
11	0.00065	0.00039	0.00040	0.00065	0.00039	0.00040
13	0.00050	0.00022	0.00028	0.00050	0.00022	0.00028
17	0.00033	0.00018	0.00013	0.00033	0.00018	0.00013
Total current injection(pu)	0.00426	0.00352	0.00291	0.00427	0.00356	0.00291

Table 5.36 CPL and CL model (28-bus RDN) total harmonic current injection comparison.

Network load level		Bus	Total harmonic current Injection (p.u)	
			CPL	CL
Light		15	0.0022	0.0002
		25	0.00017	0.00018
		33	0.00014	0.00012
Nominal		15	0.00426	0.0039
		25	0.00352	0.002
Peak		15	0.00069	0.00058
		25	0.0006	0.00023
		33	0.00049	0.00026

Table 5.37 Impact of harmonics pollution on the nominal load and CPL model performance of the IEEE 28-bus network

	tahereta	Proposed method	% reduction in THD
THD Volt max(%)	7.41	5.536	25.29
Ploss (kw)	453	449.6	
Qloss (kvar)	NR	288.3	

In all the above cases the proposed PSODV algorithm exhibited the enhanced performance**.**

5.6 Chapter Summary

In this chapter, the results and discussion on the integration of solar and wind-based distributed generators (DGs) are presented. The proposed Particle Swarm Optimization with Differential Velocities (PSODV) algorithm is implemented on 28-bus and 85-bus systems to identify the optimal placement and sizing of DGs. The results are compared with existing state-of-the-art optimization algorithms. In all cases, the proposed PSODV algorithm demonstrated superior performance in terms of power loss reduction, voltage profile improvement, and voltage stability enhancement. Additionally, a detailed comparison and Total Harmonic Distortion (THD) analysis are provided to highlight the algorithm's effectiveness. 5.6 Chapter Summary

CHAPTER 6
CONCLUSION AND FUTURE SCOPE

6.1 Conclusion

The proposed Particle Swarm Optimization with Differential Velocities (PSODV) approach optimizes both the locations and capacities of Photovoltaic (PV) and Wind Distributed Generators (DGs) to meet the growing system demand. The method is implemented on IEEE 28-bus and 85-bus systems, considering solar DG, wind DG, hybrid solar-wind DG, and various load types, including residential, commercial, and industrial. The optimal bus locations and sizes of DGs are determined, and key performance evaluation parameters, such as power loss (P_loss in kW), minimum voltage (V_min in p.u.), Voltage Stability Index (VSI_min in p.u.), and percentage reduction in power loss, are assessed across all cases. The effectiveness of the PSODV algorithm is compared with the Firefly (FF) algorithm and Gorilla Troops Optimizer (GTO) algorithm. In all scenarios, the PSODV algorithm demonstrated superior performance.

In optimal location of solar DG at 28 bus system, At residential load the power loss P_{loss}(kW) is decreased from 68.8189 kW→34.0480 kW, The voltage profile V_{min} (p.u.) is enhanced@0.9123 p.u. → 0.9613 p.u, the VSI_{min} (p.u.) is enhanced@0.6927 p.u. → 0.8539 p.u., At commercial load the power loss P_{loss}(kW) is decreased from 62.9824 kW→31.2864kW, The voltage profile V_{min} (p.u.) is enhanced@0.9161 p.u. → 0.9629 p.u, the VSI_{min} (p.u.) is enhanced@0.7044 p.u. → 0.8597 p.u., At industrial load the power loss P_{loss}(kW) is decreased from 67.3313 kW→33.3459kW, The voltage profile V_{min} (p.u.) is enhanced@0.9133 p.u. → 0.9617 p.u., theVSI_{min} (p.u.) is enhanced from 0.6957 p.u. → 0.8554 p.u.

In optimal location of solar DG at 85 bus system, At residential load the power loss P_{loss}(kW) is decreased from 313.7580 kW→202.8271kW, The voltage profile V_{min} (p.u.) is enhanced@0.871 p.u. → 0.9161 p.u, the VSI_{min} (p.u.) is enhanced@0.5767 p.u. → 0.7045 p.u.

In optimal location of wind DG at 28 bus system, At residential load the power loss P_{loss}(kW) is decreased from 68.8189 kW→33.8018kW, The voltage profile V_{min} (p.u.) is enhanced@0.9123 p.u. → 0.983 p.u, theVSI_{min} (p.u.) is enhanced@0.6927 p.u. → 0.7985 p.u., At commercial load the power loss P_{loss}(kW) is decreased from 62.9824

kW→31.0201kW, The voltage profile V_{min} (p.u.) is enhanced@0.9161 p.u. → 0.9505 p.u, theVSI_{min} (p.u.) is enhanced@0.7044 p.u. → 0.8064 p.u., At industrial load the power loss P_{loss}(kW) is decreased from 67.3313 kW→33.0940 kW, The voltage profile V_{min} (p.u.) is enhanced@0.9489 p.u. → 0.9617 p.u., the VSI_{min} (p.u.) is enhanced@0.6957 p.u. → 0.8005 p.u.

In optimal location of windDG at 85 bus system, At residential load the power loss P_{loss}(kW) is decreased from 313.7580 kW→207.1059kW kW, The voltage profile V_{min} (p.u.) is enhanced@0.871 p.u. →0.9075 p.u, theVSI_{min} (p.u.) is enhanced@0.5767 p.u. →0.6783 p.u.

In optimal location of solar and windDG at 28 bus system, At residential load the power loss P_{loss}(kW) is decreased from 68.8189 kW→35.2997kW, The voltage profile V_{min} (p.u.) is enhanced@0.9123 p.u. → 0.9422 p.u, the VSI_{min} (p.u.) is enhanced@0.6927 p.u. → 0.7881 p.u., At commercial load the power loss P_{loss}(kW) is decreased from 62.9824 kW→32.3902kW, The voltage profile V_{min} (p.u.) is enhanced@0.9161 p.u. →0.9446 p.u, theVSI_{min} (p.u.) is enhanced@0.7044 p.u. →0.7962 p.u., At industrial load the power loss P_{loss}(kW) is decreased from 67.3313 kW→34.5593kW, The voltage profile V_{min} (p.u.) is enhanced@0.9428 p.u. → 0.9617 p.u., theVSI_{min} (p.u.) is enhanced@0.6957 p.u. → 0.7901 p.u.

In optimal location of solar and windDG at 85 bus system, At residential load the power loss P_{loss}(kW) is decreased from 313.7580 kW→144.7022kW kW, The voltage profile V_{min} (p.u.) is enhanced@0.871 p.u. →0.9258 p.u, theVSI_{min} (p.u.) is enhanced@0.5767 p.u. →0.7347 p.u.

Comparison of THD analysis is presented and in the proposed method THD is significantly reduced there by enhanced the power quality.

6.2 Future scope

1. Unpredictable PV fleet loads and time-varying network conditions hinder efficiency improvement.
2. Smart charging scenarios for EV fleets offer a promising solution to optimize network performance.
3. Despite extensive studies, meta-heuristic methods for load optimization lack sufficient validation.

.

REFERENCES

[1] G. Buticchi, L. F. Costa, and M. Liserre, "Multi-port DC/DC converter for the electrical power distribution system of the more electric aircraft," *Math. Comput. Simul.*, vol. 158, 2019, doi: 10.1016/j.matcom.2018.09.019.

[2] S. Anatolii and K. Dmytro, "Using nodal specific transportation costs to determine economically beneficial distributed generation source location areas in radial electrical power distribution systems," *Prz. Elektrotechniczny*, vol. 97, no. 3, 2021, doi: 10.15199/48.2021.03.20.

[3] M. S. S. Fogliatto *et al.*, "Lifetime Study of Electrical Power Distribution Systems Failures," *J. Control. Autom. Electr. Syst.*, vol. 33, no. 4, 2022, doi: 10.1007/s40313-021-00888-6.

[4] H. Yan, B. Du, A. Marquez, and G. Buticchi, "Optimised temperature fluctuation control strategy for lifetime improvement in aircraft electrical power distribution system," *IET Electr. Syst. Transp.*, vol. 12, no. 4, 2022, doi: 10.1049/els2.12058.

[5] R. Taheri, A. Khajezadeh, M. H. Rezaeian Koochi, and A. Sharifi Nasab Anari, "Line independency-based network modelling for backward/forward load flow analysis of electrical power distribution systems," *Turkish J. Electr. Eng. Comput. Sci.*, vol. 27, no. 6, 2019, doi: 10.3906/ELK-1812-137.

[6] S. C. Rajpoot and S. K. Singhai, "A Novel Approach for Detecting and Analyzing the Shunt Fault in Electrical Power Distribution System (EPDS)," *Electr. Power Components Syst.*, vol. 51, no. 2, 2023, doi: 10.1080/15325008.2023.2168317.

[7] D. Izquierdo, A. Barrado, C. Raga, M. Sanz, and A. Lázaro, "Protection devices for aircraft electrical power distribution systems: State of the art," *IEEE Trans. Aerosp. Electron. Syst.*, vol. 47, no. 3, 2011, doi: 10.1109/TAES.2011.5937248.

[8] K. Sarwagya, S. De, and P. K. Nayak, "High-impedance fault detection in electrical power distribution systems using moving sum approach," *IET Sci. Meas. Technol.*, vol. 12, no. 1, 2018, doi: 10.1049/iet-smt.2017.0231.

[9] C. Gu *et al.*, "A Multiport Power Conversion System for the More Electric Aircraft," *IEEE Trans. Transp. Electrif.*, vol. 6, no. 4, 2020, doi: 10.1109/TTE.2020.3019446.

[10] F. Akbar and R. Shahid, "Risk management (RM) and project success (PS) of electrical power transmission and distribution systems: the moderation role of

human resource management," *Int. J. Energy Sect. Manag.*, vol. 17, no. 1, 2023, doi: 10.1108/IJESM-03-2021-0010.

[11] F. Budianto, A. Kurniawan, I. R. Kusuma, A. R. Kurniawan, and A. R. N. Gumilang, "Comparison of voltage harmonics in AC and DC shipboard electrical power distribution systems: A case study of 17,500 DWT tanker vessel," in *IOP Conference Series: Earth and Environmental Science*, 2022, vol. 972, no. 1, doi: 10.1088/1755-1315/972/1/012071.

[12] "Guide to electrical power distribution systems," *Choice Rev. Online*, vol. 30, no. 04, 1992, doi: 10.5860/choice.30-2103.

[13] M. J. Daigle, I. Roychoudhury, and A. Bregon, "Qualitative event-based diagnosis applied to a spacecraft electrical power distribution system," *Control Eng. Pract.*, vol. 38, 2015, doi: 10.1016/j.conengprac.2015.01.007.

[14] H. A. R. Florez, E. M. Carreno, M. J. Rider, and J. R. S. Mantovani, "Distflow based state estimation for power distribution networks," *Energy Syst.*, vol. 9, no. 4, 2018, doi: 10.1007/s12667-017-0269-1.

[15] A. Z. Abdullah, N. H. Hanafi, N. Azizan, and M. H. Amlus, "Optimal off point determination in electrical power distribution system using risk assessment," *J. Teknol.*, vol. 78, no. 6–2, 2016, doi: 10.11113/jt.v78.8886.

[16] M. Jamil, R. Singh, and S. K. Sharma, "Fault identification in electrical power distribution system using combined discrete wavelet transform and fuzzy logic," *J. Electr. Syst. Inf. Technol.*, vol. 2, no. 2, 2015, doi: 10.1016/j.jesit.2015.03.015.

[17] A. P. Hota, S. Mishra, D. P. Mishra, and S. R. Salkuti, "Allocating active power loss with network reconfiguration in electrical power distribution systems," *Int. J. Power Electron. Drive Syst.*, vol. 12, no. 1, 2021, doi: 10.11591/ijpeds.v12.i1.pp130-138.

[18] A. R. Kurniawan, A. Kurniawan, S. Sarwito, A. R. N. Gumilang, and F. Budianto, "Comparison of voltage drop in AC and DC shipboard electrical power distribution systems: A case study of 17,500 DWT tanker vessel," in *IOP Conference Series: Earth and Environmental Science*, 2022, vol. 972, no. 1, doi: 10.1088/1755-1315/972/1/012001.

[19] S. Gunter *et al.*, "Load Control for the DC Electrical Power Distribution System of the More Electric Aircraft," *IEEE Trans. Power Electron.*, vol. 34, no. 4, 2019, doi: 10.1109/TPEL.2018.2856534.

[20] A. R. N. Gumilang, A. Kurniawan, S. Sarwito, F. Budianto, and A. R.

Kurniawan, “Comparison of short-circuit current in AC and DC shipboard electrical power distribution systems: A case study of 17,500 DWT tanker vessel,” in *IOP Conference Series: Earth and Environmental Science*, 2022, vol. 972, no. 1, doi: 10.1088/1755-1315/972/1/012072.

[21] G. Kaur *et al.*, “Prospects of biogas and evaluation of unseen livestock based resource potential as distributed generation in India,” *Ain Shams Eng. J.*, vol. 13, no. 4, 2022, doi: 10.1016/j.asej.2021.101657.

[22] D. A. Gadanayak, “Protection algorithms of microgrids with inverter interfaced distributed generation units—A review,” *Electric Power Systems Research*, vol. 192. 2021, doi: 10.1016/j.epsr.2020.106986.

[23] G. Pepermans, J. Driesen, D. Haeseldonckx, R. Belmans, and W. D’haeseleer, “Distributed generation: Definition, benefits and issues,” *Energy Policy*, vol. 33, no. 6, 2005, doi: 10.1016/j.enpol.2003.10.004.

[24] B. Singh and J. Sharma, “A review on distributed generation planning,” *Renewable and Sustainable Energy Reviews*, vol. 76. 2017, doi: 10.1016/j.rser.2017.03.034.

[25] S. M. Ismael, S. H. E. Abdel Aleem, A. Y. Abdelaziz, and A. F. Zobaa, “State-of-the-art of hosting capacity in modern power systems with distributed generation,” *Renewable Energy*, vol. 130. 2019, doi: 10.1016/j.renene.2018.07.008.

[26] T. Ackermann, G. Andersson, and L. Söder, “Distributed generation: A definition,” *Electr. Power Syst. Res.*, vol. 57, no. 3, 2001, doi: 10.1016/S0378-7796(01)00101-8.

[27] M. E. T. Souza Junior and L. C. G. Freitas, “Power Electronics for Modern Sustainable Power Systems: Distributed Generation, Microgrids and Smart Grids—A Review,” *Sustainability (Switzerland)*, vol. 14, no. 6. 2022, doi: 10.3390/su14063597.

[28] Z. Yang, F. Yang, H. Min, H. Tian, W. Hu, and J. Liu, “Review on optimal planning of new power systems with distributed generations and electric vehicles,” *Energy Reports*, vol. 9, 2023, doi: 10.1016/j.egyr.2022.11.168.

[29] M. Almamari and M. Albadi, “Impacts of Distributed Generation on Power System Protection,” *Renew. Energy Power Qual. J.*, vol. 20, 2022, doi: 10.24084/repqj20.328.

[30] A. Ehsan and Q. Yang, “Optimal integration and planning of renewable

distributed generation in the power distribution networks: A review of analytical techniques," *Applied Energy*, vol. 210. 2018, doi: 10.1016/j.apenergy.2017.10.106.

[31] Q. Gu and Q. Qu, "Towards an Internet of Energy for smart and distributed generation: Applications, strategies, and challenges," *Journal of Computational Design and Engineering*, vol. 9, no. 5. 2022, doi: 10.1093/jcde/qwac087.

[32] Rekha and S. C. Byalihal, "Optimal allocation of solar and wind distributed generation using particle swarm optimization technique," *Int. J. Electr. Comput. Eng.*, vol. 13, no. 1, 2023, doi: 10.11591/ijece.v13i1.pp229-237.

[33] T. Bisognin Garlet, J. L. Duarte Ribeiro, F. de Souza Savian, and J. C. Mairesse Siluk, "Competitiveness of the value chain of distributed generation of photovoltaic energy in Brazil," *Energy Sustain. Dev.*, vol. 71, 2022, doi: 10.1016/j.esd.2022.10.019.

[34] Y. M. Nsaif, M. S. Hossain Lipu, A. Ayob, Y. Yusof, and A. Hussain, "Fault Detection and Protection Schemes for Distributed Generation Integrated to Distribution Network: Challenges and Suggestions," *IEEE Access*, vol. 9, 2021, doi: 10.1109/ACCESS.2021.3121087.

[35] À. Alonso-Travesset, H. Martín, S. Coronas, and J. De La Hoz, "Optimization Models under Uncertainty in Distributed Generation Systems: A Review," *Energies*, vol. 15, no. 5, 2022, doi: 10.3390/en15051932.

[36] Y. S. Ko, S. H. Kim, and G. H. Lim, "Miniaturized Distributed Generation for a Micro Smart Grid Simulator," *Energies*, vol. 15, no. 4, 2022, doi: 10.3390/en15041511.

[37] T. B. Garlet, J. L. D. Ribeiro, F. de Souza Savian, and J. C. Mairesse Siluk, "Paths and barriers to the diffusion of distributed generation of photovoltaic energy in southern Brazil," *Renew. Sustain. Energy Rev.*, vol. 111, 2019, doi: 10.1016/j.rser.2019.05.013.

[38] M. Kumar, A. M. Soomro, W. Uddin, and L. Kumar, "Optimal Multi-Objective Placement and Sizing of Distributed Generation in Distribution System: A Comprehensive Review," *Energies*, vol. 15, no. 21. 2022, doi: 10.3390/en15217850.

[39] O. P. Mahela, B. Khan, H. H. Alhelou, S. Tanwar, and S. Padmanaban, "Harmonic mitigation and power quality improvement in utility grid with solar energy penetration using distribution static compensator," *IET Power Electron.*,

vol. 14, no. 5, 2021, doi: 10.1049/pel2.12074.

[40] O. M. Bakry *et al.*, "Improvement of distribution networks performance using renewable energy sources based hybrid optimization techniques," *Ain Shams Eng. J.*, vol. 13, no. 6, 2022, doi: 10.1016/j.asej.2022.101786.

[41] S. Khunkitti, P. Boonluk, and A. Siritaratiwat, "Optimal Location and Sizing of BESS for Performance Improvement of Distribution Systems with High DG Penetration," *Int. Trans. Electr. Energy Syst.*, vol. 2022, 2022, doi: 10.1155/2022/6361243.

[42] J. Liu, H. Hu, S. S. Yu, and H. Trinh, "Virtual Power Plant with Renewable Energy Sources and Energy Storage Systems for Sustainable Power Grid-Formation, Control Techniques and Demand Response," *Energies*, vol. 16, no. 9. 2023, doi: 10.3390/en16093705.

[43] A. Luo, Q. Xu, F. Ma, and Y. Chen, "Overview of power quality analysis and control technology for the smart grid," *J. Mod. Power Syst. Clean Energy*, vol. 4, no. 1, 2016, doi: 10.1007/s40565-016-0185-8.

[44] U. Zafar, S. Bayhan, and A. Sanfilippo, "Home Energy Management System Concepts, Configurations, and Technologies for the Smart Grid," *IEEE Access*, vol. 8, 2020, doi: 10.1109/ACCESS.2020.3005244.

[45] M. L. Tuballa and M. L. Abundo, "A review of the development of Smart Grid technologies," *Renewable and Sustainable Energy Reviews*, vol. 59. 2016, doi: 10.1016/j.rser.2016.01.011.

[46] T. Dinh Pham, T. T. Nguyen, and L. C. Kien, "An Improved Equilibrium Optimizer for Optimal Placement of Distributed Generators in Distribution Systems considering Harmonic Distortion Limits," *Complexity*, vol. 2022, 2022, doi: 10.1155/2022/3755754.

[47] A. K. Mohanty, P. S. Babu, and S. R. Salkuti, "Fuzzy-Based Simultaneous Optimal Placement of Electric Vehicle Charging Stations, Distributed Generators, and DSTATCOM in a Distribution System," *Energies*, vol. 15, no. 22, 2022, doi: 10.3390/en15228702.

[48] R. Vempalle and P. K. Dhal, "Optimal analysis of time varying load radial distribution system with photovoltaic and wind generating system using novel hybrid optimization technique," *Renew. Energy Focus*, vol. 41, 2022, doi: 10.1016/j.ref.2022.03.004.

[49] A. Ansari and S. C. Byalihal, "Resource aware wind farm and D-STATCOM

optimal sizing and placement in a distribution power system," *Int. J. Electr. Comput. Eng.*, vol. 11, no. 6, 2021, doi: 10.11591/ijece.v11i6.pp4641-4648.

[50] P. I. Obi, I. I. Okonkwo, and C. O. Ogba, "Power supply enhancement in Onitsha distribution network using distribution generations," *Niger. J. Technol.*, vol. 41, no. 2, 2022, doi: 10.4314/njt.v41i2.14.

[51] S. Liasi, N. Ghiasi and R. Hadidi, "Optimal Switch Placement to Improve the Reliability of Distribution Network in Interconnected Network of Microgrids Using a Graph-Based Approach," in *IEEE Transactions on Industry Applications*, vol. 60, no. 4, pp. 5470-5479, July-Aug. 2024, doi: 10.1109/TIA.2024.3384355.

[52] Y. Khalid Hamad, A. Nasser Hussain, Y. N. Lafta, A. Al-Naji and J. Chahl, "Multi-Objective Optimization of Renewable Distributed Generation Placement and Sizing for Technical and Economic Benefits Improvement in Distribution System," in *IEEE Access*, vol. 12, pp. 164226-164247, 2024, doi: 10.1109/ACCESS.2024.3492119.

[53] K. Sivakumar, R. Jayashree, and K. Danasagaran, "Efficiency-driven planning for sizing of distributed generators and optimal construction of a cluster of microgrids," *Eng. Sci. Technol. an Int. J.*, vol. 24, no. 5, 2021, doi: 10.1016/j.jestch.2021.02.015.

[54] E. Karunarathne, J. Pasupuleti, J. Ekanayake, and D. Almeida, "The optimal placement and sizing of distributed generation in an active distribution network with several soft open points," *Energies*, vol. 14, no. 4, 2021, doi: 10.3390/en14041084.

[55] A. Ramadan, M. Ebeed, S. Kamel, A. M. Agwa, and M. Tostado-véliz, "The Probabilistic Optimal Integration of Renewable Distributed Generators Considering the Time-Varying Load Based on an Artificial Gorilla Troops Optimizer," *Energies*, vol. 15, no. 4, 2022, doi: 10.3390/en15041302.

[56] S. Nourian and A. Kazemi, "Resilience enhancement of active distribution networks in the presence of wind turbines and energy storage systems by considering flexible loads," *J. Energy Storage*, vol. 48, 2022, doi: 10.1016/j.est.2022.104042.

[57] S. Sreedevi and G. Angeline Ezhilarasi, "Optimal rating and placing of numerous distributed generators in distribution network applying spider monkey optimization," *J. Intell. Fuzzy Syst.*, vol. 43, no. 3, 2022, doi: 10.3233/JIFS-

220210.

[58] P. V. K. Babu, K. Swarnasri, and P. Vijetha, “Multi-Objective Optimal planning of Renewable Energy Sources & Electric Vehicle Charging Stations in Unbalanced Radial Distribution Systems using Harris Hawk Optimization Algorithm,” *Int. J. Renew. Energy Res.*, vol. 12, no. 1, 2022, doi: 10.20508/ijrer.v12i1.12653.g8373.

[59] A. Shaheen, A. Elsayed, A. Ginidi, R. El-Sehiemy, and E. Elattar, “Reconfiguration of electrical distribution network-based DG and capacitors allocations using artificial ecosystem optimizer: Practical case study,” *Alexandria Eng. J.*, vol. 61, no. 8, 2022, doi: 10.1016/j.aej.2021.11.035.

[60] A. K. Mohanty, P. Suresh Babu, and S. R. Salkuti, “Optimal Allocation of Fast Charging Station for Integrated Electric-Transportation System Using Multi-Objective Approach,” *Sustain.*, vol. 14, no. 22, 2022, doi: 10.3390/su142214731.

[61] A. Amin *et al.*, “Techno-Economic Evaluation of Optimal Integration of PV Based DG with DSTATCOM Functionality with Solar Irradiance and Loading Variations,” *Mathematics*, vol. 10, no. 14, 2022, doi: 10.3390/math10142543.

[62] S. Katyara *et al.*, “Leveraging a genetic algorithm for the optimal placement of distributed generation and the need for energy management strategies using a fuzzy inference system,” *Electron.*, vol. 10, no. 2, 2021, doi: 10.3390/electronics10020172.

[63] M. A. Elseify, S. Kamel, H. Abdel-Mawgoud, and E. E. Elattar, “A Novel Approach Based on Honey Badger Algorithm for Optimal Allocation of Multiple DG and Capacitor in Radial Distribution Networks Considering Power Loss Sensitivity,” *Mathematics*, vol. 10, no. 12, 2022, doi: 10.3390/math10122081.

[64] A. Norouzi, H. Shayeghi, and J. Olamaei, “Multi-objective allocation of switching devices in distribution networks using the Modified Barnacles Mating Optimization algorithm,” *Energy Reports*, vol. 8, 2022, doi: 10.1016/j.egyr.2022.09.028.

[65] H. Mubarak *et al.*, “Optimum distribution system expansion planning incorporating dg based on n-1 criterion for sustainable system,” *Sustain.*, vol. 13, no. 12, 2021, doi: 10.3390/su13126708.

[66] “Optimal Placement and Sizing of DGs in Distribution Networks Using Dandelion Optimization Algorithm: Case Study of an Algerian Distribution Network,” *Int. J. Adv. Trends Comput. Sci. Eng.*, vol. 11, no. 6, 2022, doi:

10.30534/ijatcse/2022/021162022.

[67] M. Yehia, D. Allam, and A. F. Zobaa, "A Novel Hybrid Fuzzy-Metaheuristic Strategy for Estimation of Optimal Size and Location of the Distributed Generators," *Energy Reports*, vol. 8, 2022, doi: 10.1016/j.egyr.2022.09.019.

[68] A. Gantayet and D. K. Dheer, "A data-driven multi-objective optimization framework for optimal integration planning of solid-state transformer fed energy hub in a distribution network," *Eng. Sci. Technol. an Int. J.*, vol. 36, 2022, doi: 10.1016/j.jestch.2022.101278.

[69] D. M. Osorio and J. R. Garcia, "Multi-Objective Optimization of a Microgrid Considering MBESS Efficiencies, the Initial State of Charge, and Storage Capacity," *Int. Rev. Electr. Eng.*, vol. 17, no. 3, 2022, doi: 10.15866/iree.v17i3.22053.

[70] A. Ramshanker, J. R. Isaac, B. E. Jeyeraj, J. Swaminathan, and R. Kuppan, "Optimal DG Placement in Power Systems Using a Modified Flower Pollination Algorithm," *Energies*, vol. 15, no. 22, 2022, doi: 10.3390/en15228516.

[71] T. T. Nguyen, T. T. Nguyen, N. A. Nguyen, and T. L. Duong, "A novel method based on coyote algorithm for simultaneous network reconfiguration and distribution generation placement," *Ain Shams Eng. J.*, vol. 12, no. 1, 2021, doi: 10.1016/j.asej.2020.06.005.

[72] S. Nagaballi and V. S. Kale, "A metaphor-less based AI technique for optimal deployment of DG and DSTATCOM considering reconfiguration in the RDS for Techno-Economic benefits," *J. Intell. Fuzzy Syst.*, vol. 41, no. 5, 2021, doi: 10.3233/JIFS-189891.

[73] S. K. Wankhede, P. Paliwal, and M. K. Kirar, "Bi-Level Multi-Objective Planning Model of Solar PV-Battery Storage-Based DERs in Smart Grid Distribution System," *IEEE Access*, vol. 10, 2022, doi: 10.1109/ACCESS.2022.3148253.

[74] A. Yadav, N. Kishor, and R. Negi, "Bus Voltage Violations under Different Solar Radiation Profiles and Load Changes with Optimally Placed and Sized PV Systems," *Energies*, vol. 16, no. 2, 2023, doi: 10.3390/en16020653.

[75] F. Iqbal, M. T. Khan, and A. S. Siddiqui, "Optimal placement of DG and DSTATCOM for loss reduction and voltage profile improvement," *Alexandria Eng. J.*, vol. 57, no. 2, 2018, doi: 10.1016/j.aej.2017.03.002.

[76] T. Kesavan and K. Lakshmi, "Optimization of a Renewable Energy Source-

Based Virtual Power Plant for Electrical Energy Management in an Unbalanced Distribution Network," *Sustain.*, vol. 14, no. 18, 2022, doi: 10.3390/su141811129.

[77] O. B. Adewuyi, A. P. Adeagbo, I. G. Adebayo, H. O. R. Howlader, and Y. Sun, "Modified analytical approach for pv-dgs integration into a radial distribution network considering loss sensitivity and voltage stability," *Energies*, vol. 14, no. 22, 2021, doi: 10.3390/en14227775.

[78] R. Golnazari, S. Hasanzadeh, E. Heydarian-Forushani, H. R. Sezavar, and N. Fahimi, "A techno-economic model for enhancing PV hosting capacity through capabilities of smart inverters and soft open points," *IET Renew. Power Gener.*, 2023, doi: 10.1049/rpg2.12774.

[79] M. A. Rasheed and R. Verayiah, "Investigation of Optimal PV Allocation to Minimize System Losses and Improve Voltage Stability for Distribution and Transmission Networks Using MATLAB and DigSilent," *Front. Energy Res.*, vol. 9, 2021, doi: 10.3389/fenrg.2021.695814.

[80] E. M. Getie, B. B. Gessesse, and T. G. Workneh, "Photovoltaic Generation Integration with Radial Feeders Using GA and GIS," *Int. J. Photoenergy*, vol. 2020, 2020, doi: 10.1155/2020/8854711.

[81] V. Raviprabhakaran, "Performance enrichment in optimal location and sizing of wind and solar PV centered distributed generation by communal spider optimization algorithm," *COMPEL - Int. J. Comput. Math. Electr. Electron. Eng.*, vol. 41, no. 5, 2022, doi: 10.1108/COMPEL-12-2021-0495.

[82] N. Kumar, T. Kumar, S. Nema, and T. Thakur, "A multiobjective planning framework for EV charging stations assisted by solar photovoltaic and battery energy storage system in coupled power and transportation network," *Int. J. Energy Res.*, vol. 46, no. 4, 2022, doi: 10.1002/er.7442.

[83] S. Kucuksari *et al.*, "An Integrated GIS, optimization and simulation framework for optimal PV size and location in campus area environments," *Appl. Energy*, vol. 113, 2014, doi: 10.1016/j.apenergy.2013.09.002.

[84] M. Ahmadi, M. E. Lotfy, R. Shigenobu, A. Yona, and T. Senjyu, "Optimal sizing and placement of rooftop solar photovoltaic at Kabul city real distribution network," *IET Gener. Transm. Distrib.*, vol. 12, no. 2, 2018, doi: 10.1049/iet-gtd.2017.0687.

[85] P. Dakić and D. Kotur, "Optimal placement of Pv systems from the aspect of

minimal power losses in distribution network based on genetic algorithm," *Therm. Sci.*, vol. 2018, 2018, doi: 10.2298/TSCI170528223D.

[86] M. Bazrafshan, L. Yalamanchili, N. Gatsis, and J. Gomez, "Stochastic planning of distributed PV generation," *Energies*, vol. 12, no. 3, 2019, doi: 10.3390/en12030459.

[87] R. Golnazari, S. Hasanzadeh, E. Heydarian-Forushani, and I. Kamwa, "Coordinated active and reactive power management for enhancing PV hosting capacity in distribution networks," *IET Renew. Power Gener.*, 2023, doi: 10.1049/rpg2.12773.

[88] S. Pemmada, N. R. Patne, D. Kumar, and A. Manchalwar, "A novel COVID-19 herd immunity-based optimizer for optimal accommodation of solar PV with battery energy storage systems including variation in load and generation," *Turkish J. Electr. Eng. Comput. Sci.*, vol. 31, no. 2, 2023, doi: 10.55730/1300-0632.3987.

[89] S. R. Gampa, S. Makkena, P. Goli, and D. Das, "FPA Pareto optimality-based multiobjective approach for capacitor placement and reconductoring of urban distribution systems with solar DG units," *Int. J. Ambient Energy*, vol. 43, no. 1, 2022, doi: 10.1080/01430750.2020.1713887.

[90] M. Hashem, M. Abdel-Salam, M. T. El-Mohandes, M. Nayel, and M. Ebeed, "Optimal Placement and Sizing of Wind Turbine Generators and Superconducting Magnetic Energy Storages in a Distribution System," *J. Energy Storage*, vol. 38, 2021, doi: 10.1016/j.est.2021.102497.

[91] O. Sadeghian, A. Oshnoei, M. Tarafdar-Hagh, and M. Kheradmandi, "A Clustering-Based Approach for Wind Farm Placement in Radial Distribution Systems Considering Wake Effect and a Time-Acceleration Constraint," *IEEE Syst. J.*, vol. 15, no. 1, 2021, doi: 10.1109/JSYST.2020.3040217.

[92] W. Gil-González, O. D. Montoya, L. F. Grisales-Noreña, A. J. Perea-Moreno, and Q. Hernandez-Escobedo, "Optimal placement and sizing ofwind generators in ac grids considering reactive power capability and wind speed curves," *Sustain.*, vol. 12, no. 7, 2020, doi: 10.3390/su12072983.

[93] H. Cetinay, F. A. Kuipers, and A. N. Guven, "Optimal siting and sizing of wind farms," *Renew. Energy*, vol. 101, 2017, doi: 10.1016/j.renene.2016.08.008.

[94] M. S. Mastoi, M. J. Tahir, M. Usman, D. Wang, S. Zhuang, and M. Hassan, "Research on power system transient stability with wind generation integration

under fault condition to achieve economic benefits," *IET Power Electron.*, vol. 15, no. 3, 2022, doi: 10.1049/pel2.12228.

[95] S. Shaddiq, "A Nexus among Reliability Improvement of Distribution System with Optimal Placement and Capacity of Wind-Based Distributed Generation Management," *J. ICTEE*, vol. 2, no. 2, 2021, doi: 10.33365/jictee.v2i2.1174.

[96] B. Patnaik, D. Sattianadan, M. Sudhakaran, and S. S. Dash, "Optimal placement and sizing of solar and wind based dgs in distribution systems for power loss minimization and economic operation," *Lect. Notes Electr. Eng.*, vol. 326, 2015, doi: 10.1007/978-81-322-2119-7_36.

[97] M. R. Baghayipour, A. Hajizadeh, A. Shahirinia, and Z. Chen, "Dynamic placement analysis of wind power generation units in distribution power systems," *Energies*, vol. 11, no. 9, 2018, doi: 10.3390/en11092326.

[98] M. Varan, A. Erduman, and F. Menevşeoğlu, "A Grey Wolf Optimization Algorithm-Based Optimal Reactive Power Dispatch with Wind-Integrated Power Systems," *Energies*, vol. 16, no. 13, 2023, doi: 10.3390/en16135021.

[99] A. Routray, K. D. Mistry, and S. R. Arya, "Wake Analysis on Wind Farm Power Generation for Loss Minimization in Radial Distribution System," *Renew. Energy Focus*, vol. 34, 2020, doi: 10.1016/j.ref.2020.06.001.

[100] H. S. Ramadan, A. F. Bendary, and S. Nagy, "Particle swarm optimization algorithm for capacitor allocation problem in distribution systems with wind turbine generators," *Int. J. Electr. Power Energy Syst.*, vol. 84, 2017, doi: 10.1016/j.ijepes.2016.04.041.

[101] S. Wen, H. Lan, Q. Fu, D. C. Yu, Y. Y. Hong, and P. Cheng, "Optimal allocation of energy storage system considering multi-correlated wind farms," *Energies*, vol. 10, no. 5, 2017, doi: 10.3390/en10050625.

[102] A. Jafar-Nowdeh *et al.*, "Meta-heuristic matrix moth–flame algorithm for optimal reconfiguration of distribution networks and placement of solar and wind renewable sources considering reliability," *Environ. Technol. Innov.*, vol. 20, 2020, doi: 10.1016/j.eti.2020.101118.

[103] W. Guan *et al.*, "Optimal placement and sizing of wind / solar based DG sources in distribution system," in *IOP Conference Series: Materials Science and Engineering*, 2017, vol. 207, no. 1, doi: 10.1088/1757-899X/207/1/012096.

[104] P. Kayal and C. K. Chanda, "Placement of wind and solar based DGs in distribution system for power loss minimization and voltage stability

improvement," *Int. J. Electr. Power Energy Syst.*, vol. 53, 2013, doi: 10.1016/j.ijepes.2013.05.047.

[105] N. Belbachir and M. Zellagui, "Multi-Objective Optimal Design of Solar and Wind Hybrid Renewable Energy Systems in Distribution System Considering Daily Uncertainties," *Alger. J. Renew. Energy Sustain. Dev.*, vol. 4, no. 01, 2022, doi: 10.46657/ajresd.2022.4.1.1.

[106] H. U. Rehman, A. Hussain, W. Haider, S. A. Ali, S. A. A. Kazmi, and M. Huzaifa, "Optimal Planning of Solar Photovoltaic (PV) and Wind-Based DGs for Achieving Techno-Economic Objectives across Various Load Models," *Energies*, vol. 16, no. 5, 2023, doi: 10.3390/en16052444.

[107] S. Kamel, A. Ramadan, M. Ebeed, L. Nasrat, and M. H. Ahmed, "Sizing and evaluation analysis of hybrid solar-wind distributed generations in real distribution network considering the uncertainty," in *Proceedings of the International Conference on Computer, Control, Electrical, and Electronics Engineering 2019, ICCCEEE 2019*, 2019, doi: 10.1109/ICCCEEE46830.2019.9070892.

[108] A. Ramadan, M. Ebeed, S. Kamel, M. I. Mosaad, and A. Abu-Siada, "Technoeconomic and environmental study of multi-objective integration of PV/wind-based DGs considering uncertainty of system," *Electron.*, vol. 10, no. 23, 2021, doi: 10.3390/electronics10233035.

[109] A. Padovan and D. Del Col, "Measurement and modeling of solar irradiance components on horizontal and tilted planes," *Sol. Energy*, vol. 84, no. 12, 2010, doi: 10.1016/j.solener.2010.09.009.

[110] B. K. Fontes Rodrigues, M. Gomes, A. M. Oliveira Santanna, D. Barbosa, and L. Martinez, "Modelling and forecasting for solar irradiance from solarimetric station," *IEEE Lat. Am. Trans.*, vol. 20, no. 2, 2022, doi: 10.1109/TLA.2022.9661464.

[111] J. Munkhammar and J. Widén, "Correlation modeling of instantaneous solar irradiance with applications to solar engineering," *Sol. Energy*, vol. 133, 2016, doi: 10.1016/j.solener.2016.03.052.

[112] K. Araki, Y. Ota, and M. Yamaguchi, "Measurement and modeling of 3D solar irradiance for vehicle-integrated photovoltaic," *Appl. Sci.*, vol. 10, no. 3, 2020, doi: 10.3390/app10030872.

[113] F. G. Akgül, B. Şenoɨlu, and T. Arslan, "An alternative distribution to Weibull

for modeling the wind speed data: Inverse Weibull distribution," *Energy Convers. Manag.*, vol. 114, 2016, doi: 10.1016/j.enconman.2016.02.026.

[114] M. Ahsan-ul-Haq, S. M. Choudhary, A. H. AL-Marshadi, and M. Aslam, "A new generalization of Lindley distribution for modeling of wind speed data," *Energy Reports*, vol. 8, 2022, doi: 10.1016/j.egyr.2021.11.246.

[115] Suwarno and Rohana, "Wind speed modeling based on measurement data to predict future wind speed with modified rayleigh model," *Int. J. Power Electron. Drive Syst.*, vol. 12, no. 3, 2021, doi: 10.11591/ijpeds.v12.i3.pp1823-1831.

[116] I. Pobočíková, M. Michalková, Z. Sedliačková, and D. Jurášová, "Modelling the Wind Speed Using Exponentiated Weibull Distribution: Case Study of Poprad-Tatry, Slovakia," *Appl. Sci.*, vol. 13, no. 6, 2023, doi: 10.3390/app13064031.

[117] S. Eryilmaz, İ. Bulanik, and Y. Devrim, "Computing reliability indices of a wind power system via Markov chain modelling of wind speed," *Proc. Inst. Mech. Eng. Part O J. Risk Reliab.*, 2022, doi: 10.1177/1748006X221133601.

[118] M. Zivkovic, M. Tair, K. Venkatachalam, N. Bacanin, Š. Hubálovský, and P. Trojovský, "Novel hybrid firefly algorithm: An application to enhance XGBoost tuning for intrusion detection classification," *PeerJ Comput. Sci.*, vol. 8, 2022, doi: 10.7717/peerj-cs.956.

[119] I. Fister, X. S. Yang, and J. Brest, "A comprehensive review of firefly algorithms," *Swarm Evol. Comput.*, vol. 13, 2013, doi: 10.1016/j.swevo.2013.06.001.

[120] M. Ghasemi, S. kadkhoda Mohammadi, M. Zare, S. Mirjalili, M. Gil, and R. Hemmati, "A new firefly algorithm with improved global exploration and convergence with application to engineering optimization," *Decis. Anal. J.*, vol. 5, 2022, doi: 10.1016/j.dajour.2022.100125.

[121] J. Li, X. Wei, B. Li, and Z. Zeng, "A survey on firefly algorithms," *Neurocomputing*, vol. 500, 2022, doi: 10.1016/j.neucom.2022.05.100.

[122] S. Arora and R. Kaur, "An escalated convergent firefly algorithm," *J. King Saud Univ. - Comput. Inf. Sci.*, vol. 34, no. 2, 2022, doi: 10.1016/j.jksuci.2018.10.007.

[123] Y. Xiao, X. Sun, Y. Guo, S. Li, Y. Zhang, and Y. Wang, "An Improved Gorilla Troops Optimizer Based on Lens Opposition-Based Learning and Adaptive β-Hill Climbing for Global Optimization," *C. - Comput. Model. Eng. Sci.*, vol. 130, no. 3, 2022, doi: 10.32604/cmes.2022.019198.

[124] Q. Liang, S. C. Chu, Q. Yang, A. Liang, and J. S. Pan, "Multi-Group Gorilla

Troops Optimizer with Multi-Strategies for 3D Node Localization of Wireless Sensor Networks," *Sensors*, vol. 22, no. 11, 2022, doi: 10.3390/s22114275.

[125] M. A. El-Dabah, M. H. Hassan, S. Kamel, and H. M. Zawbaa, "Robust Parameters Tuning of Different Power System Stabilizers Using a Quantum Artificial Gorilla Troops Optimizer," *IEEE Access*, vol. 10, 2022, doi: 10.1109/ACCESS.2022.3195892.

[126] T. Wu *et al.*, "A Modified Gorilla Troops Optimizer for Global Optimization Problem," *Appl. Sci.*, vol. 12, no. 19, 2022, doi: 10.3390/app121910144.

[127] B. Abdollahzadeh, F. Soleimanian Gharehchopogh, and S. Mirjalili, "Artificial gorilla troops optimizer: A new nature-inspired metaheuristic algorithm for global optimization problems," *Int. J. Intell. Syst.*, vol. 36, no. 10, 2021, doi: 10.1002/int.22535.

[128] M. Thebault, V. Clivillé, L. Berrah, and G. Desthieux, "Multicriteria roof sorting for the integration of photovoltaic systems in urban environments," *Sustain. Cities Soc.*, vol. 60, 2020, doi: 10.1016/j.scs.2020.102259.

[129] G. Moreno, P. Martin, C. Santos, F. J. Rodríguez, and E. Santiso, "A day-ahead irradiance forecasting strategy for the integration of photovoltaic systems in virtual power plants," *IEEE Access*, vol. 8, 2020, doi: 10.1109/ACCESS.2020.3036140.

[130] J. P. Pesantez, A. Ríos-Villacorta, and J. González-Redrován, "Integration of photovoltaic solar systems in the intensive and extensive shrimp sector of ecuador: El oro province study case," *Rev. Politec.*, vol. 47, no. 2, 2021, doi: 10.33333/rp.vol47n2.01.

[131] M. Thebault and L. Gaillard, "Optimization of the integration of photovoltaic systems on buildings for self-consumption – Case study in France," *City Environ. Interact.*, vol. 10, 2021, doi: 10.1016/j.cacint.2021.100057.

[132] J. D. Mariano and J. Urbanetz, "The Energy Storage System Integration Into Photovoltaic Systems: A Case Study of Energy Management at UTFPR," *Front. Energy Res.*, vol. 10, 2022, doi: 10.3389/fenrg.2022.831245.

[133] T. R. Ayodele, A. A. Jimoh, J. L. Munda, and J. T. Agee, "Challenges of grid integration of wind power on power system grid integrity: A review," *Int. J. Renew. Energy Res.*, vol. 2, no. 4, 2012.

[134] A. M. Osman and F. Alsokhiry, "Sliding Mode Control for Grid Integration of Wind Power System Based on Direct Drive PMSG," *IEEE Access*, vol. 10, 2022,

doi: 10.1109/ACCESS.2022.3157311.

[135] A. Fernández-Guillamón, K. Das, N. A. Cutululis, and Á. Molina-García, “Offshore wind power integration into future power systems: Overview and trends,” *J. Mar. Sci. Eng.*, vol. 7, no. 11, 2019, doi: 10.3390/jmse7110399.

[136] S. Pilpola and P. D. Lund, “Different flexibility options for better system integration of wind power,” *Energy Strateg. Rev.*, vol. 26, 2019, doi: 10.1016/j.esr.2019.100368.

[137] H. Lund, “Large-scale integration of wind power into different energy systems,” *Energy*, vol. 30, no. 13, 2005, doi: 10.1016/j.energy.2004.11.001.

[138] F. Hvelplund, P. A. Østergaard, and N. I. Meyer, “Incentives and barriers for wind power expansion and system integration in Denmark,” *Energy Policy*, vol. 107, 2017, doi: 10.1016/j.enpol.2017.05.009.

[139] H. Zhao, Q. Wu, S. Hu, H. Xu, and C. N. Rasmussen, “Review of energy storage system for wind power integration support,” *Appl. Energy*, vol. 137, 2015, doi: 10.1016/j.apenergy.2014.04.103.

LIST OF PUBLICATIONS

1. Aarif Shaik & Suresh Kumar Sudabattula ,2023 Optimal Power Loss Index Evaluation Using Metaheuristic Optimization Algorithms in Radial Distributed Networks.SN Computers, Science.Volume4,Page number 573.

2. Aarif Shaik & Suresh Kumar Sudabattula,2023 Optimal PV Distributed Generators Allocation Using Fire fly Algorithm to Enhance Voltage Profile.SN Computers, Science.Volume4,Page number 510.

3. Aarif Shaik & Suresh Kumar Sudabattula,2021 Placement of Solar DGs and capacitors in Distribution network combined approach. Crc press Taylor and Francis, Page number158.

4. Aarif Shaik & Suresh Kumar Sudabattula,2024 Optimal Placement of Solar and Wind Distributed Generators in Radial Distribution System, Smart grid and Electric Vehicles conference page number 020013-1 .